INTERFACIAL BONDING STRENGTH IN BILAYER TABLETS – MECHANISM AND ENGINEERING

A DISSERTATION

SUBMITTED TO THE FACULTY OF THE

UNIVERSITY OF MINNESOTA

BY

Shao-Yu Chang

IN PARTIAL FULFILLMENT OF THE REQUIREMENTS

FOR THE DEGREE OF

DOCTOR OF PHILOSOPHY

Changquan Calvin Sun, Advisor

August, 2019

Acknowledgments

First of all, I sincerely thank my advisor, Dr. Calvin Sun, with the deepest appreciation for his guidance, continuous motivation and assistance throughout the course of my Ph.D. Since the first day I joined the group, Dr. Sun always spared no efforts to teach and inspire me in the research and life so that I can develop the skills and broaden my knowledge. It is a great honor to work with him and accomplish a milestone with all the strength and courage in his lab.

I am also appreciated to my thesis committee members, Dr. Raj Suryanarayanan, Dr. Timothy S. Wiedmann, and Dr. Alex Fok. They are willing to serve on my committee and provide valuable and critical opinions and suggestions for the completion of my dissertation. In addition, Dr. Sury and Dr. Wiedmann gave the lectures for providing the fundamentals in the field and Dr. Fok was pleased to provide instruments and data analysis for the research.

I am thankful for my mentor, Dr. Raimundo Ho, during my summer internship in Abbvie. He offered me an opportunity to work in Solid State Chemistry. During the period, I had the chance to interact with excellent scientists in the pharmaceutical industry. I also learned new ideas and operated assorted instruments for the assigned experiments. It was a great memory during my Ph.D. life.

Also, I would like to thank my lab members, Limin, Reddy, Frederick, Chenguang, Shubhajit, Wei-Jhe, Jiangnan, Shenye, Kunlin, Yiwang, Hongbo, Zhu Ling, and Sibo. We always worked together as a family to pursue our common goal. I also thank Michelle,

Pinal, Mehak, Sampada, Kweku, and Hyunjoon from Dr. Sury and Dr. Panyam's groups for the support in my research and we shared the experience together.

Last but not least, I express the love and gratitude to my parents, Mr. Ching-Fa and Mrs. Jui-Pin. Thank you for their wholehearted support when I pursued my dream in these years. Even they are not here, but their heart is staying with me forever.

Dedication

To my wife, Shu-Ching Lee and to my beloved daughter, Makayla Chang.

To my caring family, my parents and my sister.

Abstract

The bilayer tablet contains two layers of materials. However, such tablets have higher tendency to crack at the interface or even layer separation. Interfacial bonding strength (IBS) is the strength that bonds two layers at the interface. Understanding the mechanism of forming an adequate IBS is critical to the successful development of a bilayer tablet product. The first step is to establish a standard measuring method for obtaining accurate IBS. Both shear and tensile tests are commonly used to measure IBS, which shows a linear correlation. However, the shear test has a more complicated result due to complex stress application and tablet testing orientation, which is not an issue for the tensile test. Therefore, the tensile test is preferred for straightforward data interpretation because of uniform applied stress. Thus, the tensile strength becomes a standard method for measuring IBS.

IBS of four layer combinations between microcrystalline cellulose (MCC) and lactose 24AN (Lac), i.e., MCC/MCC, Lac/Lac, MCC/Lac and Lac/MCC (1st/2nd), were measured under various first layer (P1) and second layer compaction pressures (P2) to validate the hypothesis that IBS is controlled by bonding area (BA) and bonding strength (BS) interplay at the interface. BA is the contact area between first layer and second layer powders at the interface and BS is the strength interactions over the contact area. As a result, any factors that influence either BA or BS affect IBS. Moreover, differential radial expansion between layers also affects IBS. In this work, BA is assessed by surface waviness and tablet porosity, while BS is assessed by tablet strength at zero porosity. Lower P1 leads to higher porosity of the first layer and higher P2 generally leads to greater surface waviness at the interface, both leading to larger BA and, thus, higher IBS.

However, higher P2 causes a larger difference in radial expansion when two layers are different materials, which weakens IBS. The materials in the two layers determine BS, which follows the descending order of MCC/MCC > MCC/Lac (Lac/MCC) > Lac/Lac. The trends in the effects of these factors on measured IBS support the hypothesis.

Further, bilayer tablets with each layer containing the mixture of MCC and lactose in different ratios with/without hydroxypropyl methylcellulose (HPMC) K15M are studied to understand the compositional effect on IBS under two P1s (20 and 100 MPa) and a fixed P2 of 200 MPa. The multi-component bilayer tablets make the trend of IBS more complicated as a function of MCC content. Still, IBS changes can be explained by the BA and BS interplay. The increase of MCC can increase BS but, at the same time, decrease BA. The addition of HPMC decreases BS for lower IBS. The interplay between BA and BS will determine IBS.

Particle size is also an important factor to affect IBS. Two sizes of microcrystalline cellulose (MCC) and lactose anhydrate were prepared to study the effect of particle size on IBS of bilayer tablets. The effect of particle size on IBS is also influenced by material mechanical properties. The results show lactose has an advantage as the first layer over MCC. With lactose in the first layer, IBS is generally higher and insensitive to particle size and materials in the second layer. However, MCC is a better fit in the second layer due to less sensitivity to particle size and materials in the first layer. The dependence of IBS on materials and particle size could be explained by the BABS interplay. The second layer prefers larger particles for higher BA but the first layer shows no preference in particle size. Besides, BS and radial expansion also influence the IBS, which necessitate being considered together between different layer combinations.

IBS alone cannot stand to judge whether or not a bilayer tablet was strong enough to sustain the downstream manufacturing processes. A survival test using tablet friabilator is developed to determine the minimum interfacial bonding strength (IBS_m) of bilayer tablets. From the result, IBS_m depends on both layer compositions and tablet size. When bilayer tablets made with more brittle materials or larger tablet sizes, a higher IBS_m was needed to pass the survival test. On the other hand, when a polymer, i.e. HPMC, was added, smaller IBS_m still passed the survival test. Considering all the composition and tablet size, an IBS_m of 0.26 MPa should be sufficient to avoid failure in bilayer tablet manufacturing in this work.

Table of Contents

List of Tables

List of Figures

Appendix Figures

CHAPTER 1. Introduction

1.1 General Introduction

Fixed dose combination (FDC) tablets have been used to deliver two or more active pharmaceutical ingredients (APIs) in a single dosing unit. [1] The FDC products provide several significant clinic advantages in some therapeutic areas by combining more than one APIs with different pharmacological mechanisms, such as anti-hypertensive, anti-viral, anti-glycemic, and anti-cholesterol areas. FDC is commonly used to treat diseases like cancer, [2] cardiovascular diseases, [3,4] infectious diseases. [5,6]

Among the FDC products, oral solid dosage form is the most popular. [7] Compared to single agent products, FDC products need more challenging formulation design and process development. [8,9] Nevertheless, oral solid FDC products have been successfully commercialized, [10] including monolithic tablets, bilayer or multi-layer tablets, and multi-particulate tablets. [11] The bilayer tablet stands out due to its unique advantages when two active drugs are chemically incompatible. In addition, either layer in the bilayer tablet can be customized to achieve its individual desired drug release profile for a better treatment outcome. [12,13] A long-standing issue for bilayer tablets is the inadequate interfacial bonding strength (IBS), which may result in bilayer tablets delamination at the interface during production or any downstream operations. If not solved, such problems can highly affect product integrity and impact drug delivery.

The overall goal of this work is to understand the bonding mechanism at the interface of bilayer tablets. A tensile method was first developed for measuring IBS. [14] The systemic variation of materials in each layer with different mechanical properties and compaction pressure was then studied to explain IBS based on the bonding model of bonding area (BA) and bonding strength (BS) interplay for the first time. BABS interplay model was

already successfully used to explain the strength of a single layer tablet. [15] In the context of IBS, BA is influenced by surface waviness and porosity, and BS is determined by tablet strength at zero porosity. Besides BA and BS, the radial expansion also affects IBS. In addition, the minimal IBS for successful development of bilayer tablets was investigated using a survival plot. With this method in place, one can determine whether or not each proposed formulation exhibits adequate IBS using a small amount of powder. This is essential for developing high quality bilayer tablet early in drug development.

1.2 Literature Review

1.2.1 Fixed Dose Combination (FDC)

The importance of fixed dose combination (FDC) products is gaining recognition by public health. FDC products are very commonly used to treat a patient population with diseases that usually require co-administration of two or more active drugs in a single dosage to achieve the claimed clinical outcome.[16] Reviews of the Physicians' Desk Reference (PDR) and United States Pharmacopeia (USP) in 2005 showed that 150 FDC products were listed in PDR and 80 in USP. [17] According to the website of Drugs@FDA in 2010, among 101 Food and Drug Administration (FDA)-approved New Drug Applications (NDAs), 26 are FDC products. [11] FDC products demonstrate a promising development in therapeutic areas due to several benefits, which includes but not limited to 1) synergistic therapeutic effects, [18] 2) enhancement of drug effectiveness, [19] 3) minimization of adverse effects, drug abuse and improvement of safety, [19-21] 4) product life cycle extension, and 5) patient compliance improvement. [3,22-24]

In spite of advantages, there are still disadvantages, such that 1) FDC products reduce the flexibility of administering drugs, 2) The cause of the adverse drug reactions in FDC products could be more difficult to pinpoint, 3) It could be a challenge for pharmacists to monitor patients' drug therapy, and 4) FDC products could be relatively large in tablet size for containing multiple drugs.

The selection of active drugs for FDC development is, in general, based on drug pharmacological mechanisms, drug–drug interactions, and pharmacokinetic profiles and product manufacturability. Therefore, many factors should be considered, all of which can contribute to the complexity in formulation design and process development. [7] For example, chemical compatibility between APIs as well as excipients is always the first step to consider in formulation design and process development. If total drug strength is high, tablet size can be too large for patients. Disproportionate drug dose combinations can cause a potential issue for content uniformity when one dose is much higher than the other. Bioequivalence (BE) needs to be conducted to demonstrate that the co-administered drugs are bioequivalent to those from a FDC product. The time to take FDC products with regard to the meal is also a challenge for GI tolerance and food effects.

Formulation design and manufacturing processes have been successfully applied in FDC products. These commonly used delivery approaches are 1) monolithic systems, 2) multi-layer systems, and 3) multi-particulate systems, which are briefly reviewed below.

Monolithic systems

When two active drugs are chemically compatible, a monolithic tablet formulation can be considered first. In this system, two drugs are mixed together and compressed to form a tablet. However, dissolution profiles and absorption mechanisms have to be evaluated for each drug.

Multi-layer systems

Multi-layer tablets can be bilayered or trilayered in most occasions. When two drugs are chemically incompatible, the multi-layer system is one of the choices for the reason that they can be physically separated into each layer. However, several aspects have to be considered, such as chemical stability of layers, layer formulation composition, process parameter, and testing methods.

Multi-particulate systems

The most used solid dosage form for this system contains pellets compressed into tablets or encapsulated into capsules. The common method to prepare pellets is to use extrusion/spheronization to manufacture pellets and then film-coated by one or multiple functional layers of coating. However, knowing how to incorporate APIs into the pellets would be an important aspect of this system.

1.2.2 Bilayer Tablet

Various formulations and manufacturing processes have been successfully used in commercial FDC products. The bilayer tablet is one of the solid dosage forms in the fixed-dose combination (FDC). [7,10] Bilayer tablets are composed of two distinct layers with functional formulation compressed in a single dosage unit, which usually needs more complicated manufacturing processes. If more than two layers in a tablet, it is commonly called multi-layer tablets. Bilayer tablets are gaining more popularity in the market and the major drivers for the bilayer tablet development are listed below.

1) When bilayer tablets carry two chemically incompatible active pharmaceutical ingredients (APIs), they can be physically separated into each layer to reduce the contact area for unwanted chemical interaction. [25]
2) Bilayer tablets can be developed to achieve a better execution of the drug release profile for one or two different APIs by utilizing the function of each layer. For example, one layer can be immediate release and the other layer can be controlled release to have a burst effect followed by stable drug release. [26-28]

The aforementioned advantages and capabilities are specific to bilayer tablets, but bilayer tablets offer a new realm of challenges in formulation design, manufacturing processes, quality control, and product performance. These challenges include. [29,30]

1) Complex weight control in individual layers and final tablet weight.
2) Inadequate layer strength.
3) Delamination or cracks at the interface.
4) API cross-contamination between layers.

5) Reduced production yields.

However, among all the challenges, the most prominent issue long-awaited to be solved is the higher tendency to delamination or layer separation at the interface. A lot of previous research have worked on understanding and predicting interface bonding strength (IBS) of bilayer tablets , such factors as effects of compaction pressure and material properties, [14,31] effects of punch curvature, [32,33] comparison of different measuring methods for determining IBS, [34] correlation with surface free energy of materials,[35] and computer modeling. [36] It is of commercial importance to study IBS because poor bilayer tablet quality can cause huge financial and reputation loss for a company. However, the complex nature of the problem has prevented a clear mechanistic understanding of the effects of formulation and process variables on IBS. Therefore, a bonding model can be proposed to fundamentally explain the effect of these factors mentioned above.

1.2.3 Formation of a Bilayer Tablet

For a single layer tablet, when a powder is compressed, the porosity between the powder is reduced under the force. [37] The powder behavior in the compaction process can be described by a series of steps involving a specific mechanism.[38,39] During the die filling, particles overcome the cohesion between particles and adhesion with the die wall to loosely fill the die. At low compaction pressure, particles move through slippage, rotation, and translation movement to reduce pores in the powder without noticeable irreversible deformation. With the increase of compaction pressure, the particles cannot

move simply by the rearrangement to accommodate the compaction pressure. Instead, they start to deform elastically and plastically, or fracture to have further pore and volume reduction, which is the main step to contribute to tablet strength. During decompression, the applied stress is reduced to zero and the compact can expand axially accordingly in the die. Then the compressed compact is pushed out of the die.

The production of bilayer tablets differs from that of a traditional single layer tablet by one more step in the filling and compaction process for second layer material. [40] A schematic illustration of the bilayer tableting process is shown in Fig. 1. Initially, first layer powder is manually loaded into the die and compressed by the first layer compaction pressure (P1) to make the first tablet layer (Fig. 1a). With the first layer staying in the die, a second layer powder is then manually added to the top of the first layer, followed by the second compaction pressure (P2) (Fig. 1b). All final bilayer tablets are ejected out of die by pushing downwards with the top punch (Fig. 1c) throughout the whole work.

The compaction behavior at the interface of bilayer tablets should be the same as that in a single layer tablet. However, when first layer powder is first compressed by P1, the mechanical properties of the compressed first layer would perform distinctly from that of the second layer powder. The degree of difference in mechanical properties between first and layer will affect IBS, which depends on materials, compaction pressures, and other manufacturing processes. These factors are briefly explained below.

Material properties

The formulation of single and bilayer tablets is composed of active pharmaceutical ingredients (APIs) and excipients, such as diluents, disintegrants, binding agents, or lubricants for different functions. Several commonly used excipients for the choice of study include microcrystalline cellulose (MCC), lactose, polyvinyl-pyrrolidone (PVP), hydroxypropyl methylcellulose (HPMC), and dicalcium phosphate dehydrate (DCP). [41] Each material possesses its specific material mechanical property, including elasticity, plasticity, and brittleness. The choice of materials should have the desired powder properties to achieve powder surface and bulk properties, especially for the first layer powder after first layer compaction is applied, which will significantly affect the bonding with second layer powder. Plastic material is usually soft and ductile, therefore, sensitive to compaction pressure, such as MCC. [42-46] During the compaction, such materials can deform easily to lose compressibility and leads to lower surface porosity and harder compact. When it is in the first layer so second layer powder will be more difficult to deform the first layer for larger interpenetration and form the bonding. However, brittle material is usually harder and less influenced by compaction pressures, i.e. lactose. [42-46] During compaction, brittle materials can maintain at higher porosity on the surface of the first layer for further deformation from second layer powder. Further deformation at the interface can induce more bonding formation.

The mixture of plastic and brittle materials can cover a wider range of mechanical properties, which can be used to achieve the balance between plasticity and brittleness of the mixture. [47,48] It is long recognized that the importance of comprehensive knowledge on the mechanical properties of the mixture for designing high-quality tablet products.

However, no literature is working on this field of research for bilayer tablet manufacturing.

In addition, particle size can affect powder compaction behavior.[49,50] Smaller particles generally form stronger tablets than larger particles because of larger surface area available for bonding between particles when compressed, such as MCC. [51-53] However, the effect of particle size is also influenced by material mechanical properties, such that the tabletability of brittle materials is not sensitive to size change i.e. dibasic calcium phosphate dihydrate and lactose. [54-56] The effects of particle size on tablet strength highlights the need for systematic study.

Compaction pressure

The bilayer tablet production is compressed twice. The first layer is compressed by first layer compaction pressure (P1), followed by second layer compaction pressure (P2) on both layers to form a bilayer tablet with interfacial bonding strength for holding the first and second layer together as a whole. Therefore, it is critical to understand the effects of P1 on the first layer and P2 on the interface for IBS.

First layer compaction pressure (P1)

The effect of P1 on the compaction behavior of the first layer of a bilayer tablet is the same as the compaction on a single layer tablet. P1 affects surface and bulk mechanical properties on the first layer, i.e. surface porosity and bulk compressibility. Lower P1

leads to higher surface porosity and retain higher bulk compressibility. With higher surface porosity in the first layer, there is more room for second layer particles to interlock. In addition, the first layer with higher bulk compressibility can induce larger interpenetration between two layers and deformation at the interface during the second layer compaction for producing larger bonding area. Conversely, higher P1 compresses the first layer into a harder compact with lower porosity, which results in smooth surface and low bulk compressibility. Thus, second layer particles will have a difficult time to form larger bonding with first layer compact.

Second layer compaction pressure (P2)

P2 affects the compaction of first, second layers and the interface. Higher P2 generally produces bilayer tablets with higher IBS. Higher P2 can drive second layer particles into the first layer compact for larger interpenetration and also contribute to greater deformation at the interface. Both of larger interpenetration and deformation cause higher boning area formation. Moreover, it is known that when the powder is compressed by higher compaction pressure, the porosity between the powder reduces. Lower porosity means that contact area between particles becomes larger, which increases bonding area. On the other hand, lower porosity can usually cause higher elastic recovery for a material.[57,58] In bilayer tablets, when first layer and the second layer are composed of different powder materials, both layers could have different radial expansion. Especially when P2 is higher, larger difference in radial expansion between first and second layers is observed. The difference in radial expansion means elastic energy between two layers is

released unevenly, which can induce shear stress at the interface and then cause cracks or even delamination. [59,60]

Manufacturing processes

In addition to material properties and compaction pressures, other factors, such as the level of lubricants, environmental conditions, compaction speed, and aging, can affect IBS. [61,62] The function of a lubricant is to reduce the friction between powders, and powder to die during the tableting process, [63] which can improve the pore reduction. However, a lubricant, such as Magnesium Stearate (MgSt), usually has low bonding strength. [64] Lower bonding strength can deteriorate IBS. As for environmental conditions, such as relative humidity or temperature, different materials have different affinity for water adsorption or distinct thermal expansion. [62,65] This difference in material–water interaction or thermal expansion can result in the difference in radial expansion, which can induce shear stress and weaken IBS. The incorporation of water in the material can alter bonding strength of layers and then IBS of bilayer tablet. Some materials have time-dependent viscoelastic relaxation in tablets, which means the porosity of tablets would change with time.[66] Therefore, the mechanical properties of these materials also change because of the change of porosity, leading to the prediction of IBS more difficult. A compressed bilayer tablet is able to keep relaxing elastically due to the effect of aging, which can not only lead to the larger difference in radial expansion for the induction of shear stress but also larger porosity for smaller bonding area.

1.2.4 Strength Measurement of a Bilayer Tablet

Determination of strength of bilayer tablets is a critical step to obtain a fundamental understanding of interfacial bonding mechanism so that the strength of bilayer tablets can be fairly compared. A testing methods is needed to compare IBS of bilayer tablets made with different materials and compaction conditions. IBS of a bilayer tablet is an important attribute to judge if the bilayer tablet has adequate strength to withstand downstream processes, such as packaging, handling, shipping, and storage. During strength measurement, bilayer tablets can fail at three different modes, i.e. first, second and interface layer. [14] When bilayer tablets fail at the interface, the measured strength is considered as IBS, which is stronger than the strength of either layer. Otherwise, the measured strength is the strength of layers in either layer.

In the literature, several methods were developed to measure IBS , such as tensile test, [14,67,68] shear test, [14,61,69] diametrical compression test, [35,70] flexural test, [59,71] and notch test. [34,72] These measuring methods are listed below and briefly mentioned.

Tensile Test

In the tensile test, one side of a bilayer tablet is glued to a loading holder and the other side is glued to the bottom of a Materials Testing Instrument (Zwick- Roell 1485, Ulm, Germany) in Fig. 1.2. The tensile force, perpendicular to the interface of the bilayer tablet, is applied. The bilayer tablet is under tension until it is pulled apart. The measured maximum force (F) can be calculated as the IBS (σ) according to Equation 1.1.

$$\sigma = \frac{F}{\pi R^2} \qquad (1.1)$$

Where *R* is the radius of bilayer tablets, when bilayer tablets are cylindrical.

Shear Test

In the shear test, one layer of a bilayer tablet was inserted into the holder cavity of a Materials Testing Instrument (Zwick- Roell 1485, Ulm, Germany) with the other layer hanging outside and the outer layer is then subjected to the shear force using a blunt blade in Fig. 1.3. The shear force is applied in parallel to the interface until the bilayer tablet is sheared apart and the maximum shear force (*F*) is obtained, which can be used to calculate IBS using the Equation 1.1.

The shear test was developed specifically in the lab, which could be different from other shear tests. [61] Nevertheless, a shear stress in parallel to the interface of bilayer tablets is exerted until the specimen is broken and the calculation of shear stress is the same as Equation 1.1.

Diametrical Compression Test

In such a test, a cylindrical bilayer tablet is used for the purpose of strength calculation. A bilayer tablet is placed between two platens of a Materials Testing Instrument (Zwick-Roell 1485, Ulm, Germany). The loading cell lowers and compresses bilayer tablets along the diameter, which exerts a tensile force diametrically along the center line of the

bilayer tablet. The maximum tensile force (*F*) that breaks the bilayer tablet into half is used to calculate IBS (σ) using Equation 1.2.

$$\sigma = \frac{2F}{\pi dt} \qquad (1.2)$$

Where d is the diameter and t is the thickness of the bilayer tablet.

Flexure Test

In the flexure test, a bilayer tablet in the form of a beam is prepared. The beam is put on two supports with a certain distance. The force is loading at the interface of a bilayer tablet until the breakage. The maximum tensile force, that breaks the beam, is located on the lower side of the beam, which can be correlated with the IBS.

Notch Test

A bilayer tablet is stressed exactly at the interface between the layers by a punch tip with a half cylinder shape. The braking force corresponds to the force needed to separate the two layers of the bilayer tablet. This force is then correlated as IBS.

IBS can be measured by the abovementioned methods. However, there is no minimum IBS (IBS_m) as a criterion acceptance to indicate if IBS of a bilayer tablet is adequate to sustain manufacturing processes. Unlike bilayer tablets, the minimal strength of a single layer tablet with cylindrical shape is identified in several papers. [45,73] When a single layer

tablet has tablet tensile strength above 2 MPa, it is generally considered sufficient tablet strength for manufacturing processes. [74] Such tablet strength was supported by the observations that the tablets with a tensile strength above 2 MPa can pass the friability test for materials that are not too brittle. [46,75,76] Tablet friability is a fundamental method used to test the durability of tablets to resist abrasion, friction or mechanical impact, [77] which is developed and described in United States Pharmacopoeia (USP).[78] In general, an acceptable friability should be below 1.0% of tablet weight loss. [79] Using tablet friability, the correlation with the acceptance criterion for tablet strength can be found.

However, there is a lack of discussion in the literature to determine the IBS_m of a bilayer tablet with any method. Therefore, a method is highly required to develop to determined IBS_m. When a criterion for IBS_m is established, this is essential for tablet formulation selection and optimization to determine whether or not each proposed formulation exhibits adequate tabletability using a small amount of powder in an early stage of drug development.

1.2.5 Predicting interfacial bonding strength of bilayer tablets

In a single layer tablet, tabletability describes the ability of a powder to be compressed into a coherent compact with specified tablet tensile strength under the effect of compaction pressure, which is plotted by the relationship between tablet tensile strength and compaction pressures. [80,81] The understanding of tabletability can be described by quantifying the bonding area (BA) (the area of contracts between particles) and bonding strength (BS) (the intermolecular force over the areas) of the material. [15,82-85] BA can be

quantified by the porosity of the tablet. BS can be obtained by fitting the tablet strength and tablet porosity to zero porosity.

Similar to tablet strength of a single layer tablet, IBS of a bilayer tablet should also depend on both BA and BS due to the same compaction behavior. During a bilayer tablet manufacturing, a powder is first compacted, usually at low pressures, to consolidate the powder bed and also make room for the second layer powder filling before a second (final) compaction pressure is applied to make a bilayer tablet. The ability of particles between the adjacent layers to inter-penetrate affects the development of the BA at the interface, and hence IBS. The extent of inter-penetration can be measured by surface waviness at the interface, which is used to assess BA of bilayer tablets at the interface. Besides, the porosity of the bilayer tablet is also taken into consideration for the actual BA. For example, same surface waviness but lower porosity can contribute to higher actual BA than with higher porosity. BS describes the level of interaction between particles at the interface following the basic mechanisms, such as van der Waal's interactions, solid bridge, and mechanical interlocking. BS, measured by the same method as single layer tablets, can be determined by the extrapolation of tablet tensile strength at zero porosity. Larger BA or/and BS can increase IBS. Radial expansion is also considered, besides BA and BS. After a bilayer tablet is ejected out of the die, the constrain of radial direction is removed. Therefore, a bilayer tablet is free to expand radially. When two layers use different materials, radial expansion of each layer can be distinct to induce shear stress at the interface, which can weaken IBS. The degree of the difference can be used to judge the deteriorating effect of shear stress on IBS.

The bonding area-bonding strength (BABS) interplay is a useful model for the goal to predict the performance by allowing a clear explanation of complex bilayer tableting behaviors. The interplay between BA and BS can lead to complex tableting behavior of materials, depending on pressure, composition, and particulate properties (e.g., size).

1.3 Objectives and Hypothesis

The primary motivation of this thesis is to understand the interfacial bonding mechanism of bilayer tablets from material properties and processing parameters as well as generalize the suitable formulation compositions for robust manufacturability of bilayer tablet products. A key missing gap is the poor understanding to identify factors that affect the interfacial bonding strength of bilayer tablets and further to ensure the development of bilayer tablets with adequate interfacial bonding strength.

The objective of chapter 2 is to determine whether or not interfacial bonding strength obtained by the shear and tensile methods could be correlated. If a statistically significant relationship is found, knowledge obtained from the tensile method can be readily adopted to guide the development and characterization of bilayer tablets.

Hypothesis: The compressive stress exerted in the shear method more closely mimics the impacting force experienced by bilayer tablets, instead of tensile stress. Although the shear method is more relevant, it is difficult to explain the IBS obtained by this method due to the more complex stress distribution at the interface during testing. In addition, the measured shear IBS may also be sensitive to the tablet orientation and placement of the

interface relative to the two planes where shear stresses are applied. In contrast, the tensile test yields unambiguous results, because the tensile stress is more uniformly applied in a direction perpendicular to the interface.

The objective of chapter 3 to 5 is to modulate material mechanical properties (size, plasticity, brittleness) in layers and processing parameters (first and second layer compaction pressures) to mechanistically understand IBS from the interplay between bonding area and bonding strength generated at the interface of bilayer tablets.

Hypothesis: IBS was controlled by the bonding area and bonding strength at the interface. Larger bonding area and bonding strength can result in lager IBS. Understanding the effects of the mechanical properties and processing parameters on bonding area and bonding strength can form the basis to predict IBS and design a high-quality bilayer tablet.

The objective of chapter 6 is to determine the minimal IBS (IBS_m) when bilayer tablets are prepared by different layer compositions and tablet size and find out if there is any correlation.

Hypothesis: IBS depends on layer compositions and tablet size. A survival test was designed to determine IBS_m using the friabilator to see if there is a relationship between IBS_m and layer compositions and tablet size. With this simple acceptance criterion, we

can know if each proposed formulation exhibits adequate strength in an early stage of drug development.

.

1.4 Research plan and Thesis organization

In Chapter 2, we developed a tensile and shear method to measure interfacial bonding strength (IBS) of bilayer tablets made with MCC and lactose. We compared IBS measured by these two methods to see if there is a significant correlation. Since tensile method gave us unambiguous data interpretation so it was used as a standard method for IBS measurement in chapter 3 to 6.

In Chapter 3, we investigated the effects of material properties and compaction pressures on interfacial bonding strength (IBS). IBS was measured under different layer compositions in each layer and a series of first and second layer compaction pressures, and the failure mode was also recorded as a supplement for IBS interpretation. We integrated bonding area- bonding strength (BABS) interplay to explain IBS of bilayer tablets.

In Chapter 4, we studied formulated bilayer tablets made with a mixture of MCC and lactose or the addition of HPMC on IBS. The mixture in varied ratio of MCC and lactose was used to mimic real-life formulation. IBS and failure mode were recorded for data interpretation. BABS interplay was applied to explain IBS under a series of the mixture.

In Chapter 5, we compared the effects of different particle size on IBS. The effect of particle size is also affected by material mechanical properties. We prepared two grades of MCC and lactose in each layer and also determined the plasticity of each material. IBS

of bilayer tablets was measured with the recording of failure mode and BABS interplay was applied to explain the effect of particle size on IBS.

In Chapter 6, we determined the minimal IBS (IBS_m) under a wide range of compositions (MCC, lactose, and HPMC) from single to multiple materials in each layer. In addition, we also studied the effect of tablet size on IBS_m. A survival test using the friabilator was developed to determine the IBS_m and discuss the generality of the application to determine IBS_m.

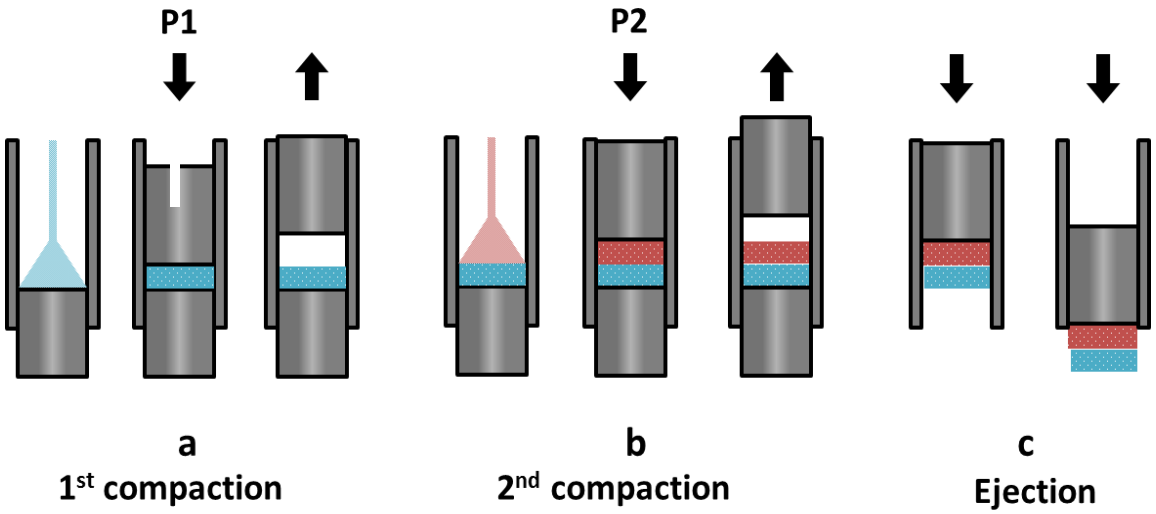

Figure 1.1 Illustration of the process for making bilayer tablets. a) The first layer was formed by compressing a powder at P1; b) Without ejecting the first layer, a second powder was added and compressed at P2 to form a bilayer tablet; c) The bilayer tablet was ejected downward out of the die.

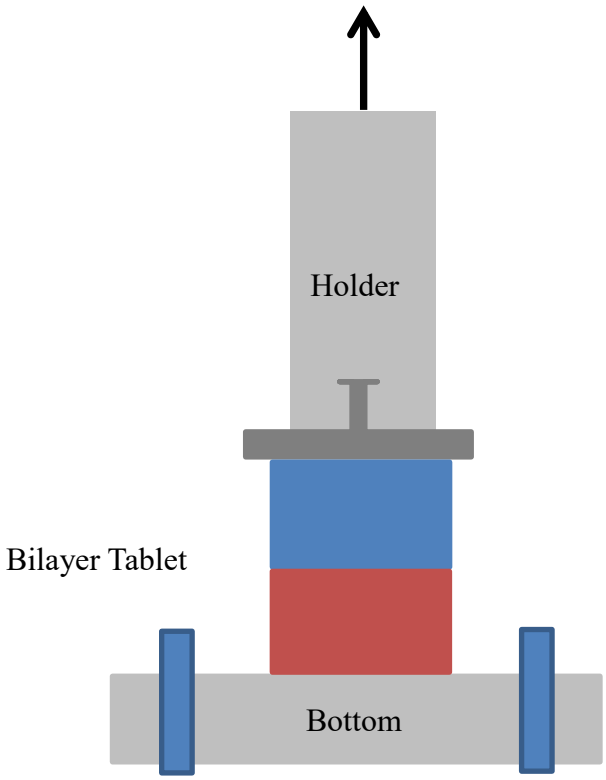

Figure 1.2 Illustration of the tensile method.

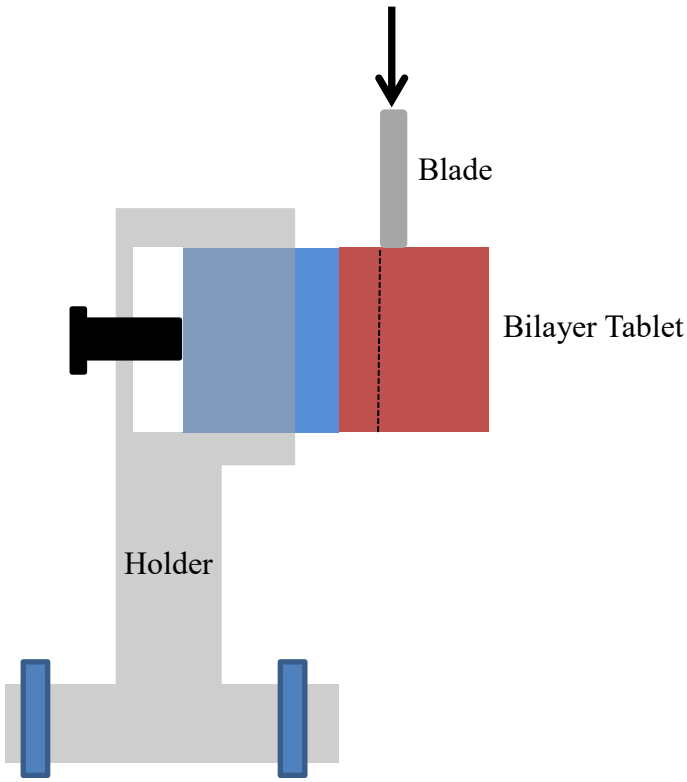

Figure 1.3 Illustration of the shear method.

CHAPTER 2. Tensile and shear methods for measuring strength of bilayer tablets

2.1 Synopsis

Both shear and tensile methods have been used to quantify interfacial bonding strength of bilayer tablets. The shear method is more convenient to perform than the tensile method. However, reproducible strength data by the shear method requires careful control of the placement of tablet and contact point for shear force application. Moreover, data obtained from the shear method depend on the orientation of bilayer tablets. Although more time-consuming to perform, the tensile method yields data that are straightforward to interpret. Thus, the tensile method is preferred in fundamental bilayer tableting research to minimize ambiguity in data interpretation. Using both shear and tensile methods, we measured mechanical strength of bilayer tablets made of several different layer combinations with lactose and microcrystalline cellulose. We observed a good correlation between strength obtained by the tensile method and carefully conducted shear method. This suggests that the shear method may be used for routine quality test of bilayer tablets on the manufacturing floors because of its speed and convenience, provided a protocol for careful control of the placement of the tablet interface, tablet orientation, and blade is implemented.

2.2 Introduction

The effective treatment of a wide range of diseases frequently requires co-administration of multiple medicines to increase the efficacy. [1] In contrast to taking tablets of each drug separately, a bilayer tablet simultaneously delivers two (or more for multi-layer tablets) drugs in one tablet. Thus, it is an effective approach for reducing pill burden. Consequently, the bilayer tablets have gained more importance and attracted attention as a dosage form. In bilayer tablets, the physical separation of drugs between layers effectively reduces the drug-drug contact surface area to minimize incompatibility among drugs. Through appropriate formulation in each layer, it is also possible to achieve desired release profiles of either a single or multiple drugs in one dosage unit. [2,3] The pharmaceutical advantages of bilayer tablets also form a basis for new intellectual property opportunities, which are important for life cycle management of drug molecules.

A main challenge in developing bilayer tablet drug products is the weak interfacial bonding strength (IBS) between the two layers, which may lead to visible cracks or even lamination at the interface after ejection or during packaging, shipping and storage. The availability of a standardized method to reliably quantify IBS is critical for investigating the causes of weak IBS. Measuring accurate IBS is the first step for developing a mechanistic understanding of the IBS evolution, which is important for effectively controlling IBS through formulation and process optimization. Accurate measurement of IBS is also required for establishing a minimally acceptable IBS that can be used to guide the formulation development of bilayer tablets, similar to the minimal diametrical tensile strength of 2 MPa proposed for single layer tablets. [4]

In the literature, several methods have been developed to quantify the strength of bilayer tablets, such as tensile test, [5-9] shear test, [10] diametrical compression test, [11-14] three point bending test, [15-18] and V-shape punch breaking test. [19] Among these, the shear and tensile methods are, by far, the most commonly used for quantifying IBS of bilayer tablets. In the shear method, a shear force parallel to the interface of bilayer tablets is applied, while a tensile force perpendicular to the interface is applied to the tablet during a tensile test.

The application of force in the shear method more closely mimics the impacting force experienced by bilayer tablets in real life, where bilayer tablets collide with each other or container wall. Thus, the stresses are more likely to compressive or shear instead of tensile. Although shear method is more relevant, it is difficult to explain IBS obtained by this method due to poorly understood stress distribution at the interface during testing. In addition, the measured shear IBS may also be sensitive to the tablet orientation and placement of the interface relative to the two planes where shear stresses are applied. In contrast, the tensile test yields unambiguous results because tensile stress is more uniformly applied to the interface in a direction perpendicular to it. However, the tensile method is much more time-consuming to perform than the shear method.

The respective advantages and disadvantages in the shear and tensile methods outlined above led to the preference of the former in the industry and the latter in academia research. A main goal of this work was to determine whether IBS values obtained by the shear and tensile methods could be correlated. If a strong and simple relationship is observed, knowledge derived from the research employing the tensile method can be readily adopted to guide the development and characterization of bilayer tablets by shear method.

2.3 Materials and Methods

2.3.1 Materials

Commonly used tablet excipients, lactose monohydrate (SuperTab 11SD and 30GR) lactose anhydrate (24AN) and microcrystalline cellulose (MCC, Pharmacel PH102) were gifts from DFE Pharm (Goch, Germany). Lactose is hard and brittle while MCC is soft and ductile. 20-24 Their binary mixtures exhibit a wide range of material properties, lying between the two pure materials. They were selected in this work for their relevance to bilayer tablet formulation and manufacturing in the pharmaceutical industry.

A portion of each powder was used to make colored tracer particles by spraying a 1% (w/w) methanol solution of a food dye. To ensure uniformity, a small amount of the solution was sprayed onto the raw powder using a spray bottle, followed by gentile mixing with a spatula and air drying. This process was repeated until the powder showed desired color intensity. Such colored powders had similar particles size and shape to the untreated powders. A small amount of the colored tracer powder (1%, w/w) was mixed with corresponding untreated powder. When making a bilayer tablet, one layer used an as-received material while the other layer used a powder containing colored tracer particles to aid the identification of the interface. Prior to compression, all powders were lubricated with 0.5% (w/w) of magnesium stearate (Mallinckrodt Pharmaceuticals, St. Louis, MO) and equilibrated in a 32% relative humidity (RH) chamber (over a saturated MgCl2 solution) before bilayer tablet compaction for at least 3 days.

2.3.2 Methods

2.3.2.1 Powder blend preparation

Powder mixing was carried out in a V-shaped blender (Blendmaster, Patterson Kelley, East Stroudsburg, PA) at 25 rpm for 10 min. A typical batch size was 100 g and the volume of the blender was 1 quart.

2.3.2.2 Bilayer tablet compaction

Cylindrical bilayer tablets were compressed on a Materials Testing Instrument (Zwick-Roell 1485, Ulm, Germany) using 8 mm flat round tooling. An illustration of the bilayer tableting process is shown in Figure 2.1. Approximately 150 mg of powder was manually loaded into the die and compressed at a pressure, P1, which was 20 MPa in this study, to make the first tablet layer (Figure 2.1a). Without ejecting the 1^{st} layer, 150 mg of a second powder was again manually added to the die and the second (final) compression was carried out at P2, which was 200 MPa in this study (Figure 2.1b). All 2^{nd} layers were always colored while the 1^{st} layers were not. All tablets were ejected out of die by pushing on the 2^{nd} layer downward with the punch (Figure 2.1c). Bilayer tablets were stored at 32% RH for overnight before they were tested, by either shear or tensile method, for IBS. Environmental RH was ~50% during compaction and IBS determination. To minimize impact of RH variation on compaction behavior, care was taken to minimize exposure of the powder to environment and compression was carried out immediately after powder was added to the die.

2.3.2.3 Force application

Both shear and tensile methods, as illustrated in Figure 2.2, force was applied using a texture analyzer (TA-XT2i, Texture Technologies Corp., Scarsdale, NY/Stable Micro Systems, Godalming, Surrey, UK).

2.3.2.4 Shear method

For each group of 6 bilayer tablets prepared under identical compaction conditions, 3 tablets were inserted into the holder cavity (round, 8.02 mm diameter) with the 1st layer inside and the other 3 tablets with the 2nd layer inside. The position of the tablets was adjusted by a screw from the back of the holder (Figure 2.2a). The inner side of the blade and the holder front surface was 1 mm apart. The tablet was placed in such a way that the interface lied at the mid-point between the holder front surface and the inner side of the blade either visually or with the aid of a portable microscope (Dyno-light pro, AnMo Electronics Corporation, Hsinchu, Taiwan). During testing, the blade was lowered in parallel to the holder front surface at a speed of 0.01 mm/s until the bilayer tablet was broken (Figure 2.2a).

After a bilayer tablet was sheared apart, the recorded maximum shear force (F) was converted to shear strength (τ) by dividing the cross-sectional area of the bilayer tablet using equation (1).

$$\tau = \frac{F}{\pi r^2} \qquad (1)$$

where r is the average radius of 1st and 2nd layers, which could slightly differ due to differential degrees of expansion post ejection.

2.3.2.5 Tensile method

One side of a bilayer tablet was glued onto a SEM stud with super glue (ethyl cyanoacrylate) and the stem of the SEM stud was inserted into the loading holder and secured with a set screw from the side (Figure 2.2b). In this configuration, the interface of the tablet was parallel to the base. A stainless steel bar with a leveled surface was fixed onto the base of the texture analyzer with clamps and a proper amount of super glue was dropped on the steel bar. The bilayer tablet was lowered at a speed of 0.01 mm/s until the lower side came in contact with the glue on the steel bar. It was then held at a force of 30 N for 5 ~ 6 min to allow the glue to harden. The holder was then lifted upward at a speed of 0.01 mm/s to apply a tensile stress to the bilayer tablet along the direction perpendicular to the tablet interface until the tablet was broken.

The tablet tensile strength (σ) was calculated as the maximum axial tensile force (F) divided by the cross-sectional area of the tablet using equation (2).

$$\sigma = \frac{F}{\pi r^2} \qquad (2)$$

where r is the average radius of 1st and 2nd layer.

2.3.2.6 Failure modes

Three failure modes could occur, i.e., fracture plane could run through either layer or at the interface (Figure 2.3). This information provides important insight for proper data interpretation, as IBS was accurately measured only when the bilayer tablets were separated along the interface. If the failure occurred within either layer, the value of IBS was higher than the measured tensile or shear strength.

2.4 Results and Discussion

2.4.1 Effects of tablet placement on IBS determined using the shear method

The placement of bilayer tablets affected the measured shear strength (τ). Careful placement of the interface between the inner surface of the blade and the holder surface improved the precision of data. At the beginning of this work, we only visually positioned the tablet so that the interface lied approximately in the mid-point between the blade and holder front surface. A high variability in the shear strength was observed, especially for MCC/MCC, 24AN/24AN layer combination, as indicated by the relatively larger standard deviations (Figure 2.4a). Subsequently, we placed the tablet precisely with the assistance of a portable microscope so that the interface was in the mid-point of the distance (1.0 mm) between the holder front surface and the inner blade (Figure 2.2a). This noticeably improved the precision of measured shear strength (Figure 2.4b). Therefore, the microscopic control of tablet placement was adopted for subsequent experiments by the shear method. In our setup of the shear method, one side of bilayer tablets was inserted to the holder cavity and the other side was pressed down by a blunt

blade. This effectively formed a lever, where the lower edge of the cavity served as a fulcrum and downward forces were applied by the upper side of the cavity to the end of tablet in the cavity and the blade from either sides of the fulcrum, respectively. For a tablet that failed at the interface, a lower force by the blade was needed to break the tablet when the interface is closer to the fulcrum, i.e., the surface of the holder. This explains the larger variability in measured strength when the placement of the interface was not precisely controlled.

2.4.2 Effects of tablet orientation on IBS values by the shear method.

Besides the placement of interface during the shear strength measurement, tablet orientation was found to also impact the failure strength when the failure occurred within a layer instead of at the interface. This was observed for MCC/24AN, 11SD/11SD, 24AN/11SD and 24AN/24AN bilayer tablets (Figure 2.4b). In all these cases, tablet failed in the 2nd layer regardless of the tablet orientation during testing (Table 2. 1). This could be understood from the lever analogy, i.e., a lower force exerted by the blade is required for the same tablet when the failure occurred at a point closer to the fulcrum. Consequently, the determined failure strength was always lower when the 2nd layer was inserted into the holder cavity for these four combinations (Figure 2.4b). It should be kept in mind that the experimentally determined failure strength in such case is lower than IBS. This highlights the value of color coding layers in bilayer tableting research, which serves for at least two purposes: a) identifying failure location (interface or not) and b) guiding accurate placement for reproducible strength data.

The knowledge of tablet failure mode (Figure 2.3) is crucial for proper interpretation of IBS measured by the shear method. In this study, tablet failure mode was not affected by tablet orientation in all cases (Table 2. 1). With color coding, we were able to explain why some bilayer tablets were sensitive to tablet orientation (when failing within a layer) while other were not (when failing at the interface, such as MCC/MCC).

2.4.3 Tensile method for measuring IBS

The complexity of stress distribution during shear testing and its impact on measured IBS can be avoided by the tensile method, which eliminates the effects of tablet orientation and the placement. Consequently, the data interpretation is straightforward. With tensile IBS data, one can unambiguously rank order IBS for different layer combinations. In this work, the 24AN/MCC combination clearly stood out with the highest tensile strength, which was followed by MCC/MCC (Figure 2.5). It should be noted that the failure mode in the tensile method (Table 2. 2) was basically identical to that in the shear method (Table 2. 1). This is consistent with the fact that the weakest location in the bilayer tablet, 1st layer, 2nd layer, or interface has the highest probability to fail.

2.4.4 The relationship between IBS determined by the tensile and shear methods

In all cases, the tensile strength was always lower than the shear strength. However, the trends in shear strength and tensile strength were visually the same (Figure 2.6). When shear strength (determined with the 2nd layer inserted into the holder cavity) was plotted

against tensile strength, an approximately linear relationship was observed ($R^2 = 0.9$, Figure 2.7) with a slope of 1.1 and an intercept of 0.42 MPa. This relationship suggests that bilayer tablets could survive at higher shear stress than tensile stress. When the shear strength was determined with the 1st layer inserted in the holder cavity, the linear relationship remained but R^2 was reduced to 0.8 (data not shown). Thus, qualitative conclusions drawn using either shear or tensile method is likely consistent. As a result, the shear method can be employed for routine testing of bilayer tablets because of its speed and convenience as long as the placement of tablet and tablet orientation are carefully controlled. For mechanistic bilayer tablet research, the tensile method is recommended due to its reliability and accuracy

2.5 Conclusions

This investigation reveals that careful placement of tablet is critical for obtaining precise data in shear method. Tablet orientation may also affect measured shear strength when tablets fail within a layer instead of at the interface. The tensile method is not affected by tablet orientation but is more time consuming to perform. There is a reasonably strong linear correlation between tablet strength determined by the shear and tensile methods. Therefore, conclusions based on the trends in shear or tensile strength of bilayer tablets in previous studies are likely consistent.

Table 2. 1 Failure mode of bilayer tablets ($1^{st}/2^{nd}$) using the shear method with the microscopically controlled placement setup. The number of tablets failed in each failure mode is shown.

In the cavity	Failed layer	MCC/ MCC	MCC/ 11SD	MCC/ 24AN	MCC/ 30GR	11SD/ MCC	11SD/ 11SD	11SD/ 24AN	24AN/ MCC	24AN/ 11SD	24AN/ 24AN	24AN/ 30GR	30GR/ MCC	30GR/ 24AN	30GR/ 30GR
1^{st} layer	2nd			**3**	**3**		**3**		**1**	**3**	**3**	**2**			
	Interface	**3**	**3***			**3***									
	1st							**3**	**2**			**1**	**3**	**3**	**3**
2^{nd} layer	2nd			**3**	**2**		**3**	**2**	**1**	**3**	**3**	**3**			**1**
	Interface	**3**	**3***		**1**	**3***									
	1st							**1**	**2**				**3**	**3**	**2**

* No intact bilayer tablets could be formed. Split at the interface occurred upon ejection.

Table 2. 2 Failure mode of bilayer tablets ($1^{st}/2^{nd}$) using the tensile method. The number of tablets failed in each failure mode is shown.

Failure mode	MCC/ MCC	MCC/ 11SD	MCC/ 24AN	MCC/ 30GR	11SD/ MCC	11SD/ 11SD	11SD/ 24AN	24AN/ MCC	24AN/ 11SD	24AN/ 24AN	24AN/ 30GR	30GR/ MCC	30GR/ 24AN	30GR/ 30GR
2nd			**3**	**3**		**3**	**2**	**2**	**3**	**3**	**3**		**2**	
Interface	**3**	**3***			**3***			**1**						
1st							**1**					**3**	**1**	**3**

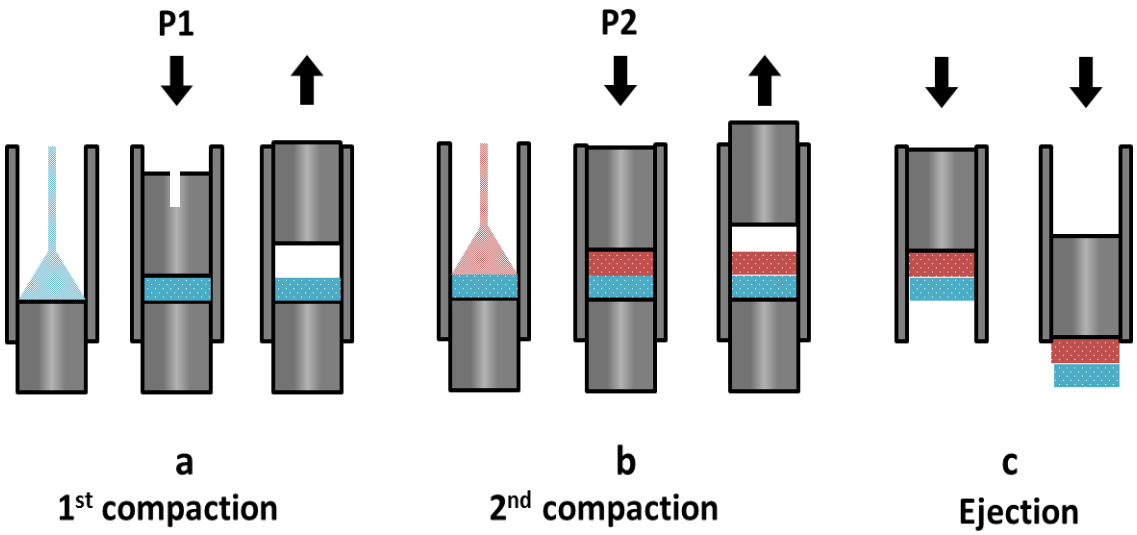

Figure 2.1 Illustration of the process for making bilayer tablets. a) The 1st layer was formed by compressing a powder at P1; b) Without ejecting the 1st layer, a 2nd powder was added and compressed at P2 to form a bilayer tablet; c) The bilayer tablet was ejected downward out of the die.

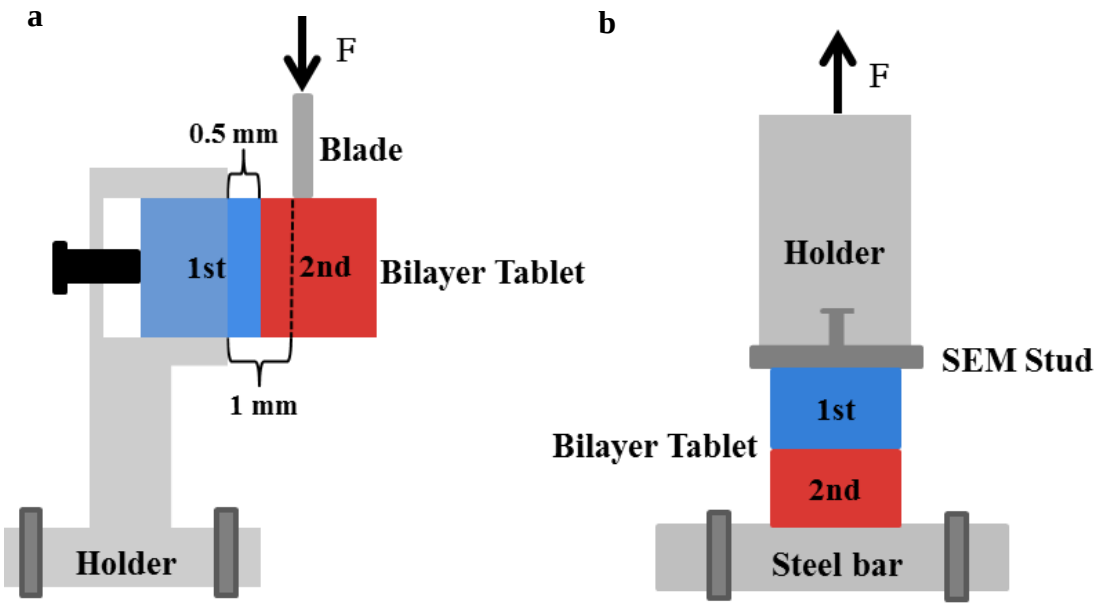

Figure 2.2 Illustration of setups for measuring interfacial bonding strength of a bilayer tablet by a) shear method and b) tensile method.

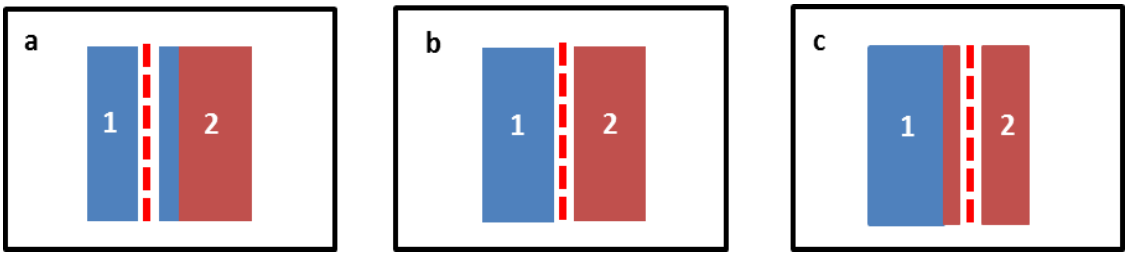

Figure 2.3 Schematic illustration of the failure modes for bilayer tablets with fracture occurring in, a) 1st layer; b) interface, and c) 2nd layer.

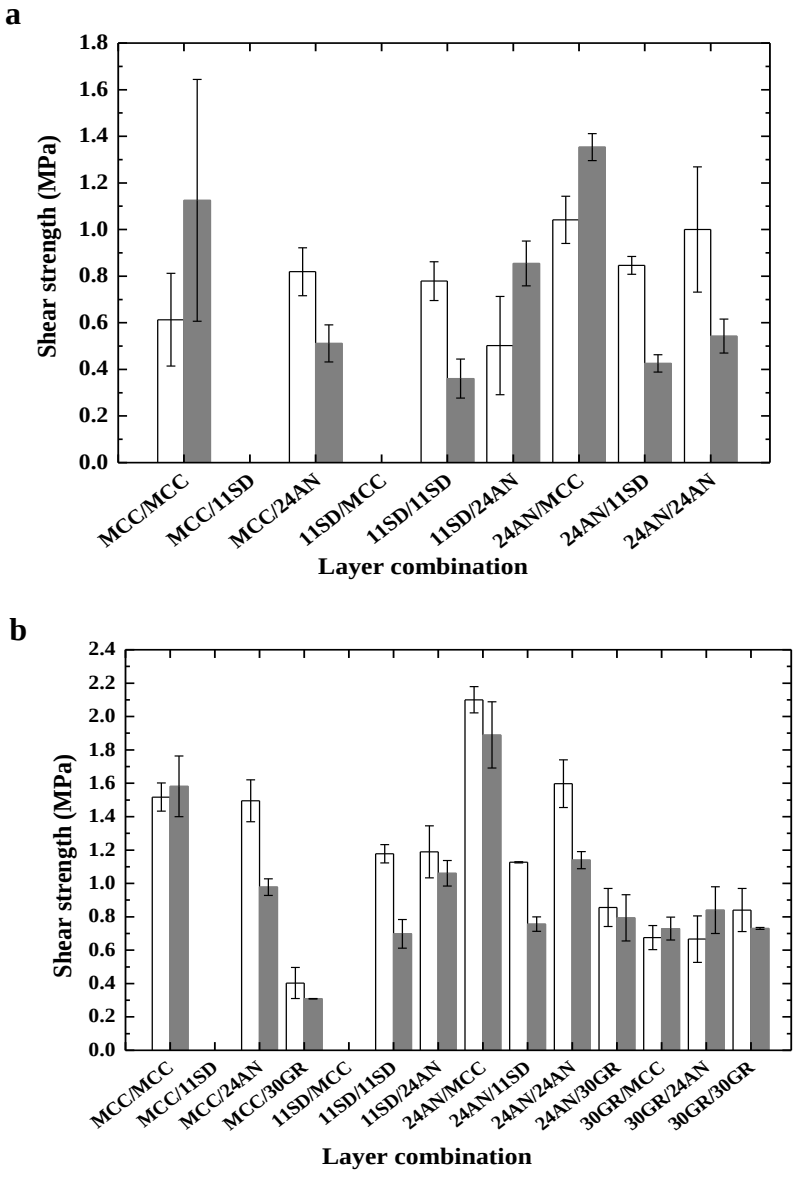

Figure 2.4 Shear strength of bilayer tablets ($1^{st}/2^{nd}$) with a) visual and b) microscopic control of the tablet placement. Open and solid bars represent 1^{st} and 2^{nd} layer in the holder cavity, respectively. Intact tablets could not be prepared for MCC/11SD and 11SD/MCC.

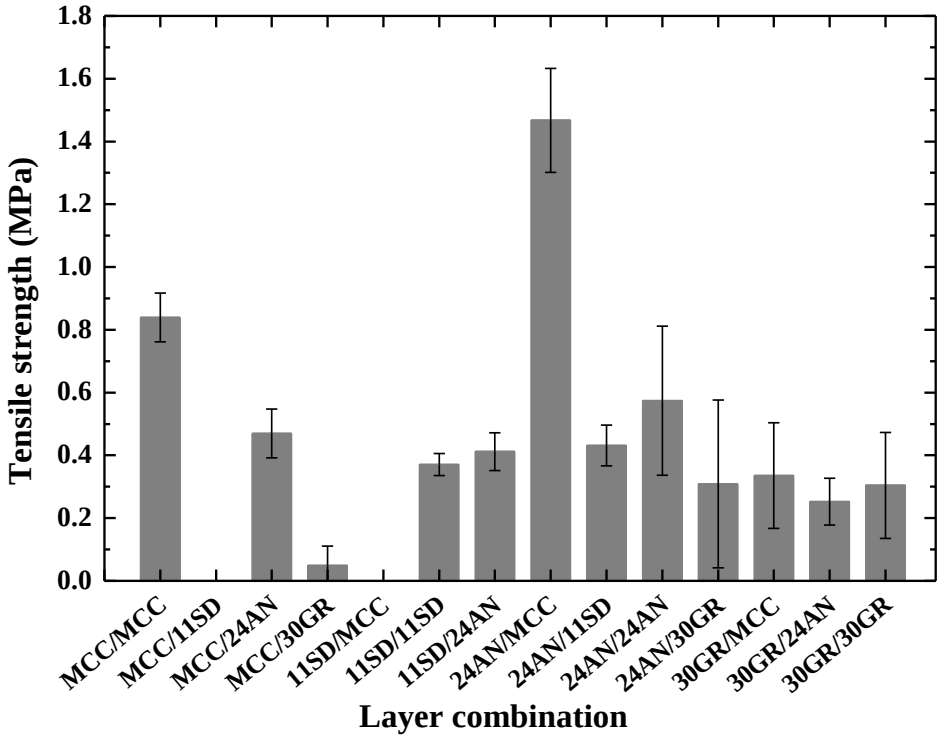

Figure 2.5 Strength of bilayer tablets ($1^{st}/2^{nd}$) measured using the tensile method. No bar is shown for MCC/11SD and 11SD/MCC because intact tablets could not be prepared.

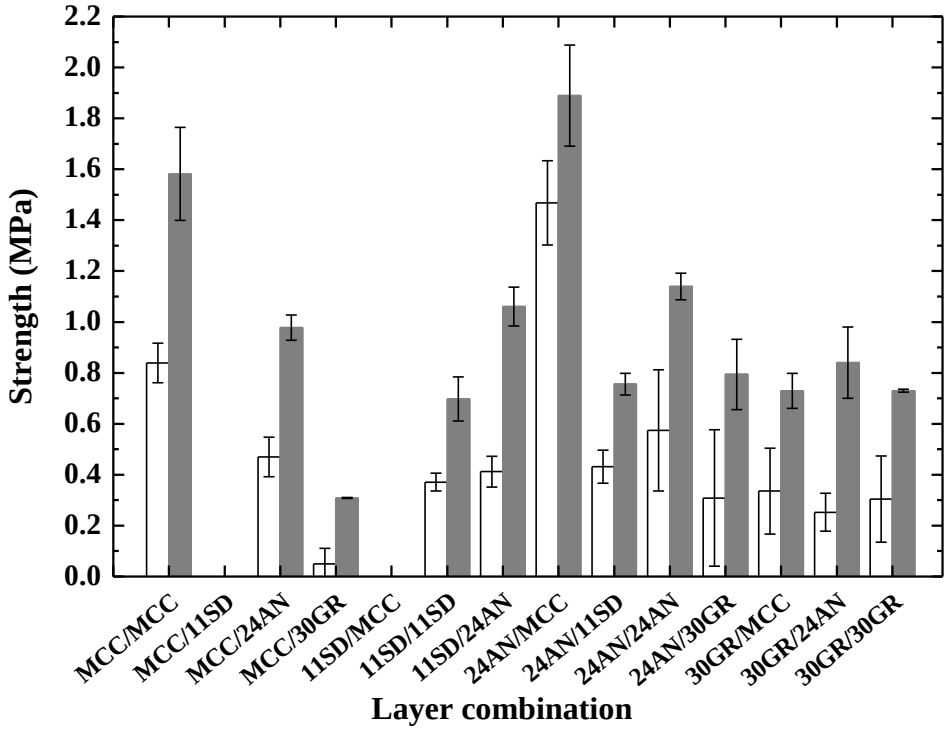

Figure 2.6 Strength of bilayer tablets ($1^{st}/2^{nd}$) measured by the tensile and shear methods. Open bar represents tensile strength and solid bar shows shear strength with 2^{nd} layer in the holder cavity.

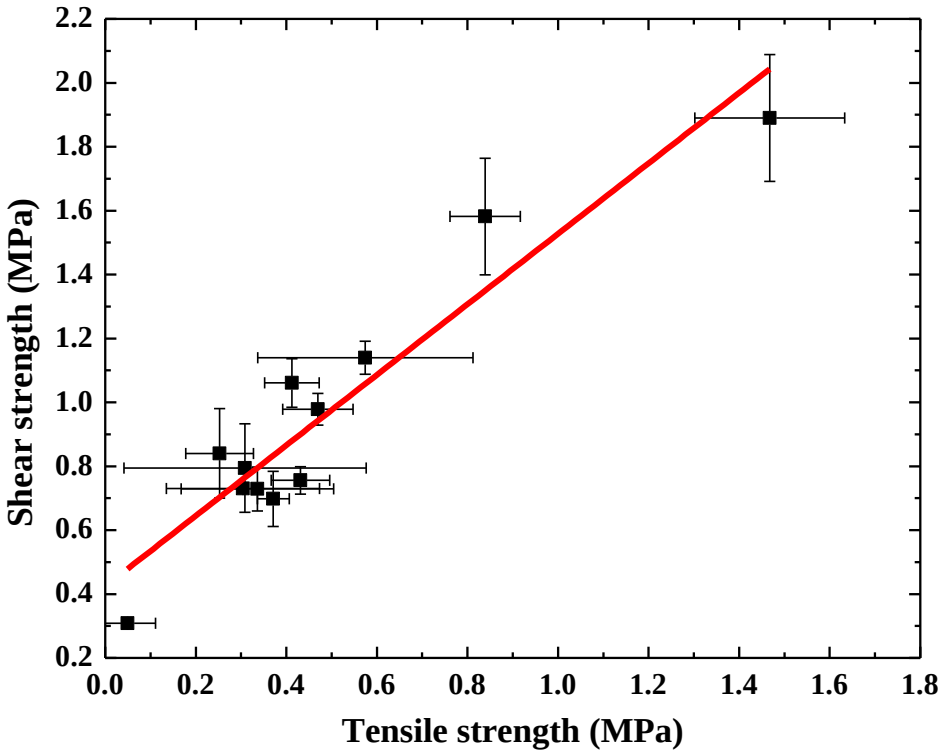

Figure 2.7 Relationship between shear and tensile strength of bilayer tablets. Shear strength was determined with the 2nd layer inserted into the cavity during shear testing.

CHAPTER 3. Insight into the effect of compaction pressure and material properties on interfacial bonding strength of bilayer tablets

3.1 Synopsis

The interfacial bonding strength (IBS) of four different layer combinations between microcrystalline cellulose (MCC) and lactose (Lac), i.e., MCC/MCC, Lac/Lac, MCC/Lac and Lac/MCC (1st/2nd) was assessed. In these studies, various first layer (P1) and second layer compaction pressures (P2) were used to test the hypothesis that IBS is controlled by bonding area (BA) and bonding strength (BS) interplay at the interface. The BA was evaluated by measurement of the surface waviness and porosity, while BS was assessed by the tablet strength at zero porosity. Lower P1 leads to higher porosity of the first layer, and higher P2 generally leads to greater surface waviness at the interface, both favor a larger BA and thereby higher IBS. However, higher P2 causes a larger difference in radial expansion, when the two layers differ, which weakens IBS. The materials in the two layers determine BS, which follows the descending order of MCC/MCC > MCC/Lac (Lac/MCC) > Lac/Lac. The trend in the effect of these factors on IBS support the hypothesis.

3.2 Introduction

High pill burden is a common problem that leads to poor patient compliance and less effective therapeutic outcome. Geriatric patients generally have difficulty in adhering to drug regimens, as evident in that approximately 50% of patients with chronic diseases do not strictly adhere to their medications as prescribed.[1,2] Non-adherence can lead to disease progression, a lower quality of life, loss of productivity, and increased morbidity.[3,4] Non-adherence was estimated to cost the healthcare system about $100 billion per year.[5] A fixed dose combination (FDC) is an attractive strategy for reducing pill burden by co-administering two or more drugs to attain the desired therapeutic outcome. [6,7] Bilayer or multi-layer tablets are a main enabling technology for the development of FDC products. Compared to single layer tablets, bilayer tablets provide unique advantages including: a) enhanced stability through physical separation of chemically incompatible drugs in different layers; [8] 2) improved patient compliance by reducing pill burden; and [9,10] 3) potential to produce complex drug release profiles for optimum delivery and clinical outcome. [11-13]

The successful development of bilayer tablets however, also faces unique challenges. One of the outstanding issues is inadequate interfacial bonding strength (IBS), which can result in quality problems, such as cracks or even layer splitting at the interface. Presently, inadequate IBS is not predictable, because there is poor understanding of the bonding. Progress towards ensuring the robust production of high quality bilayer tablets would be beneficial to the wider adoption of bilayer tablet technology. The IBS, which is the strength to bond two adjacent layers, is known to depend on both manufacturing processes and material properties. [14,15] Previous research on IBS includes effect of punch

curvature, [16,17] comparison of different methods for determining IBS, [18] correlation with surface free energy of materials,[19] and computer modeling. [20] However, the complex nature of the problem has prevented a clear mechanistic understanding of the effects of formulation and process variables on IBS.

The effects of formulation and process variables on IBS, e.g., particle size, mechanical properties, compaction pressure, and tableting speed, can be qualitatively understood by considering the compaction event occurring at the interface when manufacturing a bilayer tablet. A bilayer tablet is made by compressing the first layer of powder at a compaction pressure, P1, followed by introducing a second powder layer to the die without ejecting the first layer and then applying a compaction pressure, P2. [21] A single layer tablet may be thought as a bilayer tablet where P1 is zero and compositions are identical in the two layers. In an analogous manner, the interfacial IBS of a bilayer tablet should also depend on both bonding area (BA) and bonding strength (BS), which have been shown to control tensile strength (TS) of single layer tablets. [22-24] In the context of IBS, BA is the contact area between particles at the interface, and BS is the strength of interaction in a unit area of contact. As such, stronger interactions, contributed by larger BA and/or BS, between particles at the interface favor higher IBS. The BABS model in terms of bilayer tablet IBS is schematically illustrated in Figure 3.1.

When the first layer powder is compressed, particles initially undergo rearrangement at low compaction pressures, and then at higher compaction pressures, undergo elastic deformation, plastic deformation, or fragmentation. [25] [26] For the same material, a higher P1 tends to produce a more dense (less porous) first layer with smoother surface. This reduces the ability of particles in the second layer to penetrate into the first layer. [15,27,28]

Hence, BA is smaller, and IBS is weaker. Everything else being equal, P2 can enhance IBS by introducing larger BA between particles at the interface through promoting more interlayer particle penetration and particle deformation, similar to the rise in TS with increasing pressure for single layer tablets. [24,27]

Also, similar to the TS of single layer tablets, IBS at the bilayer interface also depends on the composition. Pore volume reduction by compression is more effective for more plastic materials. Under the same compaction pressure, a more plastic first layer powder will form a denser first layer with a smoother surface. [28-31] Therefore, more plastic materials are more sensitive to a change in compaction pressure. In contrast, harder materials undergo less plastic deformation and form a more porous first layer surface. This in turn allows more interlayer penetration during the final compression step of bilayer tablets manufacturing. An additional factor on IBS is that dissimilar radial elastic expansion of the two layers after ejection enhances the development of shear stress along the interface, which can cause splitting or crack formation, if IBS is insufficient to withstand the stress.

The aim of this work was to test the validity of the BA-BS interplay model to explain the IBS by systematically varying compaction pressure and materials in each layer. To achieve this goal, BA was inferred from surface waviness of the interface and layer porosity, because they directly correlate with the actual BA at the interface, while BS was inferred from the TS extrapolated to zero porosity. [32]

3.3 Materials and Methods

3.3.1 Materials

Two common tablet excipients, microcrystalline cellulose (MCC, Pharmacel PH102) and lactose anhydrate (Lac, Supertab 24AN) were received from DFE Pharm (Goch, Germany). MCC and Lac were chosen because of their radically different mechanical properties, where MCC is ductile, but lactose is hard and brittle. [33-37]

3.3.2 Methods

3.3.2.1 Powder blend preparation

Powder mixing was carried out in a V-shaped blender (Blendmaster, Patterson Kelley, East Stroudsburg, PA) operated at 25 rpm for 10 min. The batch size was 100 g, and the volume of the blender shell was one quart. All prepared powders were stored in 32% RH until used. To identify each layer, the second layer was blended with colored tracer particles. Tracer particles were prepared by spraying a small amount of 1% (w/w) methanol solution of a food grade dye, red for MCC and blue for lactose, followed by gentile mixing with a spatula and air drying. This process was repeated until the powder showed the desired color intensity and uniformity. Such colored powders had similar particles size and shape to the untreated powders. A small amount of the colored tracer powder (1%, w/w) was then mixed with the corresponding untreated powder. When making a bilayer tablet, one layer used an as-received material, while the other layer used a tracer particles-containing powder to aid in the identification of the interface. Prior to

compression, all powders were mixed with 0.5% (w/w) of magnesium stearate (Mallinckrodt Pharmaceuticals, St. Louis, MO) and equilibrated over a saturated $MgCl_2$ solution (32% relative humidity) in a closed chamber for at least 3 days.

3.3.2.2 Bilayer tablet compaction

Cylindrical bilayer tablets were compressed on a Materials Testing Instrument (Zwick-Roell 1485, Ulm, Germany) using 8 mm flat round tooling, following the same procedure as described before. [14] Briefly, approximately 150 mg of powder was manually loaded into the die and compressed at P1 to make the first tablet layer. Without ejecting the first layer, 150 mg of a second powder was manually added to the die and the second (final) compression was carried out at P2, which were 100, 200 or 300 MPa. Only the second layers contained colored material. All tablets were ejected from the die by pushing on the second layer downward with the punch. Bilayer tablets were stored at 32% RH overnight before IBS determination. Environmental RH was ~50% during compaction and IBS determination. To minimize the impact of RH variation on compaction behavior, care was taken to minimize environmental exposure of the powder, and compression was carried out immediately after powder was added to the die.

3.3.2.3 Tensile strength measurement

The TS of bilayer tablets was determined using a tensile test as described before. [14] One side of a bilayer tablet was glued onto a SEM stud with super glue (ethyl cyanoacrylate), and the stem of the SEM stud was inserted into the loading holder

(secured with a set screw from the side) on a texture analyzer (TA-XT2i, Texture Technologies Corp., Scarsdale, NY/Stable Micro Systems, Godalming, Surrey, UK). In this configuration, the interface of the tablet was parallel to the base. A stainless steel bar with a leveled surface was fixed onto the base of the texture analyzer with clamps. and super glue was dropped on the steel bar. The bilayer tablet was then lowered at a speed of 0.01 mm/s. until the lower side came in contact with the glue on the steel bar and reached a force of 30 N, which was held for 5 ~ 6 min to allow the glue to harden. The holder was then lifted upward at a speed of 0.01 mm/s to apply a tensile stress to the bilayer tablet along a perpendicular direction to the tablet interface until the tablet fractured. This process avoided other shear stresses that may develop due to mis-alignment between tablet and loading fixture.

The bilayer tablet TS was calculated as the maximum axial tensile force (F) divided by the cross-sectional area of the tablet using Eqn. (1).

$$TS = \frac{F}{\pi r^2} \qquad (1)$$

where r is the average radius of first and second layer, which was measured by digital calipers with 0.01 mm accuracy.

3.3.2.4 Failure modes

During a TS measurement, three failure modes could occur. The fracture plane could be located in either layer or at the interface. If bilayer tablets were separated at the interface, the TS was taken as IBS. If the failure occurred within either layers, the IBS is greater than the calculated TS.

3.3.2.5 Interface of bilayer tablets

To observe the interface of a bilayer tablet under a scanning electron microscope (SEM) (JSM-6500F, JEOL, USA), the bilayer tablet was cut diametrically from first layer to second layer using a razor, and a half tablet was mounted on a SEM stud with the cut surface up using double-sided electrical carbon tape. The sample was coated with a thin layer (50 Å) of platinum. SEM images were acquired using an acceleration voltage of 5 kV and a secondary electron detector in a vacuum of at least 10^{-3} Pa.

3.3.2.6 Surface waviness measurement by stylus profilometry

A stylus profilometer (KLA-Tencor P-16, Milpitas, CA) was used to profile the interface after separation between two layers. The stylus, normal to the surface, traversed the sample with a contact force of 1 mg (9.81 μN) to detect the asperities. The sample scan size was ~7.5 mm to cover a majority of the diameter of a tablet. The scan speed was 50 μm/s, and sampling rate was 200 Hz, approximately 30,000 data points were collected for each profile. The vertical range was set at 327 μm to allow adequately large z-direction movement of the stylus. The scans were performed three times on the same tablet surface along directions at approximately 60 degree angle to more accurately represent the surface topology.

The surface topography consists of two components, roughness and waviness, which are separated from the composite data by applying a cutoff wavelength. The profiles with feature wavelengths longer and shorter than the cutoff value are referred to as surface

waviness and surface roughness profiles, respectively. In this work, the cutoff wavelength, 80 μm, was used for surface waviness profiles, which would then capture surface size features comparable to the particle size. Such features are important to assessing bonding area at the interface of a bilayer tablet. Surface waviness, W_a, was calculated based on the summation of absolute values of the deviations with respect to a mean plane fit over the surface, as in Eqn. (2).

$$W_a = \frac{1}{L}\int_0^L |Z(x)|\, dx \qquad (2)$$

where L is sample scan length, and Z(x) is the vertical deflection of the sample at the position of x along the sample scanning.

In addition to interfacial profiles, the lateral surface of an intact bilayer tablet was also profiled to quantify the diameter mismatch between the two layers of different materials, where a larger diametrical difference indicates a larger interfacial shear stress.

3.3.2.7 Bonding strength determination

MCC, lactose, or the mixture (~200 mg) was loaded into a 8 mm round die and compressed using flat faced punches on a Zwick Materials Testing Machine (Model 1485; Zwick-Roell, Ulm, Germany) over the compaction pressure range of 25−350 MPa at the punch velocity of 5 mm/min without holding at the peak pressure. Three tablets were made at each compaction pressure and were stored in 52% RH overnight to allow relaxation. Tablet diameter (D) and thickness (T) were measured using a digital caliper with 0.01 mm accuracy and tablet weight (W) was measured using an analytical balance with 0.01 mg accuracy. Tablet flashing was carefully removed to improve accuracy of

the measured thickness.[38] Tablet density (ρ) was calculated from weight and calculated volume. True densities (ρ_t) were obtained from the tablet density – pressure data using the Sun method. [39] Tablet porosity (ε) was calculated using Eqn. (4):

$$\varepsilon = 1 - \frac{\rho}{\rho_t} \qquad (4)$$

Diametrical breaking force (F) was then measured using the texture analyzer at a testing speed of 0.01 mm/s. Diametrical tensile strength (σ) was calculated using Eqn. (5). [40]

$$\sigma = \frac{2F}{\pi DT} \qquad (5)$$

Tensile strength at zero porosity was obtained by extrapolating experimental data to zero porosity using the Ryshkewitch equation for the assessment of BS. [32]

3.4 Results and Discussion

3.4.1 Effects of pressure and materials on first layer surface property

The compaction process reduces void volume both within the powder bed and at the surface, which deteriorates the inter-layer bonding capacity. At a lower porosity, the first layer in a bilayer tablet limits penetration by particles in the second layer. Hence, bonding between the two layers is confined to the interface with little interpenetration between layers. As expected, the porosity of single layer tablets of MCC or lactose decreases with increasing compaction pressures (Figure 3.2a). Bulk MCC powder exhibited higher porosity than lactose powder, because of the less efficient packing of MCC particles. However, pore elimination in MCC tablet was more sensitive to pressure than lactose due to its higher plasticity. [41] Consequently, the compressibility curves crossed at 50 MPa, above which MCC tablets were less porous. This greater reduction

in porosity of the MCC layer with increasing pressure leads to a higher sensitivity of IBS to P1 in comparison to lactose.

The trend in waviness – pressure profiles between MCC and Lac tablets (Figure 3.2b) followed a similar trend to the porosity – pressure profiles (Figure 3.2a), where W_a of both MCC and lactose sharply decreased with increasing P1 up to 40 MPa followed by slow decrease up to 160 MPa. The W_a of MCC tablet is higher than lactose tablet below the crossover pressures of ~50 MPa, but the rank order was reversed above this pressure. This greater reduction in W_a for MCC by increasing compaction pressure is consistent with the higher sensitivity of IBS to P1 than lactose. The trends in W_a and tablet porosity were confirmed by the evident surface smoothing with increasing pressure for MCC and lactose as revealed by both SEM images (Figure 3.2c & Figure 3.2d) and profilometry surface profiles (Figure 3.2e & Figure 3.2f). In addition, profilometry surface data revealed that the tablet surface compressed by a flat punch was convex, not flat, for both MCC and lactose, which was possibly caused by the non-uniform density distribution in tablet.

The compaction pressure affects the surface curvature and smoothness, both of which influence interfacial BA. For the MCC layer, both the surface curvature and smoothness increased with increasing compaction pressure (Figure 3.2e). However, the higher pressure did not change the curvature of lactose, although the surfaces became more smooth (Figure 3.2f). Both SEM images and profilometry surface profiles suggest that the size of surface pores are as large as 200 μm at a compaction pressure of 20 MPa. With such large pores, particles of the second layer will more readily penetrate into the first layer, which will result in a larger interfacial BA. However, the higher compaction

pressure produced a smoother first layer surface, which adversely affected the development of the interfacial BA.

3.4.2 Effects of P1 and P2 on IBS

With the two excipients, MCC and lactose, there are four possible combinations of bilayer tablets, i.e. 1st layer/2nd layer: Lac/Lac, Lac/MCC, MCC/MCC, and MCC/Lac. Bilayer tablets of each combination were prepared under P1 ranging from 10 to 160 MPa and P2 of 100, 200, and 300 MPa.

3.4.2.1 Lac/Lac

The TS of the lactose/lactose bilayer tablet is given as a function of P1 in Figure 3.3a for the three different P2 values. For much of the P1 range, none of the tablets failed at the interface (Figure 3.3b). Thus, the IBS was stronger than TS of both layers, and the plateau TS was not significantly different from that of the axial TS of single compression tablet. Since the TS of individual layers directly depended on P2, the measured TS of bilayer tablets was independent of P1 until IBS was lower than layer TS. This occurred at values of P1 less than 120 MPa, when P2 was 200 or 300 MPa, but occurred at values of P1 less than 60 MPa, when P2 was 100 MPa. Above these P1 pressures, failure occurred at the interface, and the measured TS was IBS.

At the P2 of 100 MPa, all bilayer tablets prepared using P1 of 80 and 120 MPa failed along the interface, except one with P1 at 80 MPa (Figure 3.3b). When P1 was 160 MPa,

IBS was so weak that bilayer tablets spontaneously split upon ejection (Figure 3.3b). This is consistent with the BABS model, which presumes a direct correlation between IBS and BA at the interface. When the first layer was compressed at 160 MPa, lactose particles in the second layer could not easily penetrate into the first layer at a P2 of 100 MPa. This led to very small BA; and hence, low IBS. However, intact bilayer tablets could be formed at a P2 of 200 or 300 MPa, because lactose particles in the second layer could penetrate the first layer to a greater degree under a higher stress during second compression. However, the IBS of bilayer tablets was still lower than TS of the individual layers, and the bilayer tablet failed along the interface during tensile test (Figure 3.3b). Thus, P1 must be sufficiently high under a given P2 in order to induce reproducible interfacial failure mode (i.e., IBS < TS).

3.4.2.2 Lac/MCC

Lac/MCC exhibited a distinctly different trend of TS and failure mode from Lac/Lac. All tablets, except those compressed by only P2 (i.e., P1 = 0 MPa), failed at the interface (Figure 3.4b). The TS decreased with increasing P1 for all three P2, but a higher TS resulted with the use of a higher P2 (Figure 3.4a). A smoother interface was observed with increasing P1, as shown for the P2 = 200 MPa (Figure 3.5a), which would relate to a lower BA. However, the interface was only a ~2000 μm section, and the entire interface was actually concaved across the tablet, as shown in the surface profiles (Figure 3.5b), consistent with the literature. [42] As P1 increased, the interface became less concave and wavy, both contributed to smaller BA, as measured by W_a (Figure 3.5c), therefore

resulting in a smaller IBS. Data at P2 of 100 and 300 MPa qualitatively followed the same trend.

The W_a curves at different P2 crossed at a P1 of ~60 MPa (Figure 3.5c). If interfacial BA directly correlates to W_a, then the IBS for different P2 should also similarly crossed. However, IBS profiles crossed at ~160 MPa (Figure 3.4a). Thus, W_a of the Lac side of the interface was not the only factor that controlled interfacial BA. Under a higher P2, the more plastic MCC particles at the interface likely deformed to a greater extent. This would result in a lower porosity and a correspondingly greater BA, even when waviness of the Lac layer surface did not change greatly at or below P1 = 80 MPa (Figure 3.5c). Therefore, IBS is higher at a higher P2 (Figure 3.4a). However, a higher P2 can also induce a greater difference in diameters of the two layers, which may deteriorate IBS by introducing a higher shear stress along the interface. The observation that IBS is always higher at P2 = 300 MPa than P2 = 100 and 200 MPa suggests that the greater BA under higher P2 is due to more extensive permanent particle deformation, which overcomes the negative effect of shear stress. When P1 was increased to 160 MPa, intact bilayer tablets cannot be made. Due to the smoothness and mechanical rigidity of Lac layer, only a small BA developed. Consequently, IBS was insufficient to hold the two layers together.

3.4.2.3 MCC/MCC

In the case of MCC/MCC bilayer tablets, the IBS was highly sensitive to P1 and dramatically decreased with increasing P1 (Figure 3.6a) in comparison to Lac/MCC (Figure 3.4a). Despite this difference, the same explanation based on BABS interplay is

applicable to the MCC/MCC, since both failed at the interface (Figure 3.6b). For P2 of 100 MPa and as P1 is increased, the interface became smoother (Figure 3.7a). This trend is confirmed by their surface profiles (Figure 3.7b) and W_a (Figure 3.7c), both of which showed that BA decreased with increasing P1. At P2 = 200 MPa, the IBS was higher. This also was true for P2=300 MPa but the difference in IBS was less. This observation is consistent with the reduction in MCC tablet porosity, which was smaller at the higher P2 and reached near zero porosity at P2 of 200 and 300 MPa. (Figure 3.2a). Similar to Lac/MCC, the W_a curves of MCC/MCC crossed at a P1 of 70 MPa (Figure 3.7c). Thus, the deformation and associated penetration of the first MCC layer into the second layer did not further increase with the P2 change of 200 to 300 MPa.

3.4.2.4 MCC/Lac

The results with MCC/Lac bilayer tablets were complex. With each P2, TS decreased with increasing P1 (Figure 3.8a). Spontaneous layer separation (or delamination) was also observed (Figure 3.8b), but it occurred at a higher P1 when P2 was lower. Also, unlike above, the W_a curves among the different P2 were nearly superimposable (Figure 3.8c). At P1 = 0 MPa, TS was higher with increasing P2, and failure always occurred in the Lac layer. This means IBS is higher than TS of the Lac layer. At P1= 10 MPa, the same trend between TS and P2 was observed (Figure 3.8a), but failure occurred in both layers as well as at the interface (Figure 3.8b). At P1 = 20 MPa, tablets failed along the interface, when P2 was 100 MPa or 300 MPa but failure was randomly located when P2 was 200 MPa (Figure 3.8b). At P2 of 100 MPa, they all failed at the interface because P2

was low to make IBS stronger than layer strength. At P1 = 30 MPa, spontaneous layer split (delamination) occurred when P2 = 300 MPa. All of the intact tablets formed at P2 = 100 MPa and 200 MPa failed along the interface (Figure 3.8b) and yielded comparable IBS (Figure 3.8a). At P1 = 40 MPa, intact bilayer tablet could be made only under P2 = 100 MPa. The detrimental effect of increasing P2 on IBS indicated a significant role of shear stress between the MCC and Lac layers due to differential radial expansion, which is greater at higher P2 (see later discussion). At a low P1, IBS was sufficiently strong to withstand shear stress due to the large BA from the deeper interlayer penetration. Increasing P1 effectively diminished this effect and IBS to a point that spontaneous layer delamination occurred.

3.4.3 Effects of layer compositions on IBS

For a given layer combination, BS is constant and IBS is controlled by BA, which is affected by W_a and porosity. However, when different layer combinations were compared, both BA and BS must be considered. When P2 was 200 MPa, the TS followed the descending order of Lac/Lac > Lac/MCC > MCC/MCC > MCC/Lac (Figure 3.9a). The TS of Lac/Lac shows a plateau and decreased when P1 was higher than 120 MPa. The profiles of the three layer combinations displayed a continuous decrease with increasing P1 but with different slopes. Higher TS or IBS was observed when Lac was the first layer, suggesting the importance of preserving first layer with more open pores by less compressible powders to facilitate penetration by particles from the second layer.

3.4.3.1 Lac as first layer

Lac/Lac had higher TS than Lac/MCC (Figure 3.9a). Since failure occurred in the Lac layer of Lac/Lac but along the interface in Lac/MCC, TS of Lac layer must lie between the IBS of Lac/Lac and Lac/MCC. Even though BS of Lac/Lac was smaller than that of Lac/MCC (Figure 3.10), Lac/Lac still had a larger IBS than that of Lac/MCC, which can be attributed to higher BA at the Lac/Lac interface to compensate the lower BS. Another factor is that Lac/Lac had a smaller shear stress from different radial expansion (Figure 3.11a), which was significant for Lac/MCC (15-20 μm) (Figure 3.11b).

3.4.3.2 MCC as first layer

Compared to MCC/Lac, MCC/MCC showed both higher IBS and less sensitivity to increasing P1 (Figure 3.9a). Although MCC/MCC had a smaller BA due to a smoother surface (Figure 3.9b), MCC/MCC also had a higher BS than MCC/Lac (Figure 3.10) and an absence of differential radial expansion (Figure 3.11c), unlike MCC/Lac (Figure 3.11d), which more than adequately compensated the shortfall of a smaller BA.

3.4.3.3 The importance of layer sequence

For bilayer tables with different layer compositions, layer sequence can be readily changed during manufacturing to improve IBS without the need of formulation changes. A comparison of IBS profiles of Lac/MCC and MCC/Lac (Figure 3.9a), immediately reveals the significant effect of layer sequence. In this case, BS and radial expansion of Lac/MCC and MCC/Lac did not change (Figure 3.10, Figure 3.11b, and Figure 3.11d).

The dominant factor on IBS is BA. BA of Lac/MCC was higher than that of MCC/Lac (Figure 3.9b) because of the poorer compressibility of harder lactose, which leads to more open pores in the first layer to promote interlayer particle penetration.

3.5 Conclusions

The BA-BS interplay model provides a conceptual framework to explain the bonding mechanism at the interface of bilayer tablets. W_a and porosity influence the BA, and the TS at zero porosity determines BS. Radial elastic recovery is another factor that affects IBS. When bilayer tablets failed along the interface, IBS generally increases with increasing P2 but decreases with increasing P1. Higher P2 leads to greater W_a and lower porosity, which will increase the BA. However, higher P2 can also cause a larger difference in elastic recovery, which has the potential to exceed IBS, resulting in failure. Higher P1 reduces the compressibility for interpenetration, thus smaller BA. Mechanical properties of the first layer are more important than the second layer. TS or IBS of bilayer tablets with lactose as the first layer is both higher and less sensitive to P1. When MCC is the first layer, IBS is sensitive to P1 and generally weaker. Thus, layer sequence is a critical factor that should be considered during manufacturing to improve IBS, where less plastic layer should be compressed first.

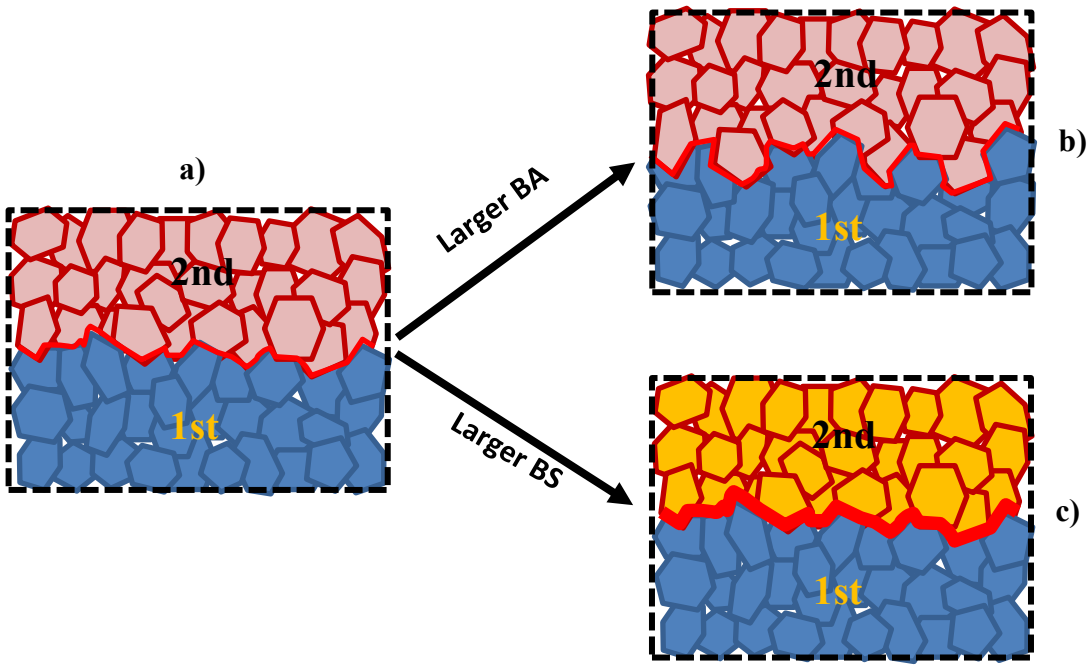

Figure 3.1 An illustration of inter-particle bonding at the bilayer tablet interface. Layer compositions in a) and b) are the same, but bonding area (BA) is larger in (b). Consequently, interfacial bonding strength in (b) is higher. BA in (c) is the same as that in (a) but bonding strength (BS) is higher than (a). Consequently, IBS in (c) is higher than (a).

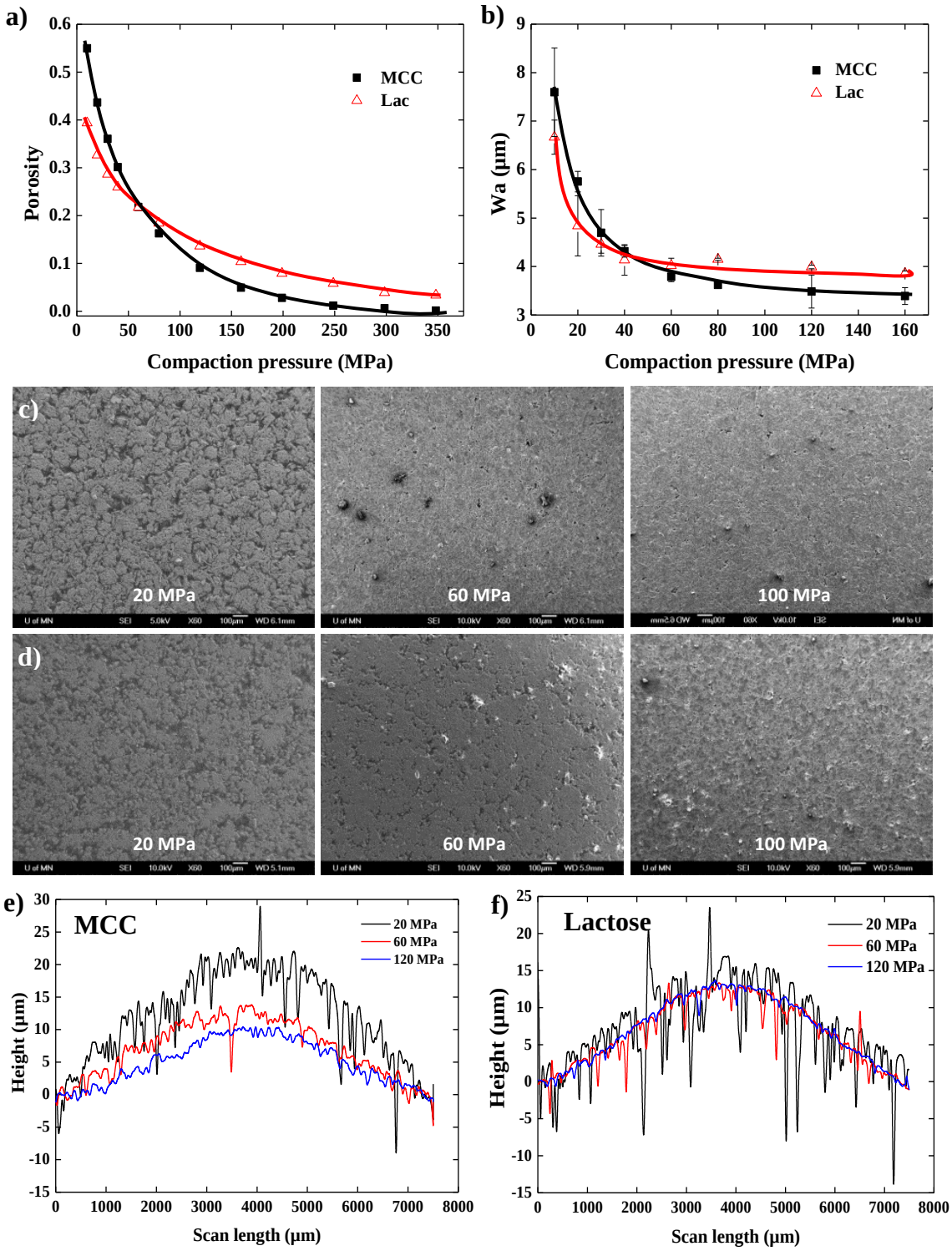

Figure 3.2 a) Compressibility and b) Surface waviness (W_a) profiles of MCC and lactose. SEM images of c) MCC and d) Lactose tablet surface at compaction pressures of 20, 60 and 120 MPa, and corresponding profilometry surface profiles of e) MCC and f) Lactose.

a)

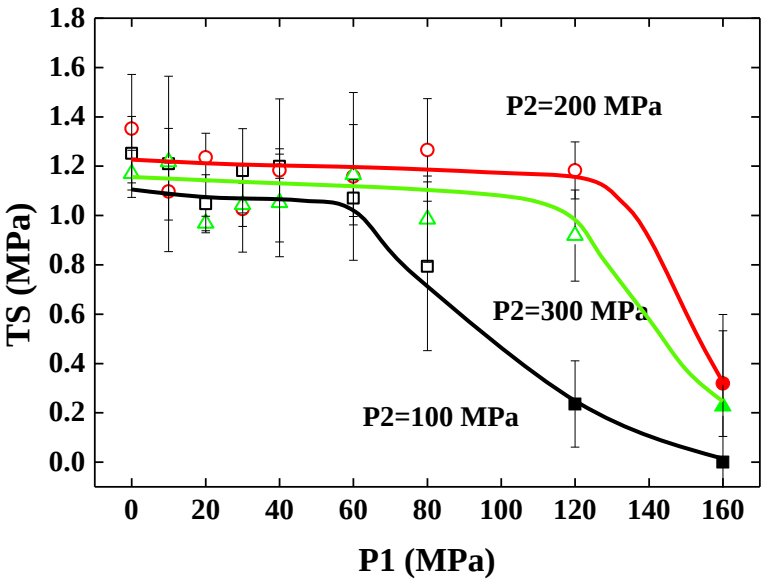

b)

P2 (MPa)	Failure	P1 (MPa)								
		0	10	20	30	40	60	80	120	160
100	2nd	3	1	-	-	1	2	1	-	-
	Interface	-	-	-	-	-	-	2	3	-
	1st	-	2	3	3	2	1	-	-	-
	Delamination	-	-	-	-	-	-	-	-	3
200	2nd	3	3	2	3	3	3	3	3	-
	Interface	-	-	1	-	-	-	-	-	3
	1st	-	-	-	-	-	-	-	-	-
300	2nd	3	3	3	3	3	3	3	3	-
	Interface	-	-	-	-	-	-	-	-	3
	1st	-	-	-	-	-	-	-	-	-

Figure 3.3 a) Effects of P1 and P2 on tensile strength (TS) of Lac/Lac (1st/2nd) bilayer tablets. Filled symbol represents bilayer tablets only failed at the interface, otherwise open symbol was used. b) Failure mode of corresponding bilayer tablets with number of failed tablets.

a)

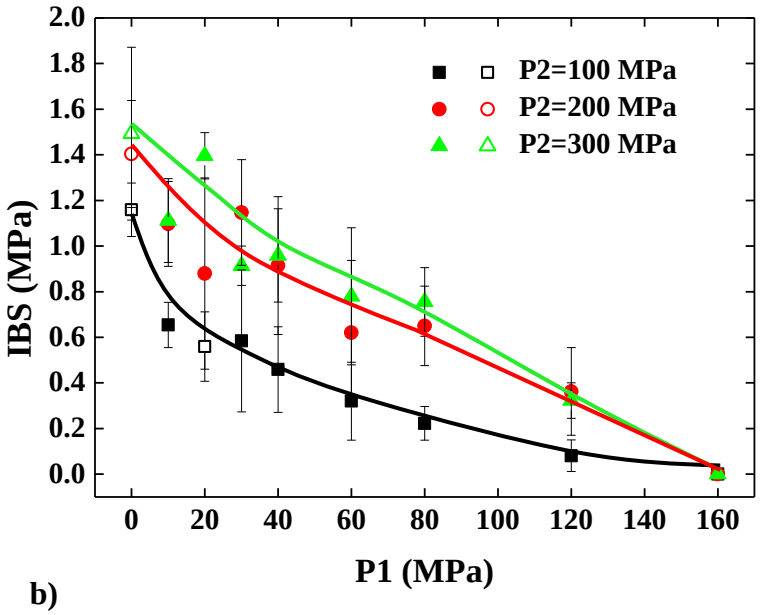

b)

P2 (MPa)	Failure	P1 (MPa) 0	10	20	30	40	60	80	120	160
100	2nd	-	-	1	-	-	-	-	-	-
	Interface	-	3	2	3	3	3	3	3	-
	1st	3	-	-	-	-	-	-	-	-
	Delamination	-	-	-	-	-	-	-	-	3
200	2nd	-	-	-	-	-	-	-	-	-
	Interface	-	3	3	3	3	3	3	3	-
	1st	3	-	-	-	-	-	-	-	-
	Delamination	-	-	-	-	-	-	-	-	3
300	2nd	-	-	-	-	-	-	-	-	-
	Interface	-	3	3	3	3	3	3	3	-
	1st	3	-	-	-	-	-	-	-	-
	Delamination	-	-	-	-	-	-	-	-	3

Figure 3.4 a) Effects of P1 and P2 on IBS of Lac/MCC (1st/2nd) bilayer tablets. Filled symbol represents bilayer tablets only failed at the interface, otherwise open symbol was used. b) Failure mode of corresponding bilayer tablets with number of failed tablets.

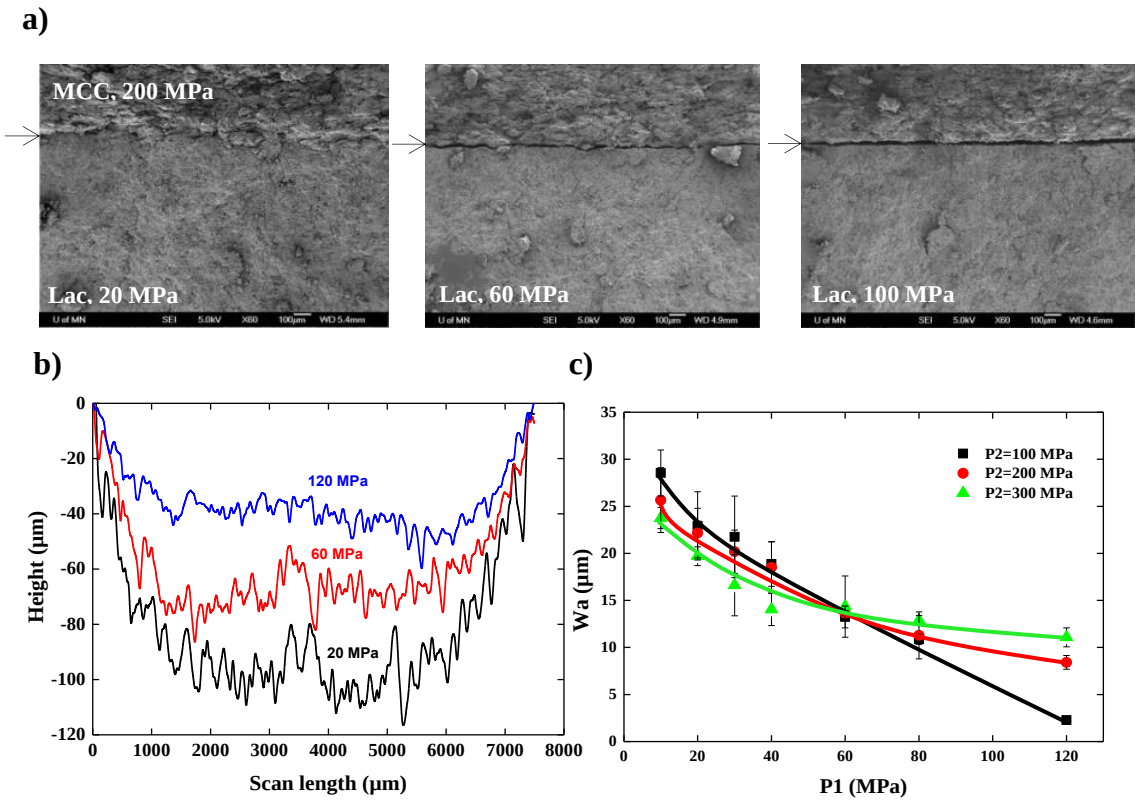

Figure 3.5 a) SEM images of the interface of Lac/MCC (1st/2nd) bilayer tablet under P1 of 20, 60 and 100 MPa, and the P2 of 200 MPa. b) Typical interface profiles (Lac side) after interfacial failure (P2 = 200 MPa). c) Surface waviness (W_a) of interface (Lac side) under different P1 and P2 combinations.

a)

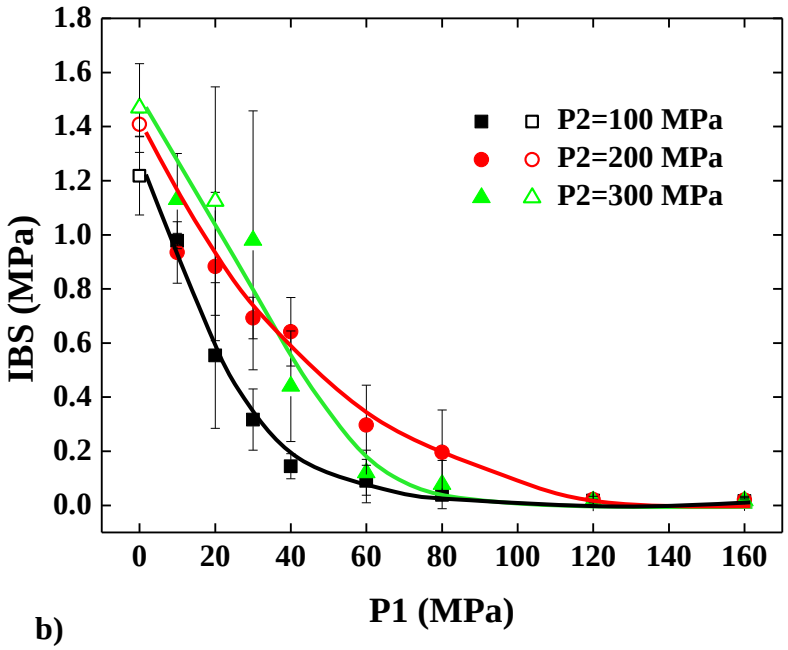

b)

P2 (MPa)	Failure	P1 (MPa)								
		0	10	20	30	40	60	80	120	160
100	2nd	3	-	-	-	-	-	-	-	-
	Interface	-	3	3	3	3	3	3	3	3
	1st	-	-	-	-	-	-	-	-	-
200	2nd	3	-	-	-	-	-	-	-	-
	Interface	-	3	3	3	3	3	3	3	3
	1st	-	-	-	-	-	-	-	-	-
300	2nd	3	-	1	-	-	-	-	-	-
	Interface	-	3	2	3	3	3	3	3	3
	1st	-	-	-	-	-	-	-	-	-

Figure 3.6 a) Effects of P1 and P2 on IBS of MCC/MCC (1st/2nd) bilayer tablets. Filled symbol represents bilayer tablets only failed at the interface, otherwise open symbol was used. b) Failure mode of corresponding bilayer tablets with number of failed tablets.

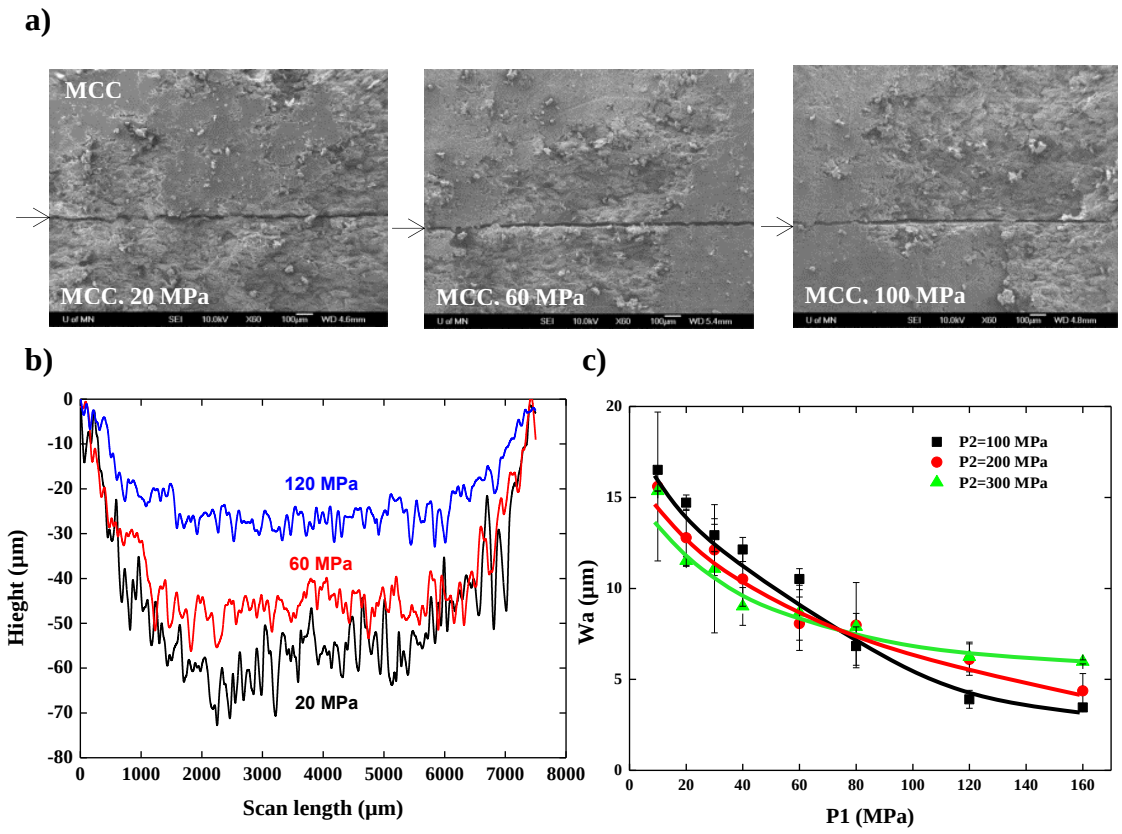

Figure 3.7 a) SEM images of the interface of MCC/MCC (1st/2nd) (P1 of 20, 60 and 100 MPa, and P2 = 200 MPa). b) Surface waviness profiles of the first layer MCC (P2 = 200 MPa). c) Surface waviness (W_a) of the interface (first MCC layer) under different P1 and P2.

a)

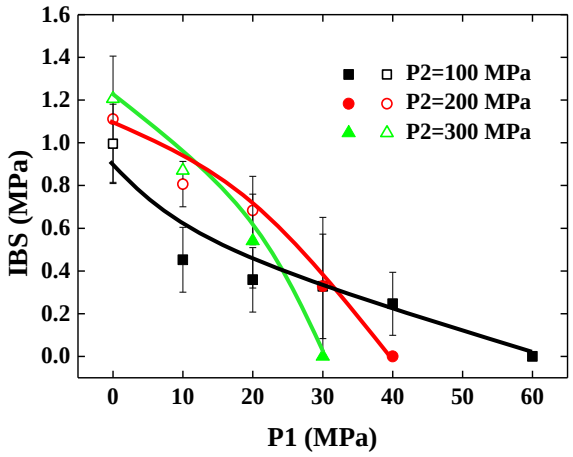

b)

P2 (MPa)	Failure	P1 (MPa)					
		0	10	20	30	40	60
100	2nd	3	-	-	-	-	-
	Interface	-	3	3	3	3	-
	1st	-	-	-	-	-	-
	Delamination	-	-	-	-	-	3
200	2nd	3	1	2	-	-	-
	Interface	-	2	1	3	-	-
	1st	-	-	-	-	-	-
	Delamination	-	-	-	-	3	-
300	2nd	3	1	-	-	-	-
	Interface	-	2	3	-	-	-
	1st	-	-	-	-	-	-
	Delamination	-	-	-	3	-	-

c)

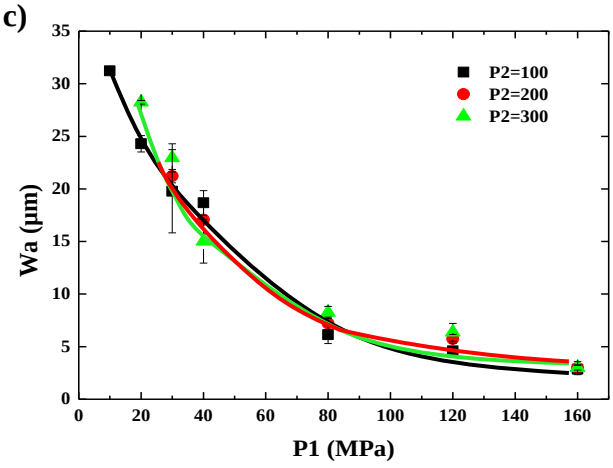

Figure 3.8 a) Tensile strength (TS) of MCC/Lac (1st/2nd) under a series of P1 and P2. Filled symbol represents bilayer tablets only failed at the interface, otherwise open symbol was used. b) Failure mode of corresponding bilayer tablets with number of failed tablets. c) Surface waviness (W_a) of the interface on MCC side under different P1 and P2.

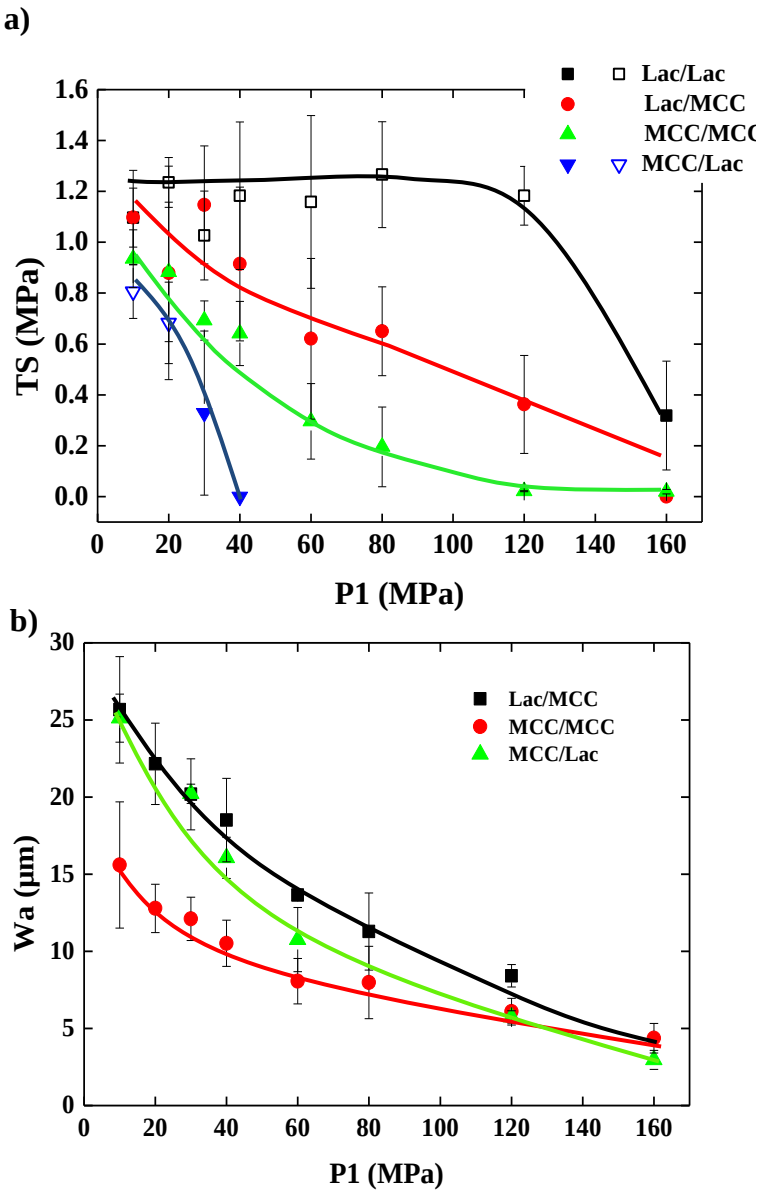

Figure 3.9 Effects of P1 on a) Tensile strength (TS) of bilayer tablets at P2 = 200 MPa for Lac/Lac, Lac/MCC, MCC/MCC, and MCC/Lac. Filled symbol represents bilayer tablets only failed at the interface, otherwise open symbol was used. b) Surface waviness (W_a) of the corresponding bilayer tablets.

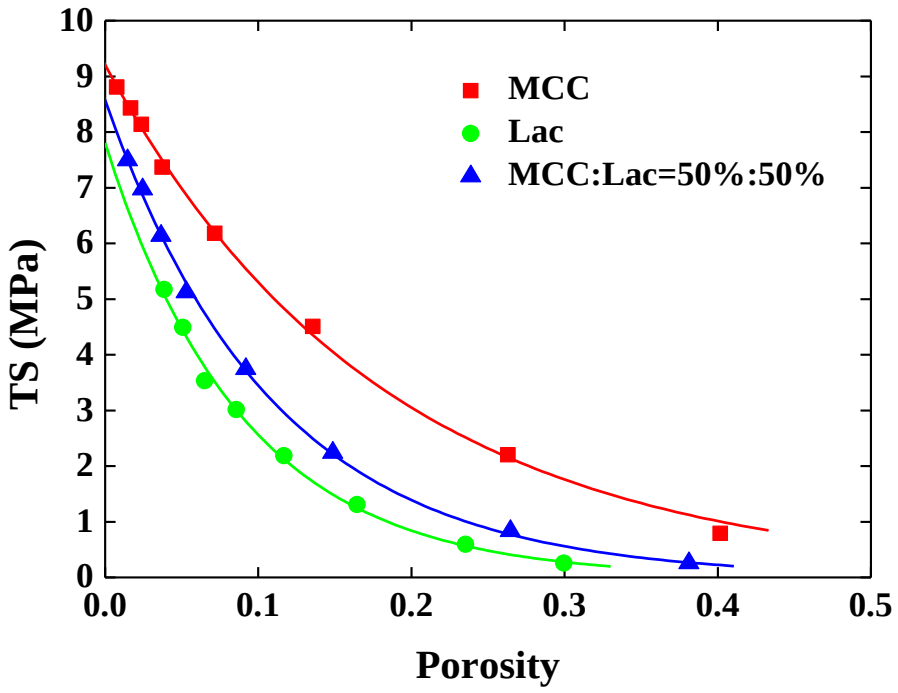

Figure 3.10 Tensile strength (TS) of MCC, lactose and the mixture of 50% MCC and 50% lactose. Bonding strength is assessed by TS at zero porosity. TS at zero porosity of MCC, lactose and the mixture is 9.21, 8.57 and 7.80 MPa, respectively.

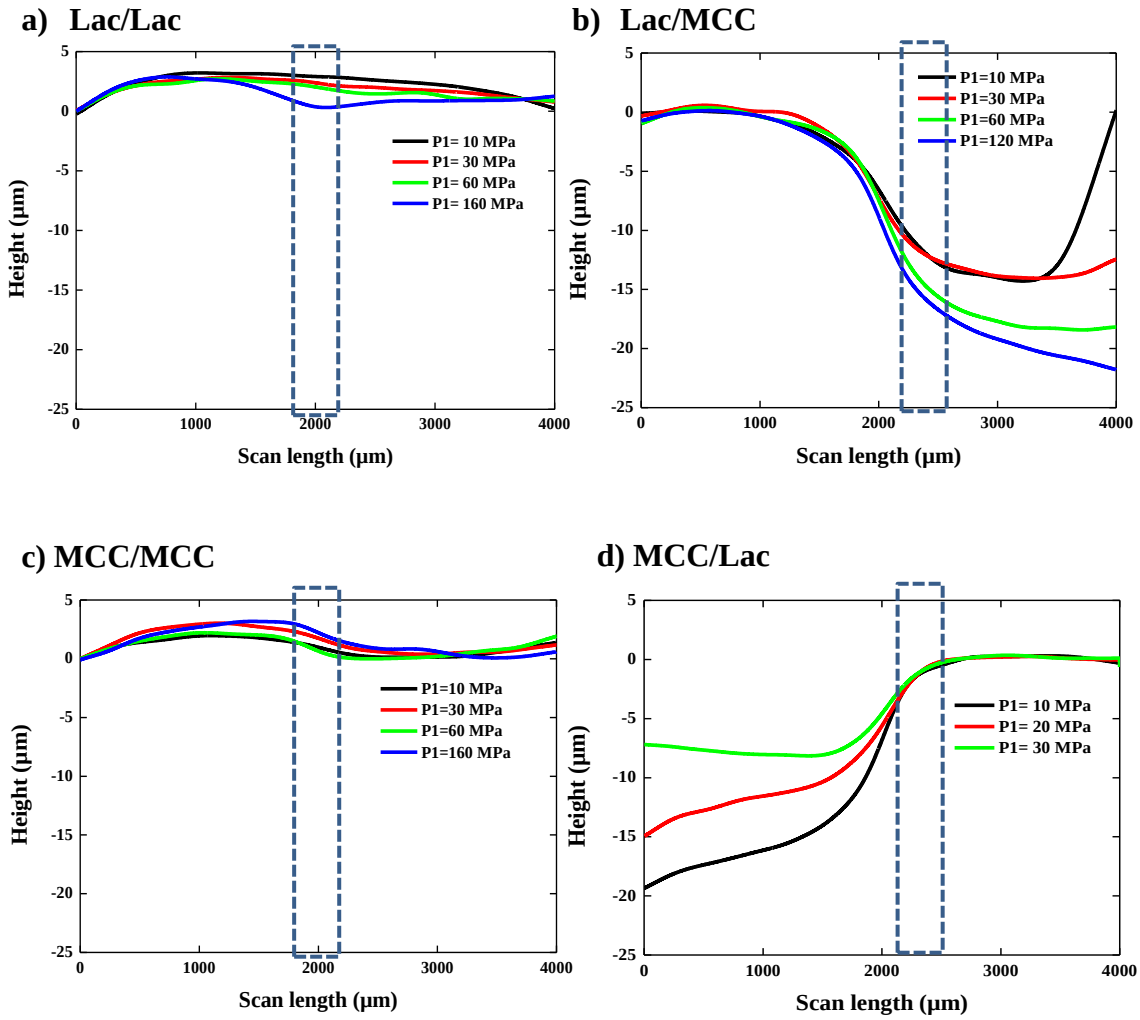

Figure 3.11 Lateral surface profiles of a) Lac/Lac, b) Lac/MCC, c) MCC/MCC and d) MCC/Lac under different P1 and P2 = 200 MPa. The boxes mark expected region of the interfaces.

CHAPTER 4. Interfacial bonding in formulated bilayer tablets

4.1 Synopsis

To take full advantage of the drug delivery advantages offered by bilayer tablets, the common associated issue of weak interfacial bonding strength (IBS) with manufacturing must be overcome. This work seeks to characterize the effect of composition in individual layers and compaction pressure on the IBS. Mixtures of MCC and lactose in different ratios with/without HPMC were used where the first layer was compacted with two different pressures (20 and 100 MPa) followed by a second layer compaction pressure of 200 MPa. After identifying the failure mode as either at the interface or within a layer, the complex trends of bilayer tablet tensile strength as a function of MCC content were explained by considering the interplay between particle bonding strength and bonding area at the interface.

4.2 Introduction

Fixed dose combination (FDC) products are commonly used to treat diseases that require co-administration of two or more drugs to achieve desired clinical outcome.[1,2] FDC products can simultaneously deliver two (or more) drugs in one tablet so that the number of doses can be reduced to considerably alleviate pill burden. The convenience offered by such combination products plays an important role in tackling the problem of medication non-adherence.[3-5] Among the common FDC formulation designs, the bilayer tablet is gaining more attention due to its advantages over the monolithic tablet. For instance, the physical separation of drugs in different layers effectively avoids the problem of chemical stability between two incompatible drugs by minimizing the contact surface area between them. Moreover, a bilayer tablet can be designed to provide both a rapid release layer and a slow release layer and thereby produce the desired overall drug release kinetics for optimal therapeutic outcome.[6-10] However, the successful development of bilayer tablet products must also overcome new challenges in formulation design, manufacturing process, controls and product performance requirements unseen in traditional monolithic tablets. One of the critical issues is the weak interfacial bonding strength (IBS) between adjacent layers, which can lead to cracking or splitting during manufacturing, shipping, storage or other processes. [11,12] Such defective or substandard bilayer tablets lead to lower yield, batch rejection, and sometimes even product recalls.[11,13] Understanding the interfacial bonding mechanism in bilayer tablets is a key to design a formulation strategy and implement process control for successful production of high quality bilayer (or multi-layer) tablets.

The tabletability of monolithic tablets is explained by a bonding area (BA) – bonding strength (BS) interplay model,[14-16] in which the tablet strength is a consequence of the contact area between particles and the intermolecular forces over the contact area.[17,18] This model was also extended to explain IBS in bilayer tablets, [19] based on the fact that the compaction interactions among particles at the interface are fundamentally the same as those in a compacted monolithic tablet. During the manufacturing process, a powder is first compacted, usually at low pressures, to consolidate the powder bed and also make room for the second layer powder before a final compaction pressure is applied to make a bilayer tablet. The ability of particles between the adjacent layers to inter-penetrate affects the development of BA at the interface, and hence IBS. The extent of inter-penetration depends on both material properties and compaction pressures, which affect surface waviness and porosity at the interface. The BS between particles at the interface depends on van der Waal's interactions, solid bridge, and mechanical interlocking, and it can be assessed by the tablet tensile strength extrapolated to zero porosity. [20,21]

As in monolithic tablets, bilayer tablets are composed of active pharmaceutical ingredients (APIs) and excipients, including fillers, disintegrants, flavors, colors, lubricants, glidants, preservatives, and sweeteners. [22,23] These excipients are used to attain certain desired tablet properties and performance, such as mechanical strength and drug dissolution profiles. Since each excipient has unique mechanical properties and compaction behavior, the selection of excipients in a bilayer tablet impact tablet properties, including IBS. Previous research on IBS of bilayer tablets exclusively studied single component in each layer, [24-27] which allows for simple data interpretation but ignores the complexity of bilayer tablets used as products. In this work, the effect of

composition on IBS using multi-component formulations was assessed using the BA-BS interplay model.

4.3 Materials and Methods

4.3.1 Materials

Two common tablet formulation excipients, microcrystalline cellulose (MCC, Pharmacel PH102) and lactose anhydrate (Supertab 24AN) and one polymer, Benecel™ Hydroxypropyl methylcellulose (HPMC, K15M), were used in this work. MCC and lactose were provided by DFE Pharm (Goch, Germany) and HPMC K15M was provided by Ashland (Wilmington, DE).

4.3.2 Experimental Methods

4.3.2.1 Bilayer tablet compaction

Prior to compaction, all powders were mixed with 0.5% (w/w) of magnesium stearate (Mallinckrodt Pharmaceuticals, St. Louis, MO) in a V-shaped blender (Blendmaster, Patterson Kelley, East Stroudsburg, PA) at 25 rpm for 10 min. A typical batch size was 100 g, and the volume of the blender was 1 quart. All final blend were equilibrated in a 32% relative humidity (RH) chamber (over a saturated $MgCl_2$ solution) for at least 3 days before bilayer tablet compaction. Cylindrical and flat-surfaced bilayer tablets (8 mm diameter) were compressed on a Materials Testing Instrument (Zwick- Roell 1485, Ulm,

Germany) following the same procedure described earlier. [26] A powder (~150 mg) was manually added into the die and compressed under a compaction pressure (P1) of 20 MPa or 100 MPa to make the first layer. Another 150 mg of a second powder was then manually poured on top of first layer followed by compression at a compaction pressure (P2) of 200 MPa.

In order to clearly identify the boundary between two layers, each layer was added with some colored tracer particles, as described in a previous publication. [26] Colored MCC and lactose tracer particles were prepared by spraying with a 1% (w/w) methanol solution of food grade dyes, i.e., red for MCC and blue for lactose, and dried until desired color intensity was achieved. The colored tracer powder (1%, w/w) was then added into corresponding untreated powder for tableting. The second layer was always composed of blue colored lactose and uncolored MCC with or without HPMC, and first layer consisted of red colored MCC and uncolored lactose to assist easy delineation of the interface (Figure 4.1). All tablets were ejected out of die by pushing on the second layer downward with the punch. Bilayer tablets were stored at 32% RH for overnight before their tensile strength was measured. Environmental RH was ~50% during compaction and IBS determination. To minimize the impact of RH variation on compaction behavior, care was taken to minimize exposure of the powder to environment and compression was carried out immediately after powder was transferred to the die.

4.1.1.1 Tensile strength measurement

The tensile strength (TS) of bilayer tablets was determined by a tensile test using a texture analyzer (TA-XT2i, Texture Technologies Corp., Scarsdale, NY/Stable Micro Systems, Godalming, Surrey, UK) as described before. [26] In brief, one side of a bilayer tablet was glued onto a SEM stud with super glue (ethyl cyanoacrylate) and the stem of the SEM stud was inserted into the loading holder and secured with a set screw from the side. A stainless steel bar with a leveled surface was fixed onto the base of the texture analyzer with clamps and a proper amount of super glue was dropped on the steel bar. The bilayer tablet was lowered at a speed of 0.01 mm/s until the lower side came in contact with the glue on the steel bar. It was then held at a force of 30 N for 5 ~ 6 min to allow the glue to harden. The holder was then lifted upward at a speed of 0.01 mm/s to apply a tensile stress to the bilayer tablet along the direction perpendicular to the tablet interface until the tablet was broken.

The bilayer tablet TS was calculated as the maximum axial tensile force (*F*) divided by the cross-sectional area of the tablet using Eq. (1).

$$\mathrm{TS} = \frac{F}{\pi r^2} \qquad (1)$$

where r is the average radius of first and second layer, measured using a digital caliper with an accuracy of 0.01 mm.

4.1.1.2 Failure modes

Three types of failure modes were observed after the tensile test. Bilayer tablets can split in either first layer, second layer, or at the interface. When bilayer tablets failed only at

the interface, the measured TS is designated as IBS. If the failure occurred within either layer, the value of IBS of the bilayer tablet was higher than the measured TS.

4.1.1.3 Determination of surface waviness using stylus profilometry

Interfacial surface topography assessment was performed using bilayer tablets split at interface. The surface was profiled by stylus profilometry (KLA-Tencor P-16, Milpitas, CA) as described previously. [19] The stylus traversed normal to the surface of a sample with the contact force of 1 mg (9.81 μN) to detect the asperities. The sample scan size was ~7500 μm to cover the diameter of a tablet as wide as possible. The scan speed was set at 50 μm/s at a sampling rate of 200 Hz, approximately 30,000 data points were collected in total. The vertical range was set at 327 μm for adequate z-direction movement of the stylus. The scans were triplicated on the interface for the determination of surface profiles.

The surface topography consists of roughness and waviness components, which are separated by a cutoff wavelength. The profiles featuring longer wavelengths than the cutoff are referred to as surface waviness and shorter wavelengths as surface roughness. In this work, the cutoff wavelength at 80 μm was chosen, which is comparable to the mean size of the particles. Consequently, surface waviness data is more relevant for assessing BA at the interface of a bilayer tablet. Surface waviness was calculated as the summation of absolute deviations from a mean plane fit over the surface. Surface waviness parameters (W_a) is defined in Eq. (2).

$$W_a = \frac{1}{L}\int_0^L |Z(x)|\, dx \qquad (2)$$

where L is sample scan length, and Z(x) is the vertical deflection of the sample at the position of x along the line of scan.

4.1.1.4 Bonding strength determination

Each mixture (∼200 mg) of MCC and lactose, with or without HPMC, was loaded into an 8 mm round die and compressed using flat faced punches on a Zwick Materials Testing Machine (Model 1485; Zwick-Roell, Ulm, Germany) at the pressures of 25, 50, 100, 150, 200, 250, 300, and 350 MPa at the punch velocity of 5 mm/min without holding at the peak pressure. Three tablets were made at each compaction pressure and relaxed in 52% RH overnight. The binary mixtures of MCC and lactose in different ratios cover a wide range of material properties varying between soft and ductile MCC and hard and brittle lactose. [28-32]

The tablet diameter (*D*) and thickness (*T*) were measured using a digital caliper with 0.01 mm accuracy, and tablet weight was obtained using an analytical balance with 0.01 mg accuracy. The tablet density (ρ) was calculated from the calculated volume and weight. To avoid measurement errors in *T*, tablet flashing was gently removed. [33] True densities (ρ_t) was obtained using the Sun method from tablet density – compaction pressure data. [34] The tablet porosity (ε) was then calculated using Eq. (3):

$$\varepsilon = 1 - \frac{\rho}{\rho_t} \qquad (3)$$

The breaking force (*F*) was measured by the diametrical compression test using a texture analyzer (TA-XT2i, Texture Technologies Corp., Scarsdale, NY/Stable Micro Systems, Godalming, Surrey, UK) at a testing speed of 0.01 mm/s. The diametrical tensile strength (σ) was calculated with Eq. (4). [35]

$$\sigma = \frac{2F}{\pi DT} \qquad (4)$$

The BS was assessed using σ_0, which was obtained by extrapolating σ to zero porosity from the fitted Ryshkewitch Eq. (5). [18]

$$\sigma = \sigma_0 \, e^{-b\varepsilon} \qquad (5)$$

where b is an empirical constant.

4.4 Results and Discussion

4.4.1 IBS of MCC-Lactose mixtures

4.4.1.1 Effects of percent MCC on IBS

The binary mixtures of MCC and lactose in different ratios exhibit a wide range of mechanical properties, which cover properties of typical immediate release tablet formulations. The TS of bilayer tablets showed a complicated trend with the compositional change at P1 of 20 MPa and P2 of 200 MPa (Figure 4.2a). With increasing amount of MCC, TS initially increased up to 20% MCC, decreased in the range of 20% - 80% MCC, and then rose again above 80% MCC.

Pure lactose bilayer tablets failed in either the first or second layer but never at the interface (Figure 4.2b), suggesting that IBS of these tablets is higher than TS of individual layers. As a brittle material, pure lactose tablet were porous when compressed at 20 MPa. This made the penetration of lactose particles from the second layer into the first layer easier to take place. In other words, the two layers developed a more intimate contact at the interface than a more compressed first layer with a smoother surface under the same P2. With 10% and 20 % MCC, failure still occurred in either first or second layer (Figure 4.2b). Thus, the IBS was higher than the TS of either layer. Although the contributions to IBS was reduced by BA due to reduced W_a (Figure 4.2c), the contribution by larger BS arising from the higher percentage of MCC more than sufficiently compensated the loss in IBS. This explains the increasing TS with increasing MCC content, since MCC exhibits much better tabletability than lactose, and binary mixtures containing more MCC are expected to form stronger tablets under the same P2. [36,37]

However, the TS of bilayer tablets of mixtures containing 30% MCC was lower than that containing 20% MCC. This is accompanied by failure occurring either at the interface or within individual layers (Figure 4.2b), indicating a similarity between IBS and TS of individual layers, due to the interplay between reduced IBS caused by smaller BA and increased TS by higher BS. At MCC content above 30%, all failures occurred at interface (Figure 4.2b). Thus, the measured TS was IBS, which almost linearly decreased with increasing MCC contents (Figure 4.2a). The BS is expected to be higher when MCC is higher in the mixtures. Thus, the decreasing IBS reflected decreasing BA, according to the BA-BS interplay model. This point is supported by the reduced W_a with increasing

MCC content (Figure 4.2c). Therefore, the detrimental effect of lower BA overwhelmed the positive contribution from the higher BS when MCC content increased. The smaller W_a can be caused by both a more shallow curvature and less rugged surface, as it was shown between two bilayer tablets containing 40% and 80% MCC prepared under identical conditions (P1 of 20 MPa and P2 of 200 MPa) (Figure 4.2d). Although 80% MCC mixture has a slightly higher BS (8.56 MPa) than 40% MCC mixture (8.36 MPa) (Figure 4.3), the interface BA is much lower, as shown by the much lower W_a (Figure 4.2c). W_a of bilayer tablets containing 30% or less MCC could not be measured (Figure 4.2c) because tablets did not fail cleanly along the interface.

However, at MCC higher than 80%, the IBS increased again with increasing MCC content (Figure 4.2a). Here, all bilayer tablets failed at the interface (Figure 4.2b). Therefore, the trend must also be explained based on interactions at the interface. As the interface continued to become smoother for these powders (Figure 4.2c), the BA is expected to decrease with increasing MCC content. Thus, the rising trend indicates that the contributions by the higher BS of MCC richer mixtures outweighed their detrimental effects on BA. Therefore, the complex trend s a result of the transition of the dominating factor for TS from BS to BA and then back to BS, accompanied by a change in failure mode from within individual layers to at the interface.

4.1.1.1 Effects of P1 on IBS

The explanation provided above for the complex trend in TS at P1 of 20 MPa can be further examined by changing P1 to a higher value, i.e. 100 MPa. For a given material, a

higher P1 can lead to further consolidation of the first layer resulting in a smoother surface and more resistance to penetration by particles from the second layer. [19,38] Consequently, the IBS should be lower. Since P2 was kept the same, the strength of individual layers should not change significantly. Indeed, the TS of bilayer tablets of all mixtures universally decreased, when P1 was increased from 20 MPa to 100 MPa (Figure 4.2a). The change was the greatest for plastic MCC and least for lactose. However, the failure mode was similar except for 30% MCC (Figure 4.2b), which always failed at the interface. Thus, the TS of individual layers was higher than IBS in this case. Recall, at P1 of 20 MPa, IBS and TS of individual layers were comparable and random failure either at the interface or within individual layers was observed. Therefore, a higher P1 led to a lower IBS for bilayer tablets of this mixture. A striking consequence of the higher P1 was the significantly lower W_a for all bilayer tablets (Figure 4.2c & Figure 4.2d). Under this condition, increasing MCC content only slightly decreased W_a (Figure 4.2c). Thus, the consolidation and surface smoothing of the first layer contributed by the higher P1 were greater than that by the increasing MCC content.

However, there was no observation of second rise on IBS above 80% MCC when P1 was 100 MPa (Figure 4.2a) and all bilayer tablets failed at the interface (Figure 4.2b). That means that the deteriorating effect of lower BA on IBS under P1 of 100 MPa was greater than the increasing BS. Consequently, no rise in IBS is seen. Since bilayer tablets of lactose and mixture containing 80% and 90% lactose did not fail at the interface, the BS still had a dominant role that led to higher IBS than TS of individual layers.

4.4.2 The effect of HPMC on IBS

One important application of the bilayer tablet is to release drugs simultaneously at different rates, for example, sustained release of one drug from one layer but immediate release of another drug from the other layer, such as Mucinex® DM. The most common formulation strategy for achieving sustained release of a drug is the use of HPMC to form a matrix layer, where HPMC forms a thick viscous layer upon contact with an aqueous medium, through which drug slowly diffuses out into the medium.[39] Hence, the effect of MCC/lactose ratio on IBS was also investigated using the second layer containing 40% w/w of HPMC.

In this case, the first layer mimics an immediate release formulation and the second mimics a controlled release formulation. Similar to the bilayer tablets of MCC and lactose binary mixtures at P1 of 100 MPa (Figure 4.2a), the measured TS of HPMC containing bilayer tablets increased up to 12 % of MCC before decreasing with the increasing amount of MCC when P1 was 20 MPa and 100 MPa (Figure 4.4a). A second rise of IBS with the increase of %MCC was absent in the profile. In the mixture of MCC and lactose, the second rise in IBS in MCC rich binary mixtures was attributed to the enhancing effect of BS on IBS, which outweighs the effect due to reduced BA when more MCC is in the mixture. The absence of such a second rise in HPMC containing mixtures suggests that the BS was not increased sufficiently to offset the negative effect on IBS due to lower BA caused by increased amount of MCC in the mixtures. This is consistent with the fact that HPMC has lower BS than either MCC or lactose, and therefore the BS of the HPMC containing layer did not contribute sufficiently to generate the second rise. The amount of 6% ~ 12% MCC in the first layer made negative

contribution that W_a decreases with MCC (Figure 4.4c), but MCC strengthened TS of layers and BS at the interface. The increase in BS could outweigh the decrease in BA so IBS increases.

From 18% to 60% MCC in the second layer, even though more MCC can enhance BS, W_a decreases more (Figure 4.4c), therefore the effect of BA loss dominates over BS and weaken IBS for both P1 at 20 and 100 MPa. However, when P1 is 20 MPa, the bilayer tablet failed in the second layer or at the interface (Figure 4.4b); instead bilayer tablets failed only at the interface with P1 at 100 MPa. In the surface profile (Figure 4.4d), 24% MCC shows a larger curvature and more rugged surface than 48% MCC when P1 is at 20 MPa or 100 MPa, indicating 24% MCC can have higher W_a than 48% MCC and thus IBS. One interesting observation is that, judging from layer color, the protrusions in the W_a profile (Figure 4.4d) of the split tablet prepared at P1 of 20 MPa originated from the second layer powder. This indicated that IBS, caused by smaller W_a, and TS of individual layers (reduced by the addition of HPMC), was similar. Therefore, no clear interface was obtained. At P1 of 100 MPa, no protrusions were detected, and all bilayer tablets failed at the interface. Therefore, higher P1 led to lower IBS, which became lower than TS of individual layers.

The overall TS with the addition of HPMC in the second layer was weaker than that without HPMC. The reasonable explanation is that HPMC in the mixture greatly lowers BS (Figure 4.5). When comparing at the same ratio of MCC to lactose with and without HPMC, we found out the difference in TS can reach almost 4 MPa, which indicates BS of pure HPMC should be even lower than BS of the mixture with HPMC. The W_a and surface profile of bilayer tablets with HPMC, however, is larger (Figure 4.4c-d) than that

without HPMC (Figure 4.2c-d) for both P1. A higher W_a theoretically should increase the IBS, but it did not happen due to the low BS of HPMC with other materials. The effect of a lower BS caused by HPMC outweighed the higher BA, leading to lower IBS for bilayer tablets with HPMC. Moreover, the TS difference between them is larger than that without HPMC. The possible reason is that the HPMC is relatively soft and more sensitive to compaction pressure. Therefore, at higher P1, TS abruptly decreases to near zero when MCC is only 30%.

4.5 Conclusions

The complex trend in IBS of bilayer tablets prepared with mixtures of MCC and lactose can be understood by considering BA-BS interplay of particles at the interface. The addition of a small amount of MCC to lactose increased the BS at the interface, resulting in a higher IBS. However, when too much MCC was in the mixture, the negative effect on IBS due to reduction of BA of the more plastic mixture outweighed the positive contribution to IBS by higher BS. Consequently, continuous decreased in IBS was observed when MCC amount increased. The effects of BA-BS interplay on IBS depended on P1, where higher P1 aggravated the negative effects of lower BA on IBS, thus changing the dependence of IBS on MCC%. The addition of HPMC weakens BS, thus also shifts the dependence of IBS on MCC%. This work confirmed the usefulness of the BS - BA interplay model in explaining IBS of formulated bilayer tablets.

Figure 4.1 An image of a bilayer tablet (8 mm diameter). The first layer (Bottom layer) consisted of red colored MCC and uncolored lactose, while the second layer (Top layer) was composed of blue colored lactose and uncolored MCC.

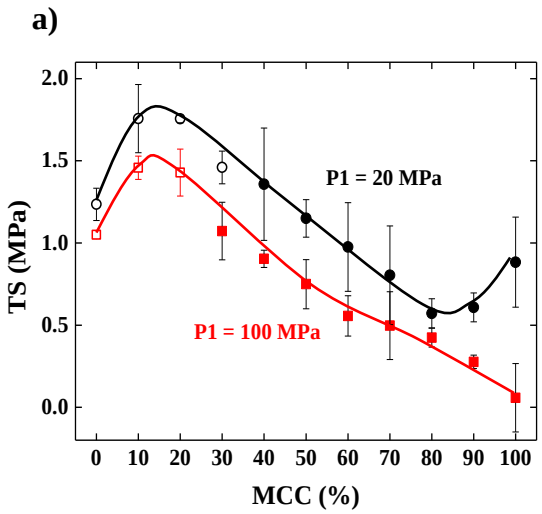

b)

P1	Failure	MCC (%)										
		0	10	20	30	40	50	60	70	80	90	100
20	2nd	2	3	3	-	-	-	-	-	-	-	-
	Interface	-	-	-	2	3	3	3	3	3	3	3
	1st	1	-	-	1	-	-	-	-	-	-	-
100	2nd	-	2	3	-	-	-	-	-	-	-	-
	Interface	-	-	-	3	3	3	3	3	3	3	3
	1st	3	1	-	-	-	-	-	-	-	-	-

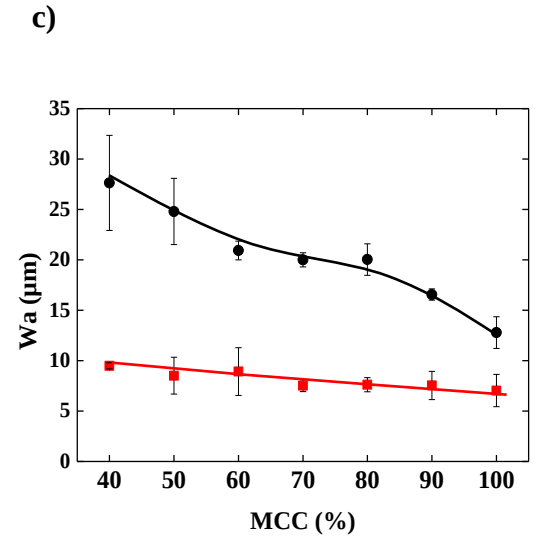

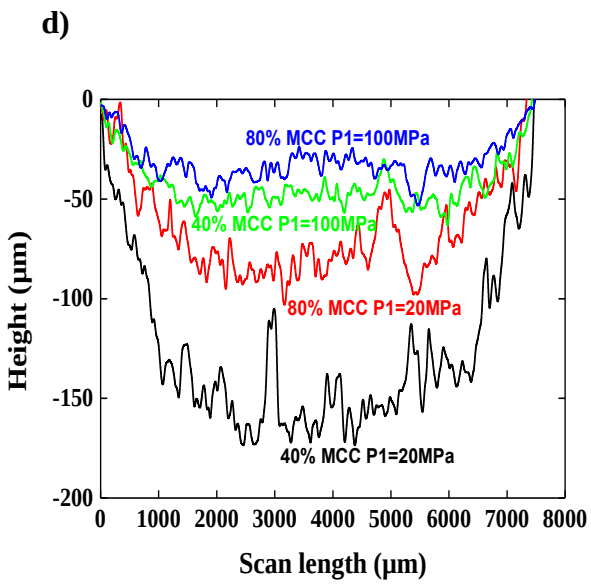

Figure 4.2 a) Tensile strength (TS) of bilayer tablets made with the mixture of MCC and lactose (P1 = 20 or 100 MPa, P2 = 200 MPa). Filled symbol represents bilayer tablets only failed at the interface, otherwise open symbol was used. b) Failure mode of corresponding bilayer tablets. c) Surface waviness (W_a) on the first layer side of interface. d) Surface height profiles of bilayer tablets with 40% and 80% MCC under P1 at 20 MPa or 100 MPa.

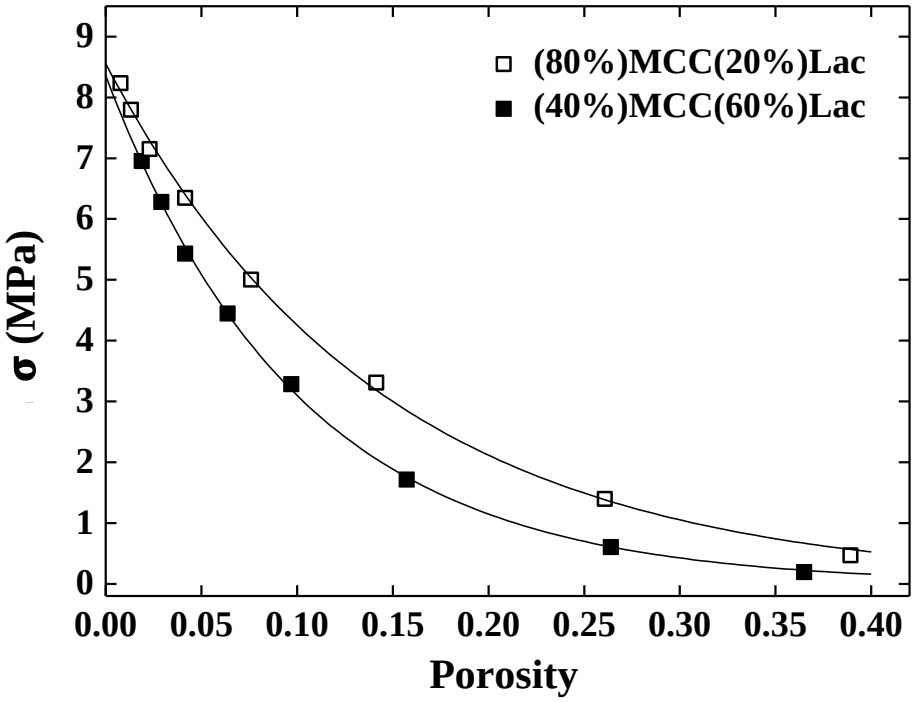

Figure 4.3 Diametrical tensile strength (**σ**) of single layer tablet made from (80%)MCC(20%)Lac and (40%)MCC(60%)Lac as a function of porosity. TS at zero porosity ($\boldsymbol{\sigma}_0$) for (80%)MCC(20%)Lac and (40%)MCC(60%)Lac is 8.56±0.07 and 8.36±0.07 MPa, respectively.

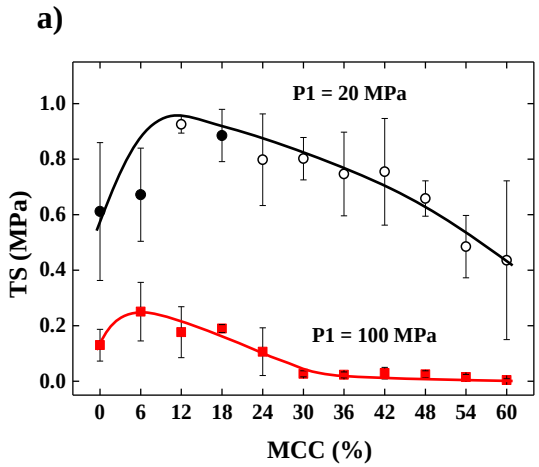

b)

P1	Failure	2nd	MCC(%) 0	6	12	18	24	30	36	42	48	54
		1st	0	10	20	30	40	50	60	70	80	90
		2nd	-	-	2	-	2	2	2	1	1	1
20	Interface		3	3	1	3	1	1	1	2	2	2
		1st	-	-	-	-	-	-	-	-	-	-
		2nd	-	-	-	-	-	-	-	-	-	-
100	Interface		3	3	3	3	3	3	3	3	3	3
		1st	-	-	-	-	-	-	-	-	-	-

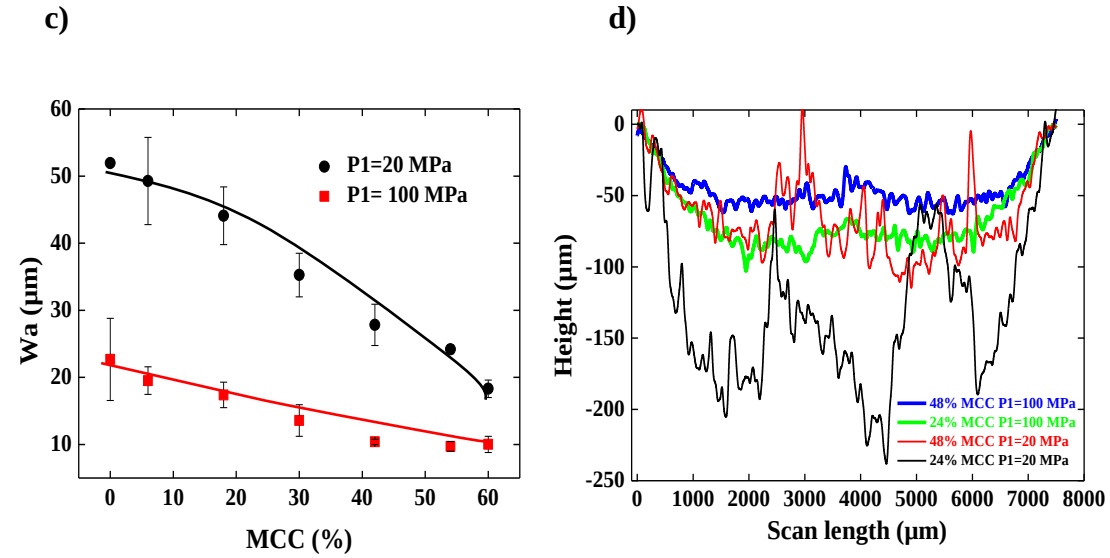

Figure 4.4 a) Tensile strength (TS) of bilayer tablets containing 40% (w/w) HPMC in the second layer, where P1 was 20 or 100 MPa, and P2 was 200 MPa. Filled symbol represents bilayer tablets only failed at the interface, otherwise open symbol was used. b) The failure mode of corresponding bilayer tablets with the number of failed tablets. c) Surface waviness (W_a) on first layer surface of bilayer tablets. d) Surface height profiles at the interface after bilayer tablets were separated at the interface.

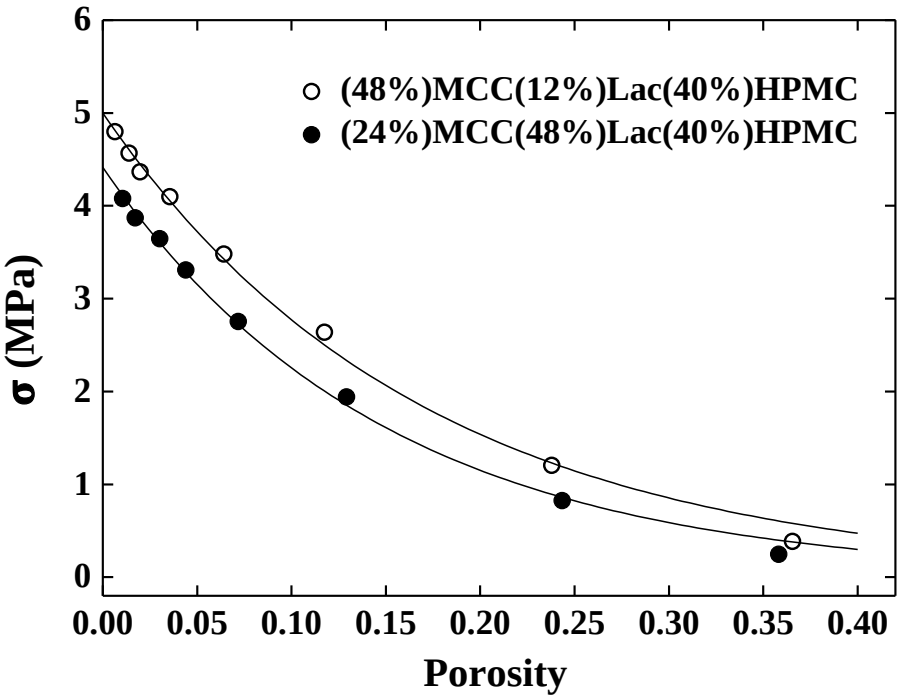

Figure 4.5 Diametrical tensile strength (**σ**) of single layer tablet made from (48%)MCC(12%)Lac(40%)HPMC and (24%)MCC(48%)Lac(40%)HPMC as a function of porosity. TS at zero porosity ($\boldsymbol{\sigma}_0$) for (48%)MCC(12%)Lac(40%)HPMC and (24%)MCC(48%)Lac(40%)HPMC is 4.99±0.06 and 4.41±0.06 MPa, respectively.

CHAPTER 5. The effect of particle size on interfacial bonding strength of bilayer tablets

5.1 Synopsis

The effect of particle size on interfacial bonding strength (IBS) of bilayer tablets was studied using microcrystalline cellulose (MCC) and lactose anhydrate. When MCC is in the first layer, IBS is generally lower and more sensitive to particle size and mechanical properties of the second layer material. In contrast, when lactose is in the first layer, the IBS is higher and less influenced by either of these properties. On the other hand, the use of MCC in the second layer leads to higher IBS than lactose. The dependence of IBS on material and particle size can be explained by bonding area (BA) - bonding strength (BS) interplay. IBS generally increases with increasing BA, which is favored by larger particles in the second layer. However, variations in particle size of the first layer powder did not significantly affect IBS.

5.2 Introduction

The effect of particle size on powder compaction behavior has been extensively studied and relatively well understood [1-6]. In general, smaller particles form stronger tablets than larger particles. The rationale is that a larger surface area is available for bonding between particles resulting in strong compacts as in the case of starch and microcrystalline cellulose (MCC) [7,8]. However, the compaction property of MCC was also reported to be independent of particle [3]. The contradiction in the reported effect of particle size on tablet strength of MCC highlights the need for further examination of particle size effects. The particle size effect can also be influenced by material mechanical properties. While it is commonly accepted that particle size influences tabletability of plastic materials, such an effect is much smaller for brittle materials e.g., dibasic calcium phosphate dihydrate and lactose [7,9,10]. Thus, mechanical properties of the material need to be considered in order to better understand the particle size effect on tablet strength.

Bilayer or multi-layer tablets have been commonly used to either deliver multiple drugs in one dosage for synergistic therapeutic effect or to modify release profile of a drug by controlling its dissolution from different layers through appropriate formulations [11-13]. The influence of both particle size and mechanical properties on tabletability of a material can be explained by the bonding area (BA) and bonding strength (BS) interplay model in monolithic tablets [14-16]. The BABS model was similarly used to explain effects of several parameters on interfacial bonding strength (IBS) of bilayer tablets, since the deformation and bonding of particles at the interface are fundamentally the same as that in the bulk [17,18]. The bilayer tablet is manufactured by first compressing a layer of powder

without ejection, followed by filling and compressing a second layer of powder [19,20]. The mechanical properties of the compressed first layer powder bed, which is distinctively different from the original powder, depend on the compaction conditions during first layer compression. A higher compaction pressure to prepare the first layer limits the extent of particle rearrangement in response to intrusion of particles from the second layer, which is essential for developing large BA to have optimal bonding along the interface of the bilayer tablet [21]. This explains why IBS can significantly decrease with increasing first layer compaction pressure [17].

One of the quality problems associated with bilayer tablets is the cracking or layer splitting along interface due to insufficient IBS [22,23]. There is a need for strategies to improve IBS. Particle size was shown to affect interfacial bonding strength (IBS) of bilayer tablets [24]. However, the discussion surrounding the effect of particle size on IBS is limited. The purpose of this work was to gain a better understanding of the effect of particle size on IBS from the angle of BABS interplay by comparing the results when the same and different materials were used in the two layers.

5.3 Materials and Methods

5.3.1 Materials

Microcrystalline cellulose (MCC, Pharmacel PH102) and lactose anhydrate (Lac, Supertab 24AN) were commonly used excipients for bilayer tablet formulation. Both excipients were received from DFE Pharm (Goch, Germany). Two size fractions o both

MCC and Lac were obtained by sieving. A batch of MCC was sieved using standard sieves to obtain two fractions: <63 µm, (MCC(S)) and 180-250 µm (MCC(L)). For lactose, the sieve fractions were <63 µm (Lac(S)) and 250-350 µm (Lac(L)).

5.3.2 Methods

5.3.2.1 Bilayer Tablet Compaction

Red colored MCC and blue colored lactose tracer particles were prepared in each size fraction for ease of identification of layers and bilayer failure mode as previously described. [25] Each final colored blend was prepared by mixing one gram of the tracer particles, 99 g of corresponding untreated powder, and 0.5 g of magnesium stearate (Mallinckrodt Pharmaceuticals, St. Louis, MO) in a V-shaped blender (Blendmaster, Patterson Kelley, East Stroudsburg, PA) at 25 rpm for 10 min. The uncolored blend was similarly prepared by mixing 100 g of untreated powder with 0.5 gram of magnesium stearate. First layer was always colored, while the second layer was not. All powders were equilibrated in a 32% relative humidity (RH) chamber (over a saturated $MgCl_2$ solution) for at least 3 days before they were used to prepare bilayer tablets. Bilayer tablets are designated as 1^{st} layer/2^{nd} layer, for example, MCC(S)/Lac(L) refers to a bilayer tablet with the first and second layers consisting of MCC(S) and Lac(L), respectively.

Cylindrical flat-faced bilayer tablets, 8 mm in diameter, were prepared using a Materials Testing Machine (Zwick- Roell 1485, Ulm, Germany). [25] Both first and second layer weight was ~150 mg. The first layer compaction pressure (P1) was 20 MPa, and the

second layer compaction pressure (P2) was 200 MPa. All bilayer tablets were ejected out of die by pushing from the second layer side with the punch. Bilayer tablets were then stored at 32% RH for overnight before they were tested for IBS.

5.3.2.2 Tensile strength measurement

Axial tensile strength (TS) of bilayer tablets was measured using a texture analyzer (TA-XT2i, Texture Technologies Corp., Scarsdale, NY/Stable Micro Systems, Godalming, Surrey, UK) as detailed previously. [25] In brief, one surface of a bilayer tablet was attached onto a SEM stud with super glue (ethyl cyanoacrylate), and the stem of the SEM stud was fixed in the loading holder. A stainless steel bar with a leveled surface was fixed onto the base of the texture analyzer with clamps, and super glue was dropped on the steel bar. The bilayer tablet was lowered at a speed of 0.01 mm/s, until the lower side came in contact with the glue on the steel bar. It was then held at a force of 30 N for 6 min to allow the glue to harden. The holder was then raised at a speed of 0.01 mm/s to apply a tensile stress along a direction perpendicular to the interface until the bilayer tablet broke. When bilayer tablets separated at the interface, the TS equals the IBS. Otherwise, if failure occurred within either the first or second layer, the TS must be lower than IBS.

The TS is the maximum axial tensile force (*F*) divided by the cross-sectional area of the tablet given by Eqn. (1).

$$\mathrm{TS} = \frac{F}{\pi r^2} \qquad (1)$$

where *r* is the average radius of first and second layer.

5.3.2.3 Assessing bonding area using surface waviness

To characterize the interface, interfacial topography was measured using stylus profilometry (KLA-Tencor P-16, Milpitas, CA). [17] A limitation of this approach was that the interface could not be probed, if failure was not along the surface. During the surface profiling, the stylus traversed along the surface with the contact force of 1 mg (9.81 µN). The scan length was ~7500 µm, and the scan speed was 50 µm/s with a sampling rate of 200 Hz. Approximately 30,000 data points were collected for each scan. The largest vertical range of 327 µm was chosen. The scans were performed in triplicate on the same interface at three different directions differing by a 60^o angle.

The surface profile consists of roughness and waviness components, which are separated by an arbitrary cutoff wavelength. The component at wavelengths longer than the cutoff value is referred as surface waviness. and the component at shorter wavelength is referred as surface roughness. In this work, the cutoff wavelength of 80 µm was chosen. To assess BA at the interface, surface waviness (W_a) is calculated as the summation of absolute deviations from a mean line along the surface, using Eqn. (2).

$$W_a = \frac{1}{L}\int_0^L |Z(\mathrm{x})|\,\mathrm{dx} \qquad (2)$$

where L is sample scan length and Z(x) is the vertical deflection of the sample at the position of x along the scan path.

5.3.2.4 Bonding strength assessment

For each powder, tablets were made using the 8 mm round die and flat faced punches on a Zwick Materials Testing Machine (Model 1485; Zwick-Roell, Ulm, Germany) at compaction pressures of 25, 50, 100, 150, 200, 250, 300 and 350 MPa. Punch velocity was 5 mm/min. Punch withdrew without holding once the target pressure was achieved. Tablets were triplicated at each compaction pressure and were stored in 32% RH overnight to allow relaxation.

The diameter (*D*) and thickness (*T*) were measured using a digital caliper (0.01 mm accuracy). To obtain accurate thickness, both tablet surfaces were gently polished to remove the flashing.[26] Tablet weight (*W*) was determined using an analytical balance (0.01 mg accuracy). Tablet density (ρ) - compaction pressure data were used to obtain true density (ρ_t) and a plasticity (1/*C*) by model fitting using the Sun method. [27] The porosity (ε) of tablets was calculated using Eqn. (3):

$$\varepsilon = 1 - \frac{\rho}{\rho t} \qquad (3)$$

Diametrical breaking force (*F*) of each tablet was then measured using a texture analyzer (TA-XT2i, Texture Technologies Corp., NY) at a testing speed of 0.01 mm/s. Tensile strength (σ) was calculated according to Eqn. (4). [28]

$$\sigma = \frac{2F}{\pi DT} \qquad (4)$$

σ - ε data were fitted using the Ryshkewitch Eqn. (5). [29]

$$\sigma = \sigma_0 \, e^{-b\varepsilon} \qquad (5)$$

where σ_0 is the σ extrapolated to zero porosity and b is an empirical constant.

5.4 Results

5.4.1 Effects of second layer material

5.4.1.1 MCC in first layer

When the first layer consisted of MCC(S), the TS of varying second layer materials followed the descending order of MCC(S) > MCC(L) > Lac(L) > Lac(S) (Table 5. 1). Since all bilayer tablets failed at the interface (Table 5. 1), the IBS followed the same order as TS. Larger MCC particles in the second layer had a lower TS, but larger Lac particles in the second layer had a higher TS.

When the first layer consisted of MCC(L), the rank order of TS was MCC(S) ≈ MCC(L) > Lac(L) > Lac(S) (Table 5. 1), which is similar to the case of MCC(S) in the first layer. The TS of MCC(L)/Lac(S) tablets was zero, because all bilayer tablets delaminated upon ejection out of die. Particle size of MCC in the second layer did not affect TS, but larger sized lactose had a higher TS. In this series, two of the MCC(L)/Lac(L) tablets failed in the Lac(L) layer, and one along the interface. Thus, IBS of MCC(L)/Lac(L) tablets is comparable to the TS of the Lac(L) layer. Therefore, with MCC(S) and MCC(L) in the first layer material, both material type and particle size of materials in the second layer influenced TS. In both cases, MCC(S) and MCC(L) in the second layer had a significantly higher TS than Lac(S) and Lac(L).

5.4.1.2 Lac in first layer

When the first layer consisted of Lac(S), the TS followed the order of MCC(L) >> Lac(S) ≈ MCC(S) ≈ Lac(L) (Table 5. 1). Lac(S)/MCC(L) always failed along the interface, while failures in the Lac layer were observed in other cases (Table 5. 1). Thus in this set, TS of Lac(S)/MCC(L) bilayer tablet is the highest, but it is unknown how its IBS compares to that in other bilayer tablets. The size of Lac in the second layer did not affect TS, which is aligned with the similar tensile (σ) of Lac(S) and Lac(L) at 200 MPa as well as other pressure studied (Figure 5.1). This explains why TS of Lac(S)/MCC(S) is close to that of Lac(S)/Lac(S), since failure occurred in the Lac(S) layer in both cases. Both are also similar to TS of Lac(S)/Lac(L), which failed in the Lac(L) layer.

When the first layer consisted of Lac(L), the TS followed the order of MCC(S) >MCC(L) ≈ Lac(S) ≈ Lac(L) (Table 5. 1). When the second layer was MCC(S) and MCC(L), all tablets failed at the interface, except one Lac(L)/MCC(S) tablet that failed in the Lac(L) layer (Table 5. 1), which indicates IBS is comparable to that of TS of the Lac(L) layer. However, when the second layer was Lac(S) and Lac(L), all tablets failed in the second layer. Smaller sized MCC in the second layer corresponded to higher TS. The particle size of Lac in the second layer did not affected TS, which is the same as the case where the first layer consisted of Lac(S). Finally, bilayer tablets with Lac in the second layer generally exhibited higher TS than those with MCC in the first layer (Table 5. 1).

5.4.2 Effect of first layer material

5.4.2.1 MCC in second layer

When the second layer consisted of MCC(S) but first layer material varied among the four powders, TS followed the order of Lac(L) > MCC(S) ≈ MCC(L) ≈ Lac(S) (Table 5. 1). Both MCC(S)/MCC(S) and MCC(L)/MCC(S) failed at the interface and variations in particle size of MCC in the first layer had no obvious effect on IBS. With Lac(S) and Lac(L) in first layer, bilayer tablets could fail either along the interface or in Lac layer, indicating IBS is similar to σ of the lactose layers. When the second layer consisted of MCC(L) while the first layer material varied, TS followed the order of Lac(S) > Lac(L) ≈ MCC(L) > MCC(S) (Table 5. 1). All tablets failed at the interface (Table 5. 1). larger MCC in the first layer corresponded to higher TS. However, larger Lac in the first layer led to lower TS.

5.4.2.2 Lac in second layer

When the second layer was comprised of Lac(S) while first layer materials varied, the order of TS followed Lac(S) ≈ Lac(L) >> MCC(S) > MCC(L) (Table 5. 1). With MCC(S) and MCC(L) in the first layer, all bilayer tablets failed at the interface (Table 5. 1). MCC(L)/Lac(S) delaminated upon ejection out of the die. Bilayer tablets with Lac(S) and Lac(L) in the first layer only failed in the second Lac(S) layer (Table 5. 1). Larger MCC in the first layer corresponded to lower TS. However, particle size of Lac in the first layer had no significant effect on TS.

When the second layer consisted of Lac(L), the order of TS with varying first layer material was Lac(S) ≈ Lac(L) > MCC(S) > MCC(L) (Table 5. 1), similar to the earlier case of Lac(S) in the second layer. When MCC(S) was in the first layer, all bilayer tablets failed at the interface (Table 5. 1). When MCC(L) was in the first layer, two tablets failed in the Lac(L) layer and one failed at the interface. When Lac(S) and Lac(L) was in the first layer, bilayer tablets always failed in the second Lac(L) layer. Consequently, TS is expected to be independent of particle size of lactose in the first layer. Compared to MCC(S) and MCC(L) in the second layer, TS of Lac(S) and Lac(L) in the second layer was more sensitive to materials in the first layer.

5.5 Discussion

5.5.1 Role of BABS interplay on IBS

In order to apply the BABS interplay model to explain the observed effect of particle size on IBS, [14-16,30] values of BA and BS are needed. Since these may not be directly measured, BA and BS are indirectly assessed by surface waviness (W_a) and tensile strength at zero porosity (σ_0), respectively.[29] The assumption is that a larger W_a corresponds to larger BA, while higher σ_0 corresponds to higher BS. When different materials are used in the adjacent layers, the BS at the interface is approximated by the geometric average of BS of the two materials.

TS positively correlates with W_a, ranging from 5 to 30 μm (Figure 5.2). This suggests that BA plays a significant role on IBS. The extent of radial expansion for both MCC (0.25%) and Lac (0.75%) were both small (Table 5. 2) but can be considered for a more

accurate comparison. The BA is affected by particle size and mechanical properties of materials, e.g., plasticity. The plasticity of both MCC and lactose was independent of particle size but smaller MCC was more plastic than larger MCC ($p < 0.05$) (Table 5. 2 and Figure 5.3a). The plasticity of MCC is significantly lower than that of Lac, as shown by the difference in the plasticity parameter, 1/C, of MCC ($p < 0.05$) (Table 5. 2). This confirms the plastic nature of MCC. [31-35] Therefore, MCC should have more facile plastic deformation than lactose, regardless of particle size. Bilayer tablets with lactose as the first layer had larger W_a (Figure 5.2), which is consistent with the lower plasticity of Lac. Based on σ_0, BS of MCC(S) is the highest, followed by MCC(L), Lac(S), and then Lac(L) (Table 5. 2). The BS of MCC depends on particle size but that of lactose does not (Figure 5.3b), which is consistent with the high tendency of lactose to undergo fragmentation during compression while MCC does not.

In addition to BA and BS, differential radial expansion between two layers can induce shear stress along the interface, which is expected to weaken IBS. The radial expansion in the Lac layer is higher than that of MCC (Table 5. 2). The radial expansion depends on the material but was independent of particle size.

5.5.2 Size effect with MCC in first layer

When MCC is in the first layer, except for MCC(L)/Lac(S) with a W_a of 5 μm, W_a spreads in a narrow range of 12 - 20 μm (Figure 5.2). When MCC(S) is in the first layer while the second layer material varies, W_a follows the order of Lac(L) > Lac(S) ≈ MCC(S)> MCC(L) (Figure 5.2). This order does not match that of IBS (Table 5. 1).

Among the four second layer materials tested, BS followed the order of MCC(S) > MCC(L) ≈ Lac(S) ≈ Lac(L) (Table 5. 2). Thus, the highest IBS of MCC(S)/MCC(S) in this series is attributed to its highest BS, which outweights its smaller BA than Lac(L). In comparison to MCC(S)/Lac(L), MCC(S)/MCC(S) also does not suffer the deleterious effect of differential radial expansion between MCC and Lac layers. The lower IBS of MCC(S)/MCC(L) is due to its lower BS and BA than MCC(S)/MCC(S). The IBS of MCC(S)/Lac(S) was the lowest due to both lower BS and different radial expansion between layers. MCC(S)/Lac(L) had higher IBS than MCC(S)/Lac(S) because of its larger BA (Figure 5.1).

When the MCC(L) consists of the first layer and the second layer material varies, both IBS and BA roughly followed the order of MCC(L) > MCC(S) > Lac(S) (Figure 5.2). Although BS of MCC(S) was higher than MCC(L) (Table 5. 2), the positive effect of larger BA on IBS for MCC(L)/MCC(L) lessened the negative effect of BS. Consequently, IBS of MCC(L)/MCC(L) is similar to MCC(L)/MCC(S). MCC(L)/Lac(S) showed zero IBS because bilayer tablets delaminated upon ejection, which is consistent with the unfavorable combined effects of very low BA, lower BS, and differential radial expansion between the layers.

5.5.3 Size effect with lactose in first layer

When Lac(S) is in the first layer, only Lac(S)/MCC(L) fails along the interface (Table 5. 1), which exhibits both the highest W_a and the highest IBS in this work. Therefore, the positive effect of larger BA on IBS outweighed the negative effect due to the differential

radial expansion between Lac and MCC layers. When Lac(L) is in the first layer, Lac(L)/MCC(L) shows a slightly higher W_a than Lac(L)/MCC(S) (Figure 5.2), suggesting larger MCC in the second layer favors IBS by increasing BA. However, the positive effect of larger BA on IBS of Lac(L)/MCC(L) was outweighed by the positive effect of higher BS on IBS in Lac(L)/MCC(S). Consequently, IBS is higher for Lac(L)/MCC(S) (Table 5. 1).

In general, larger particles in the second layer tend to cause larger W_a, regardless it is MCC or lactose.

5.5.4 Size effect with MCC in second layer

When the the second layer consists of MCC(S) and first layer material is allowed to vary, both IBS and W_a follow the descending order of Lac(L) > MCC(S) > MCC(L) (Figure 5.2). The IBS of Lac(L)/MCC(S) is the highest, despite that it suffers from both the differential radial expansion between the two layers (Table 5. 2) and lower BS than MCC(S)/ MCC(S) (Table 5. 2). Thus, the larger BA dominates the BABS interplay to result in a higher IBS. The slightly higher IBS of MCC(S)/MCC(S) than MCC(L)/MCC(S) is attributed to the positive effects of larger BA and higher BS in MCC(S)/MCC(S), since differential layer expansion is not an factor in either tablets.

When MCC(L) is in the second layer and the first layer material is allowed to vary, IBS follows the order of Lac(S) > Lac(L) ≈ MCC(L) > MCC(S) (Table 5. 1). This rank order roughly follows that of W_a (Figure 5.2). Thus, the higher IBS of Lac(S)/MCC(L) and Lac(L)/MCC(L) is attributed to their larger BA , which outweights negative effects by the

different radial expansion and lower BS (Table 5. 2). The particle size effect of second layer material on IBS in this case is material dependent, where smaller Lac or larger MCC lead to larger BA and higher IBS.

5.5.5 Size effect with lactose in second layer

When Lac(S) is in the second layer, MCC(S)/Lac(S) had higher IBS than MCC(L)/Lac(S) (Table 5. 1). Given the same different radial expansion, higher IBS is attributed to the higher BA (Figure 5.2) and higher BS of MCC(S)/Lac(S) (Table 5. 2). With MCC(L) in the first layer, bilayer tablet delamination upon ejection indicates very low BA. While Lac(L) is in the second layer, only MCC(S)/Lac(L) fails along the interface (Table 5. 1). Hence, relative contributions to IBS by BA cannot be compared.

5.5.6 Effects of layer sequence

For each pair of material, the layer sequence is also important to the IBS of bilayer tablets. [17] This is confirmed in this study, where the IBS follows the order of MCC(S)/Lac(L) < Lac(L)/MCC(S) and MCC(L)/Lac(S) < Lac(S)/MCC(L) (Table 5. 1). Since a simple change in layer sequence does not change BS and radial expansion, the change in IBS is attributed to a change in BA. Generally, when a more plastic material is used in the first layer, BA is smaller because of their higher compressibility leading to a more consolidated powder bed that is more resistant to penetration by particles in the second layer. This is supported by the observation that Lac/MCC tablets generally exhibited higher TS than those of MCC/Lac regardless of size (Table 5. 1).

5.6 Conclusions

Particle size can profoundly influence IBS of bilayer tablets but the effect is material dependent. For a given material in one layer, variations of material (size or type) in the other layer affect IBS. Size reduction can lead to either higher or lower IBS, which is in contrast to its general effect to improve tablet tensile strength. Material plasticity plays a prominent role in the development of IBS by affecting BA. When the first layer material is brittle lactose, regardless of particle size, IBS is less sensitive to variations in the second layer material. In contrast, when the fist layer consists of plastic MCC, IBS is sensitive to the second layer composition. However, when the second layer is MCC, high IBS is preserved despite change of particle size and material in the first layer. The BABS interplay model, assessed by Wa and σ_0, facilitates a better understanding of the effect of particle size on IBS of bilayer tablets. IBS generally increases with increasing BA, which is attained by larger particles in the second layer. Variation in particle size of the first layer materials does not significantly affect BA.

Table 5. 1 Mean tensile strength (TS) of 16 combinations of bilayer tablets made of MCC(S), MCC(L), Lac(S) and Lac(L) with standard deviation given in parenthesis. Tablets failed along the interface are marked with *.

1st layer / 2nd layer	MCC(S)	MCC(L)	Lac(S)	Lac(L)
MCC(S)	0.82 (0.12)*	0.70 (0.23)*	0.73 (0.03)	1.02 (0.15)
MCC(L)	0.57 (0.10)*	0.79 (0.23)*	1.25 (0.15)*	0.87 (0.12)*
Lac(S)	0.20 (0.02)*	0.00*	0.80 (0.13)	0.73 (0.24)
Lac(L)	0.38 (0.09)*	0.27 (0.14)	0.65 (0.09)	0.77 (0.07)

Table 5. 2 Tensile strength at zero porosity (σ0), plasticity (1/C), true density (ρ_t) and tablet radial expansion of MCC(S), MCC(L), Lac(S) and Lac(L). Standard deviation is shown in parenthesis

Materials	**MCC(S)**	**MCC(L)**	**Lac(S)**	**Lac(L)**
σ_0 **(MPa)**	9.63(0.14)	8.45(0.05)	8.41(0.52)	8.53(0.67)
1/*C* (MPa)	107.5(13.7)	84.1(8.6)	377.2(58.2)	372.4(62.1)
ρ_t **(g/cm^3)**	1.43(0.004)	1.43(0.001)	1.45(0.01)	1.45(0.01)
Radial expansion (%)	0.23(0.04)	0.22(0.05)	0.67(0.06)	0.63(0.03)

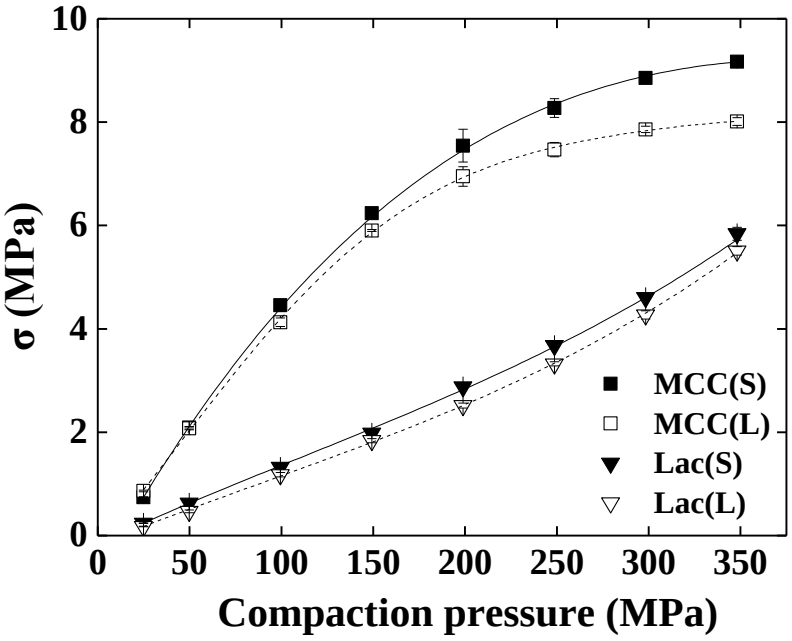

Figure 5.1 Tabletability of MCC(S), MCC(L), Lac(S) and Lac(L).

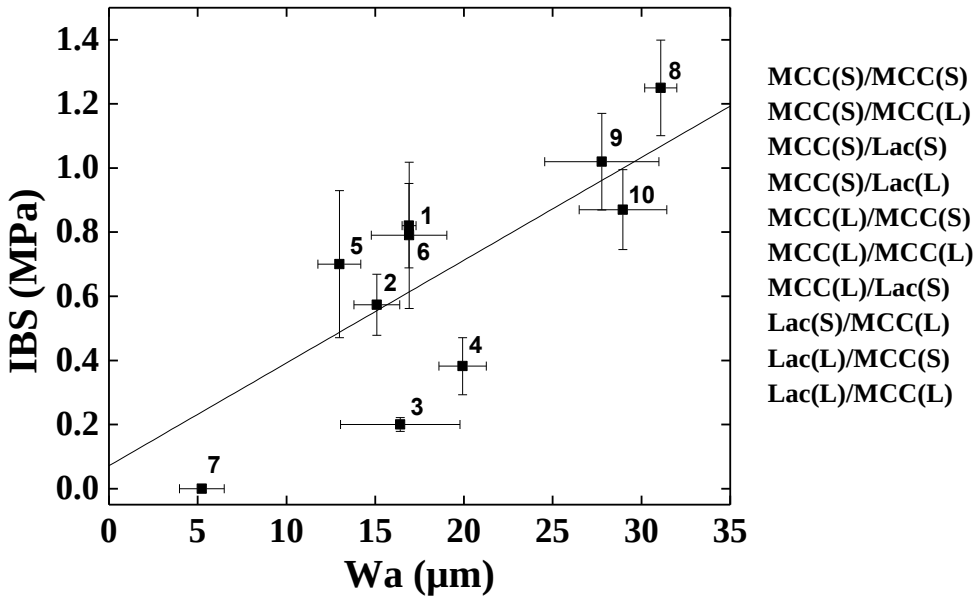

Figure 5.2 Correlation between interfacial bonding strength (IBS) and surface waviness (W_a) on the first layer after separation of two layers.

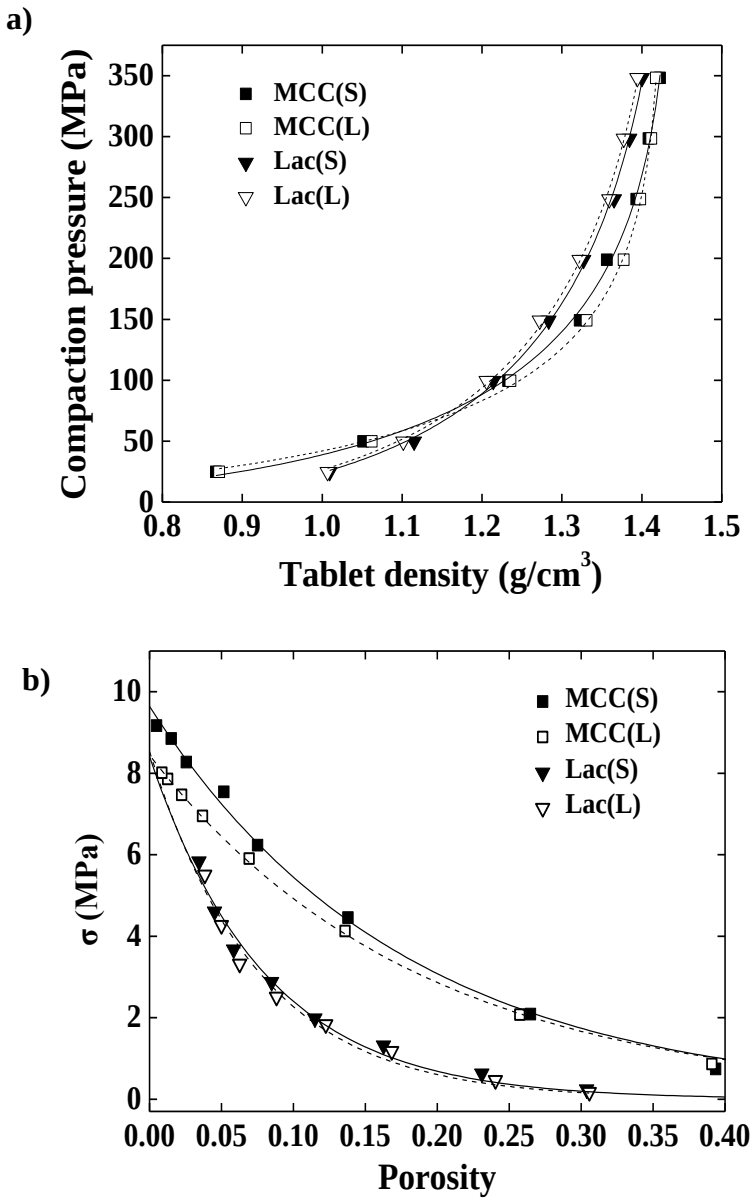

Figure 5.3 a) Fitting of compaction pressure tablet density data to obtain true density and plasticity parameter, 1/C, and b) Compactibility of MCC(S), MCC(L), Lac(S), and Lac(L).

CHAPTER 6. Minimum interfacial bonding strength for bilayer tablets determined using a survival test

6.1 Synopsis

A critical quality attribute of bilayer tablets, Interfacial Bonding Strength (IBS), can be experimentally measured by several methods. Presently, the IBS alone cannot stand to judge the ability of bilayer tablets to sustain the stresses experienced during the manufacturing, transportation, and handling processes. A survival test using tablet friabilator was developed, where bilayer tablets were repeatedly dropped at a fixed height and integrity of the interface was periodically examined. The number of tablets that survived the stress test was plotted as a function of the number of drops to obtain a survival plot. Using the survival test, the minimum IBS (IBS_m) for bilayer tablets to be free from defects, such as layer cracking or lamination, was determined for a number of single component powders and blends. Results suggest that IBS_m depends on both layer composition and tablet size. When bilayer tablets were made with more brittle materials or larger tablet sizes, a higher IBS_m was required to pass the survival test. On the other hand, when the polymer, HPMC, was added, a lower IBS_m was sufficient to pass the survival test. Considering all the compositions and tablet sizes studied in this work, an IBS_m of 0.26 MPa is recommended as a tentative criterion for bilayer tablets of most materials to avoid quality issues arising from inadequate IBS.

6.2 Introduction

The bilayer tablet is an important dosage form for drug delivery, especially when two chemically incompatible drugs are delivered in one dose. The separation of drugs in different layers effectively reduces their direct contact and thereby minimizes unwanted chemical interactions between them.[1] The modified drug release achievable by bilayer tablets, such as the combination of immediate release from one layer and prolonged release from the other layer, can provide a distinct therapeutic advantage. [2,3] However, the development of bilayer tablets still faces challenges in formulation and manufacturing. One of the critical issues is weak interfacial bonding strength (IBS). A bilayer tablet with low IBS can crack or even split at the interface, which results in problems with product quality and therapeutic effectiveness. [4,5]

Previous research on the bilayer tablet has focused on exploring 1) factors that can affect IBS, such as compaction pressure and material properties, [6] punch curvature, [7,8] and particle size, [9] 2) test methods to determine IBS, such as tensile test, [10-13] shear test, [14] diametrical compression test, [15-18] three point bending test, [19-22] wedging test, [8,23] and 3) comparison of different methods. [24,25] However, in absence of an acceptance criterion, a specified value of the IBS is insufficient for judging whether or not a bilayer tablet can be sustained during the downstream manufacturing processes, such as handling, coating, packaging, and shipping. For monolithic tablets, 2 MPa has been used as an acceptance criterion for tablet tensile strength, above which tablets are deemed sufficient to maintain tablet integrity. [26] Such a criterion was supported by the observations that tablets with tensile strength $\geq$ 2 MPa can pass the friability test for materials that are not too brittle. [27-30] With this simple acceptance criterion in place, one can determine whether or not each

proposed formulation exhibits adequate tabletability using a small amount of powder. This is essential for material-sparing tablet formulation selection and optimization in an early stage of drug development, where APIs are usually not available in a sufficient quantity to prepare a batch of tablets for the friability test, which requires 6.5 g of tablets under each set of compaction parameters. [27] Similarly, the identification of a criterion for IBS is useful to guide bilayer tablet development. Generally, a higher IBS should correspond to a lower tendency to layer splitting. When a criterion for minimum IBS (IBS_m) is established, the material- and time-consuming friability test could be avoided during the course of bilayer formulation and process development.

The goal of this research was to examine effects of layer composition and tablet size on IBS_m, for the purpose of guiding efficient formulation and process development for the optimization of bilayer tablets.

6.3 Materials and Methods

6.3.1 Materials

Microcrystalline cellulose (MCC, Pharmacel® PH102) and lactose anhydrate (Supertab® 24AN) were received from DFE Pharm (Goch, Germany), and Hydroxypropyl methylcellulose (HPMC, K15M, Benecel™) was received from Ashland (Wilmington, DE). MCC, lactose, and HPMC are known to exhibit plastic, brittle, and viscoelastic deformation behavior, respectively. [30-35]

6.3.2 Experimental Methods

6.3.2.1 Bilayer Tablet Compaction

Bilayer tablets were prepared using a Materials Testing Machine (Zwick-Roell 1485, Ulm, Germany) with 6, 8 or 10 mm diameters flat round tooling. When making 8 mm bilayer tablets, the first layer was made by compressing approximately 150 mg of powder at a series of compaction pressures (P1) in increments of 10 MPa. Without ejecting the first layer, 150 mg of a second powder was added to the same die, and a second compaction pressure (P2) was applied to form a bilayer tablet. For 6 mm and 10 mm bilayer tablets, each layer contained 60 mg and 300 mg powder, respectively, to maintain the similar aspect ratio to that of 8 mm bilayer tablets. After compression, the upper punch was used to push the second layer downwards to eject the bilayer tablets out of the die. The bilayer tablet compaction was conducted at ~50% RH, and bilayer tablets were stored at 32% RH overnight before they were tested for IBS measurement and survival test were carried out at 50% RH. To minimize the RH effect, caution was taken to minimize exposure of the powder and bilayer tablets to the environment.

In order to visually identify each layer, red MCC and blue lactose tracer particles were prepared following a published procedure. [25] To prepare a batch of mixture, 1 gram of the tracer particles, 99 grams of corresponding untreated powder, and 0.5 gram of magnesium stearate (Mallinckrodt Pharmaceuticals, St. Louis, MO) were mixed in a V-shaped blender (Blendmaster, Patterson Kelley, East Stroudsburg, PA) at 25 rpm for 10 min. All samples were equilibrated in a 32% relative humidity (RH) chamber (over a

saturated $MgCl_2$ solution) for at least 3 days before they were used to prepare bilayer tablets.

When bilayer tablets were made with a single component in each layer, the second layer was always colored, but first layer was uncolored. For layers of binary or ternary blends, the first layer contained red-colored MCC tracer particles, and the second layer contained blue-colored lactose tracer particles.

6.3.2.2 Interfacial bonding strength measurement

The IBS of bilayer tablets was measured using a published tensile test. [25] [25] In this method, one flat surface of a bilayer tablet was fixed with super glue (ethyl cyanoacrylate) onto a SEM stud. The stem of the SEM stud was then inserted into the upper loading holder of texture analyzer (TA-XT2i, Texture Technologies Corp., Scarsdale, NY/Stable Micro Systems, Godalming, Surrey, UK) and fixed in position using a set screw. A rectangular stainless steel bar was fixed onto the platform of the texture analyzer and super glue was dropped onto the steel bar. The bilayer tablet was lowered at a speed of 0.01 mm/s until the bilayer tablet came in contact with the glue and then was held under a contact force of 30 N for 5 ~ 6 min to allow the glue to harden. In this configuration, the interface of the tablet was approximately parallel to the base. The holder was then lifted upward at a speed of 0.01 mm/s to apply a tensile stress to the bilayer tablet along the direction perpendicular to the tablet interface until the tablet was broken.

The tensile strength (TS) was calculated as the maximum axial tensile force (F) divided by the cross-sectional area of the tablet using Eqn. (1). When bilayer tablets failed at the

interface, TS is the same as IBS. Otherwise, TS < IBS, when the bilayer tablet failed in either layers.

$$\mathrm{TS} = \frac{F}{\pi r^2} \qquad (1)$$

where *r* is the average radius of first and second layer, measured by digital calipers with 0.01 mm accuracy.

6.3.2.3 Survival test

Five identically prepared bilayer tablets (composition, size, P1, and P2) were coded for performing the survival test. For a given layer composition, bilayer tablets were made under different P1 but the same P2 to obtain different IBS. [36] A total of 20 bilayer tablets (4 sets of tablets made under four different sets of conditions) were loaded to the drum of a tablet friabilator (EF-2, Electrolab, Mumbai, India), which was run at 25 rpm for 4 min each time. The number of bilayer tablets free from noticeable defects was recorded after careful visual inspection. This process was repeated for 10 times. The number of intact bilayer tablets against number of drops yielded a survival plot.

The IBS_m could be determined from upper and lower limit of IBS. When all five bilayer tablets of each set survived, the corresponding IBS was deemed sufficient to avoid layer cracking or splitting, i.e., IBS > IBS_m. When any of the five tablets failed, the corresponding IBS was considered insufficient for avoiding the generation of interfacial defects during handling and storage, i.e., IBS < IBS_m. The window where IBS_m resides

was narrowed down by repeating the test using bilayer tablets with systematically varied IBS.

6.4 Results and Discussion

6.4.1 Single component in each layer

Survival plots of different bilayer tablets are shown in Figure 6.1. For a given combination of first and second layer materials, IBS can be varied by controlling P1 and P2, where higher P1 or lower P2 generally leads to lower IBS. [36] In the case of Lac/Lac, bilayer tablets did not fail unless P1 was 120 MPa or higher (Figure 6.S1). When P1 was low, tablets failed in the Lac layer instead of along the interface and TS was approximately constant regardless of P1 (Figure 6.S1a). This is to be expected since the strength of individual Lac layers was determined by P2, which was 100 MPa. In all systems, IBS decreased with increasing P1 when bilayer tablets failed along the interface (Figure 6.S1). Thus, it was possible to perform survival test on bilayer tablets with different IBSs. Based on the survival data (Figure 6.1), the IBS_m of Lac/Lac, Lac/MCC, MCC/MCC and MCC/Lac (1^{st} layer/2^{nd} layer) was bracketed as 0-0.16 MPa, 0-0.05 MPa, 0.05-0.09 MPa, and 0-0.07 MPa, respectively. Lac/Lac appeared to possess the highest IBS_m, followed by MCC/MCC, and then Lac/MCC and MCC/Lac, which suggested that IBS_m was higher when both layers were brittle. The broad brackets for IBS_m of Lac/Lac, Lac/MCC, and MCC/Lac reflected the sensitivity of IBS to changes in P1, where an increase of P1 by 10 MPa led to delamination along the interface. However, it would have been reasonable if IBS_m of Lac/Lac is higher than that of MCC/MCC because Lac is

more brittle than MCC, [34] which means cracks propagate faster and more easily in a Lac/Lac bilayer tablets. [37] Since Lac is among the more brittle excipients, results so far suggest that 0.16 MPa IBS_m is likely adequate for other single component bilayer tablets of similar sizes.

6.4.2 Multiple components bilayer tablets

Although not conclusive based on single component data, the IBS_m appeared materials-dependent. To further explore this, IBS_m values of systematically varied layer compositions were determined using binary mixtures of MCC and lactose, and ternary mixtures of MCC, lactose, and HPMC. As in the single component systems, IBS of multiple-component bilayer tablets was modified by changing P1 (Figure 6.S2). When the composition was (30%)MCC/(70%)Lac and (70%)MCC/(30%)Lac, the IBS_m lied between 0.05-0.15 MPa and 0.05-0.17 MPa, respectively (Figure 6.2a and Figure 6.2b). After adding the fixed amount of 40% HPMC in both layers, the IBS_m was 0.02-0.04 MPa for (18%)MCC(42%)Lac(40%)HPMC (Figure 6.2c), and 0.03-0.1 MPa for (42%)MCC(18%)Lac(40%)HPMC (Figure 6.2d). Both of which were smaller than those without HPMC, thus, confirming the effects of material properties on IBS_m. This suggests that HPMC can more effectively absorb impact energy at the interface so that bilayer tablets are more resistant to cracking and delamination.

Further studies involved making bilayer tablets using the binary mixtures in first layer and the ternary mixture in second layer, which mimics the bilayer tablets consisting of both immediate release (the binary mixture) and extended release (the ternary mixture)

functions. The IBS_m was 0.12-0.2 MPa for (30%)MCC(70%)Lac/(18%)MCC(42%)Lac(40%)HPMC (Figure 6.2e) and 0.03-0.06 MPa for (70%)MCC(30%)Lac/(42%)MCC(18%)Lac(40%)HPMC (Figure 6.2f). These data showed that the use of more brittle lactose in the two layers led to significantly higher IBS_m. In other words, more brittle bilayer tablets required higher IBS to survive external stresses. This is understandable because brittle materials are more sensitive to crack propagation during impact. [37] Consequently, higher IBS_m is needed to keep interface intact during the survival test. With multiple components, an IBS_m of 0.2 MPa is then sufficient to preserve integrity of these bilayer tablets under the test conditions.

6.4.3 Effect of tablet size

Tablet size is expected to affect IBS_m because larger tablets would induce higher stresses throughout the bilayer tablet, including along the interface, to counter the larger momentum of a heavier tablet at the point of impact with the friabilator drum wall. This possible effect was studied using bilayer tablets with diameters of 6 mm, 8 mm, and 10 mm and the same thickness to diameter ratio of 2:3. The weight of a 6 mm and 8 mm bilayer tablet was 22% and 52% of that of a 10 mm bilayer tablet, respectively. Due to the effect of weight difference, the IBS_m ranged 0.04 -0.09 MPa, 0.05 - 0.15 MPa, and 0.10 - 0.26 MPa for 6 mm, 8 mm, and 10 mm bilayer tablets, respectively (Figure 6.3) based on IBS data in Figure 6.S3. At a minimum, the IBS_m of 10 mm bilayer tablets was higher than that of 6 mm.

The IBS_m of 0.2 MPa sufficient to preserve bilayer tablet integrity in earlier sections was determined using 8 mm bilayer tablets. If smaller bilayer tablets are manufactured, an IBS_m below 0.2 MPa should be sufficient because of the lower impact energy by smaller tablets. The same reason explains why 10 mm bilayer tablets of the same materials required higher IBS_m of 0.26 MPa to successfully pass the survival test.

6.4.4 Relationship with friability

The use of survival plots to determine IBS_m should not be confused with the conventional tablet friability test. The latter test usually measures weight loss after 100 drops in a friabilator [27,30]. If desired, friability of bilayer tablets can be obtained by weighing tablet weight after 100 drops. A successful bilayer tablet should exhibit both good friability and pass the survival test. Moreover, tablet friability may correlate with IBS_m since, both IBS_m and tablet friability are affected by materials mechanical properties [30].

6.5 Conclusions

A survival test was proposed to determine the minimum interfacial bonding strength (IBS_m) of bilayer tablets. Using this survival test, it has been shown that IBS_m depends on both layer compositions and tablet size. In general, more brittle materials or larger tablets require a higher IBS_m. An IBS of 0.26 MPa was sufficient to avoid gross defects in bilayer tablets for all materials studied in this work. Given the diverse mechanical properties of materials investigated here, this value likely holds for most tablet

formulations. For each specific formulation and tablet size, the actual IBS_m can be determined using the survival test described here. The survival test described in this work provides the first common technology platform for systematically studying bilayer tablets to meet a key quality requirement.

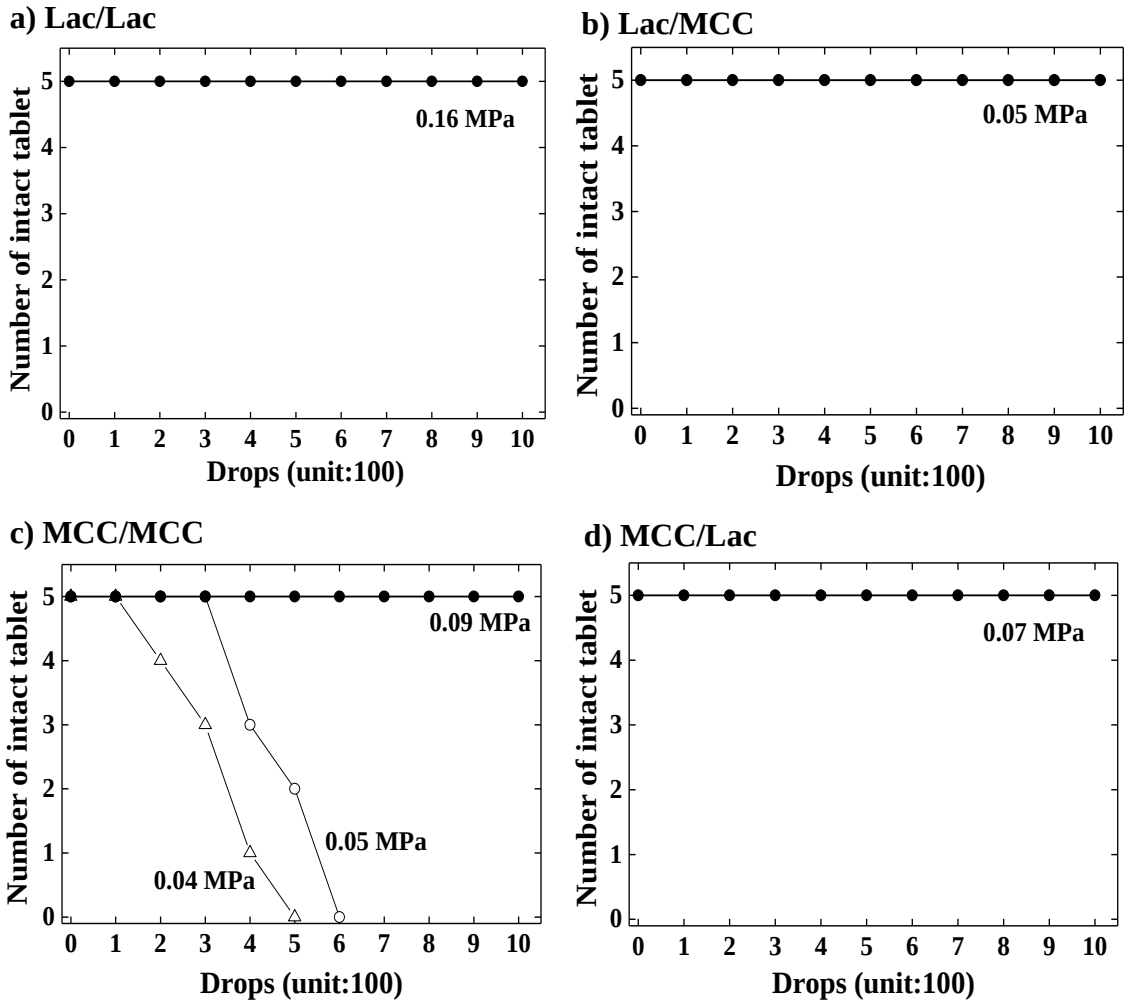

Figure 6.1 Survival plot of a) Lac/Lac, b) Lac/MCC, c) MCC/MCC and d) MCC/Lac with interfacial bonding strength indicated (n=3).

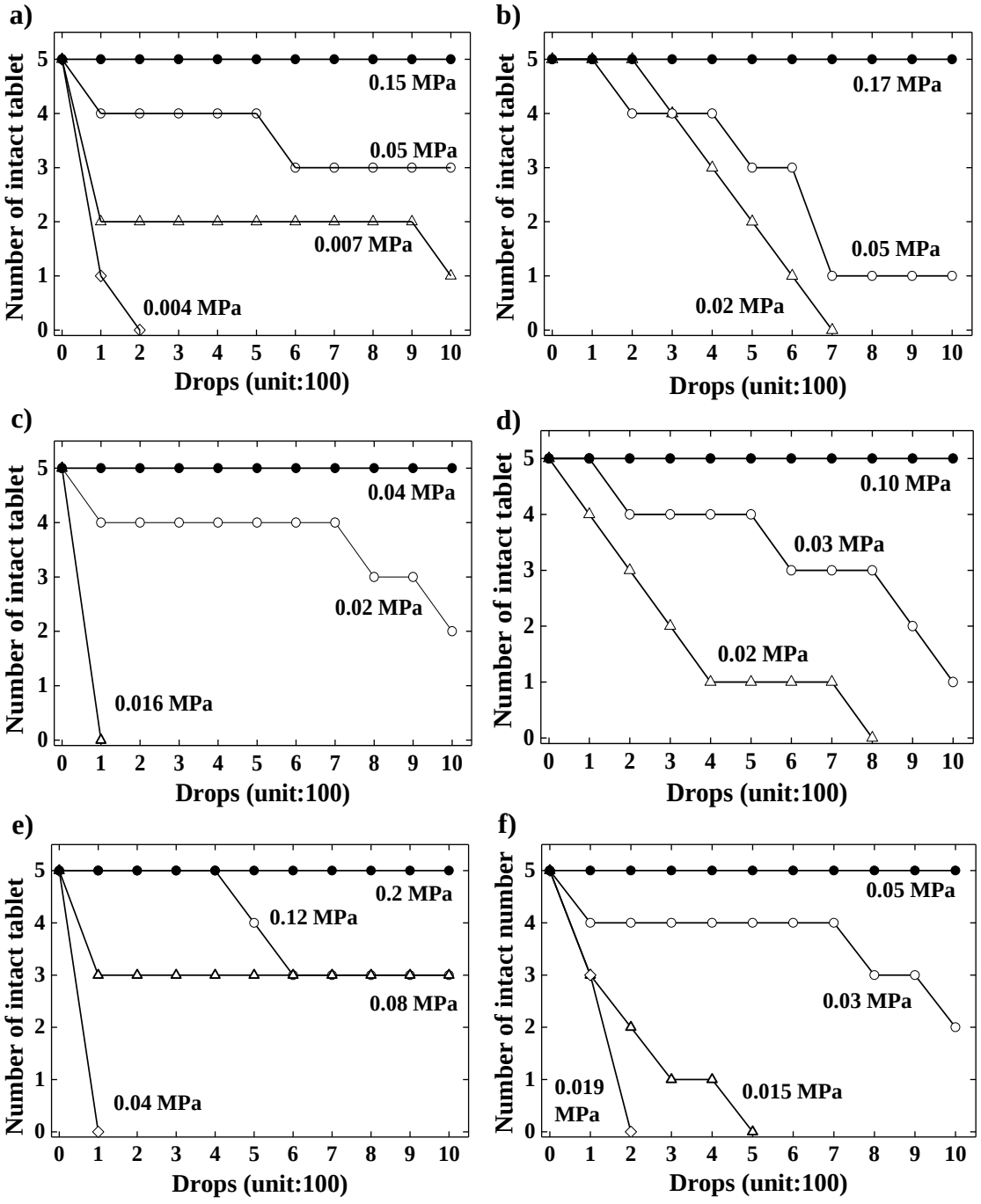

Figure 6.2 Survival plots of a) (30%)MCC(70%)Lac, b) (70%)MCC(30%)Lac, c) (18%)MCC(42%)Lac(40%)HPMC, d) (42%)MCC(18%)Lac(40%)HPMC, e) (30%)MCC(70%)Lac in first layer and (18%)MCC(42%)Lac(40%)HPMC in second layer and f) (70%)MCC(30%)Lac in first layer and (42%)MCC(18%)Lac(40%)HPMC in second layer with interfacial bonding strength indicated (n=3).

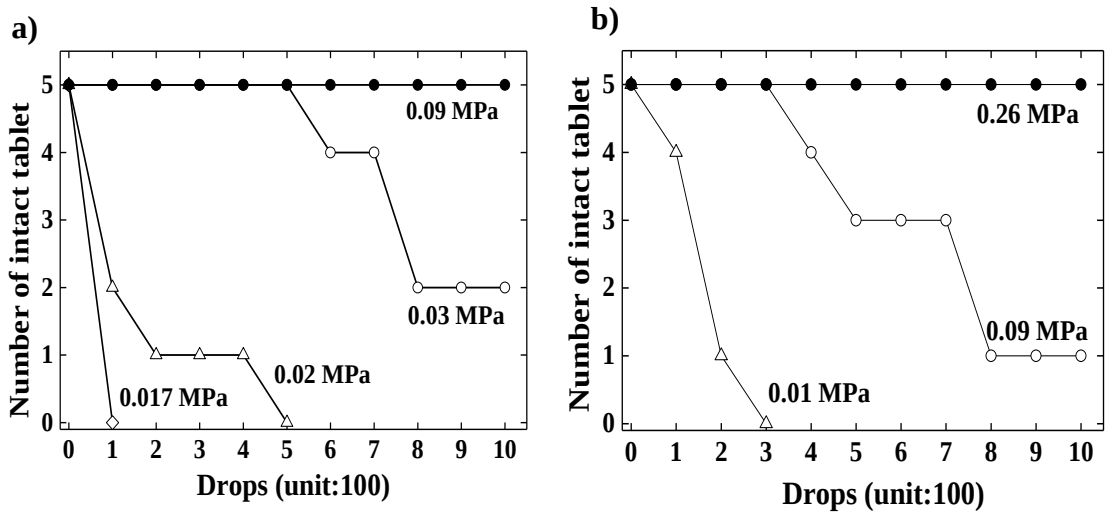

Figure 6.3 Survival plot of a) 6 mm and b) 10 mm bilayer tablets with interfacial bonding strength indicated. Both bilayer tablets were made of (30%)MCC(70%)Lac (n=3).

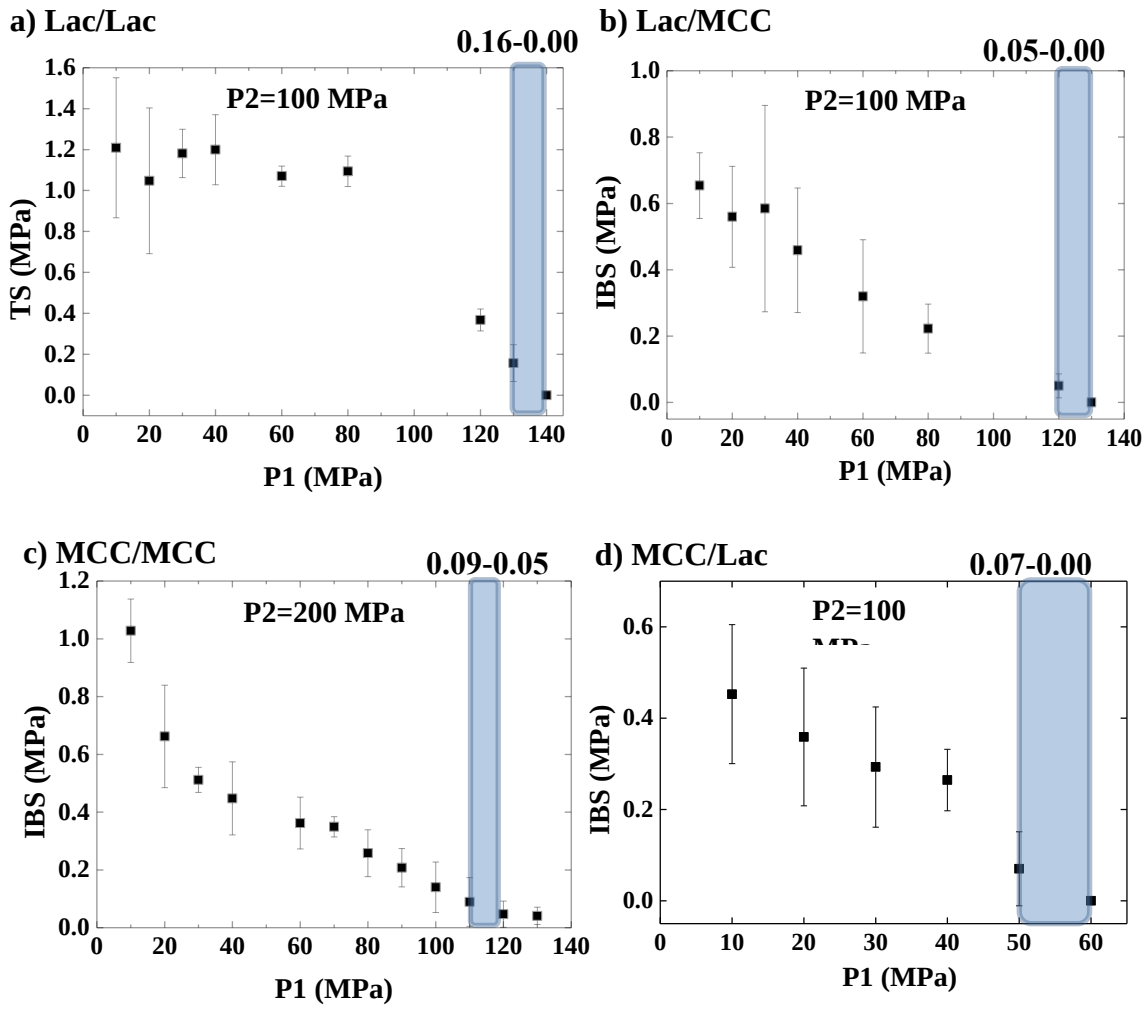

Figure 6.S1 Tensile strength (TS) or interfacial bonding strength (IBS) of a) Lac/Lac, b) Lac/MCC, c) MCC/MCC, and d) MCC/Lac under a series of first layer compaction pressure (P1) and a fixed second layer compaction pressure (P2). Blue box indicates the range of minimal IBS (n=3).

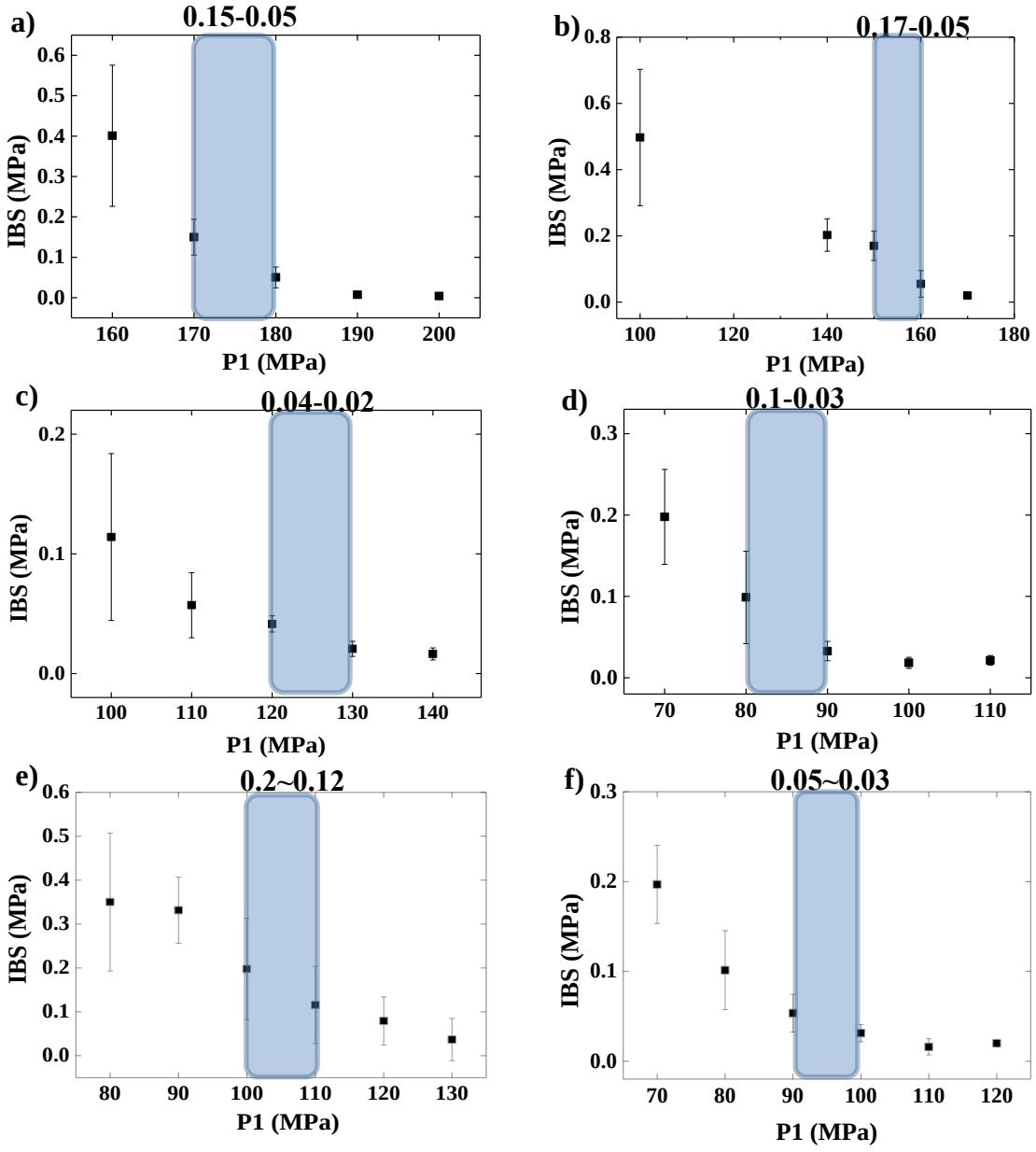

Figure 6.S2 Interfacial bonding strength (IBS) of bilayer tablets made with a) (30%)MCC(70%)Lac, b) (70%)MCC(30%)Lac, c) (18%)MCC(42%)Lac(40%)HPMC, d) (42%)MCC(18%)Lac(40%)HPMC, e) (30%)MCC(70%)Lac in first layer and (18%)MCC(42%)Lac(40%)HPMC in second layer and f) (70%)MCC(30%)Lac in first layer and (42%)MCC(18%)Lac(40%)HPMC in second layer under a series of first layer compaction pressure (P1) and the fixed second layer compaction pressure (P2= 200 MPa). Blue box indicates the range of minimal IBS (n=3).

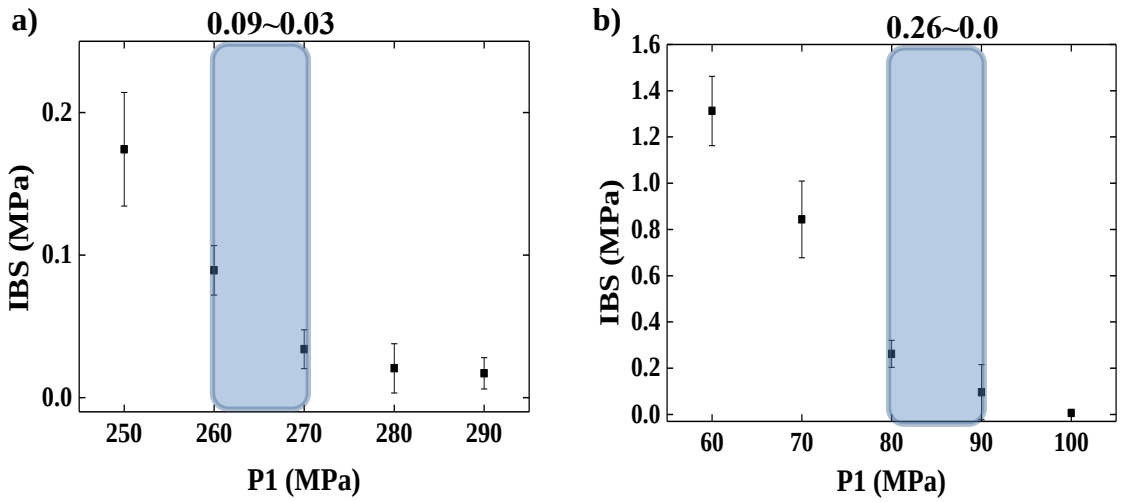

Figure 6.S3 Interfacial bonding strength (IBS) of a) 6 mm and b) 100 mm bilayer tablet. Both bilayer tablets were made of (30%)MCC(70%)Lac under a series of first layer compaction pressure (P1) and a fixed second layer compaction pressure (P2) at 200 MPa. Blue box indicates the range of minimal IBS (n=3).

CHAPTER 7. Research summary and future work

Research Summary

The overall goal of the thesis is to understand the interfacial bonding strength of bilayer tablets made with different materials and compaction pressures and determine the minimal interfacial bonding strength. The key message of each chapter is summarized below.

Chapter 2.

Inadequate interfacial bonding strength (IBS) was a long-standing challenge for manufacturing bilayer tablets. Before understanding the bonding mechanism, the tensile method and shear method were developed. The tensile method used tensile force to pull bilayer tablet apart and shear method applied shear force on the side to shear bilayer tablets. In real life impact, the shear force is more likely to happen than a tensile force. However, comparing the measured IBS in each method, the tensile method can produce unambiguous data interpretation. Instead, the shear method can have two measured IBS for the same bilayer tablets, which might be due to the complex stress distribution and layer orientation. Even though the shear method was more appropriate in terms of force wise, the difficulty for data interpretation makes the tensile method more relevant for further IBS measurement. The tensile method is then considered as the standard method to determine IBS in chapters 3 to 6.

Chapter 3.

Understanding the mechanism of interfacial bonding strength of bilayer tablets is critical for robust manufacturing and avoid layer separation. We prepared bilayer tablets made of

materials with two different mechanical properties, MCC and lactose, and a series of first layer compaction pressures (P1) and second layer compaction pressure (P2) at 100, 200, 300 MPa. There are four types of bilayer tablets, MCC/MCC, MCC/Lac, Lac/Lac, Lac/MCC. IBS was measured using the tensile method developed in Chapter 2 and the failure mode was recorded. IBS of Lac/Lac maintains and independent of P2 at lower P1 but IBS decreases when P1 increases higher, which can be explained by the change of failure mode from layer to interface failure. The other three types of bilayer tablets, IBS decrease when P1 increases and P2 decreases. IBS was clearly explained by the bonding area (BA) and bonding strength (BS) interplay. The BA or BS increases for larger IBS. BA and BS were assessed by surface waviness and tablet strength at zero porosity of the two materials at the interface, respectively. Besides of BA and BS, porosity and radial expansion of each layer should be considered for more accurate IBS comparison. Smaller porosity can contribute to the actual bonding area and different in radial expansion induces shear force to weaken IBS.

Chapter 4.

A formulation typically contains multiple compositions to achieve better mechanical properties and clinical outcomes. We investigated the effect of the mixture of MCC and lactose in a 10% increment and first layer compaction pressures (P1) at 20 and 100 MPa on interfacial bonding strength (IBS). The result shows an unexpected trend of IBS with the increase of MCC. First, IBS increases when MCC increases to 20-30%. With MCC from 30% to 80%, IBS decreases and bilayer tablets fail at the interface. However, IBS increases again with over 80% of MCC when P1 is 20 MPa. Instead, no second rise of

IBS is observed when P1 is 100 MPa. Also, higher P1 gives lower IBS. All of The phenomena can be explained by the bonding area (BA) and bonding strength (BS) interplay. With a small amount of MCC, BS increases for higher IBS. However, when MCC is above 30%, lower IBS is attributed by a smaller BA. As for the second rise in IBS, it is caused by the decrease of the defect. Higher P1 compresses the first layer more than lower P1 so BA is greatly reduced, thus lower IBS for higher P1. Both BA and BS changes accordingly to affect IBS and failure mode.

Chapter 5.

The particle size of materials can be an important factor that affects interfacial bonding strength (IBS) of bilayer tablets. However, the effect of particle size is also influenced by material mechanical properties. Therefore, particle size and mechanical properties of a material act together to influence IBS. In this work, two sizes of MCC and lactose are prepared and plasticity of each material is measured. The result shows lactose is more suitable as the first layer because IBS maintains higher and is less sensitive to second layer materials and particle size. On the other hand, MCC prefers in the second layer. The change of IBS can be explained by the bonding area (BA) and bonding strength (BS) interplay. IBS generally increases with the increase of BA, which is related to the particle size. The second layer prefers larger particles for higher BA but the first layer shows no preference in particle size for BA. Besides, BS and radial expansion also influence the IBS, which necessitate being considered together for more precise comparison between different layer combination.

Chapter 6.

Knowing the minimal interfacial bonding strength (IBS_m) is an essential step to determine whether or not each proposed formulation exhibits adequate IBS for any manufacturing process. A survival test was developed to determine IBS_m of bilayer tablets using a wide range of materials (MCC, lactose, and HPMC) from single to multiple compositions in each layer to ensure generality. The result shows IBS_m depends on both layer materials and tablet size. In general, more brittle materials or larger tablets corresponded to a higher IBS_m. The addition of HPMC can alleviate the impact and reduce the IBSm. We observed an IBS of 0.26 MPa should be sufficient to avoid gross defects in bilayer tablets for all materials studied in this work. Given the diverse mechanical properties among these materials, this value likely holds for most tablet formulations. For each specific formulation and tablet size, the actual IBSm can be determined using the survival test described here.

Future Work

In the work, we first demonstrated the successful application of BABS interplay to explain interfacial bonding strength (IBS) of bilayer tablets with the simple formulation. Then a more complex formulation of the mixture and different particle sizes were used to verify BABS interplay. However, the materials used in the work are limited to two excipients, MCC and lactose, and one polymer, HPMC. The next step would be to systematically use materials with different mechanical properties including APIs and excipients to further test the BABS interplay. The approach can be similar to this work starting from simple to more complex formulation.

We have studied single and multiple compositions and the effect of particle size on interfacial bonding strength (IBS). Still, there is a multitude of factors that are worth discussing.

1) Environmental conditions

Different materials have a different response to environmental conditions, i.e. relative humidity. Different water content in the environment can change crystal surface, level crystallinity or mechanical properties, all of which will affect the bonding area and bonding strength interplay. This will highlight the importance of the RH effect on IBS.

2) Lubrication level

The level of lubricant can have an effect on compaction behavior. Lubricant usually has lower bonding strength, which can reduce IBS. However, it can reduce the friction

between particles and with the die wall to increase the compaction efficiency to increase BA. It is informative to study the level of lubricant to find an appropriate amount for better IBS.

3) Tablet shape

A tablet is not limited to cylindrical shape as tested in this work. Different shapes of tablets can have different stress distribution upon testing IBS. In this work, the tensile method was used to measure IBS, which applied a uniform tensile force on the surface to pull cylindrical bilayer tablets apart. With a curved surface, a special design of the tensile method should be made. However, the information obtained can be critical to have a standard method to determine IBS for any further analysis.

We have established the minimal IBS (IBSm) on a variety of material compositions and tablet size with the survival test. In this work, the determination of IBSm was measured one day after the manufacturing of bilayer tablets. The next step could investigate the aging effect on IBS. The bilayer tablet product is usually stored for a period of time in the bottle before the expiration date. It is useful to determine the IBSm when bilayer tablets are stored for longer days before testing to see if IBSm reaches a plateau. Finding the IBSm plateau makes the bilayer tablet production more robust without unexpected failure.

In the work, we have studied factors that affect the interfacial bonding strength of bilayer tablets. The effect of these factors should have the same influence on multi-layer tablets. However, the mutual influence will be more complex with the increase of layers. The next step should be applying BABS interplay to discuss the effect of these factors on the

IBS of multilayers tablets. A successful demonstration of agreement between bilayer and multi-layer tablets can validate the generality of BABS interplay to approach IBS.

BIBLIOGRAPHY

CHAPTER 1.

1. FDA 2015. Fixed-Combination and Co-Packaged Drugs: Applications for Approval and Combinations of Active Ingredients Under Consideration for Inclusion in an Over-the-Counter Monograph.
2. W. Humphrey R, M. Brockway-Lunardi L, T. Bonk D, Dohoney KM, Doroshow JH, Meech SJ, Ratain MJ, Topalian SL, M. Pardoll D 2011. Opportunities and challenges in the development of experimental drug combinations for cancer. Journal of the National Cancer Institute 103:1222-1226.
3. Gupta AK, Arshad S, Poulter NR 2010. Compliance, safety, and effectiveness of fixed-dose combinations of antihypertensive agents: a meta-analysis. Hypertension 55:399-407.
4. Bakris GL, Weir MR, Hypertension So, Investigators tEoLiD 2003. Achieving goal blood pressure in patients with type 2 diabetes: conventional versus fixed-dose combination approaches. The Journal of Clinical Hypertension 5:202-209.
5. Friedland GH, Williams A 1999. Attaining higher goals in HIV treatment: The central importance of adherence. AIDS (London, England) 13:S61-72.
6. Blomberg B, Spinaci S, Fourie B, Laing R 2001. The rationale for recommending fixed-dose combination tablets for treatment of tuberculosis. Bulletin of the world health organization 79:61-68.
7. Desai D, Wang J, Wen H, Li X, Timmins P 2013. Formulation design, challenges, and development considerations for fixed dose combination (FDC) of oral solid dosage forms. Pharm Dev Technol 18:1265-1276.
8. Wechsler J 2005. Combination products raise manufacturing challenges. Pharm Tech 29:32-40.
9. Siew A 2014. Tackling challenges in the development of fixed-dose combinations. Pharm Technol 38:57.
10. Koo O 2010. Manufacturing Process Considerations for Fixed-Dose Combination Drug Products.

11. Desai D, Wang J, Wen H, Li X, Timmins P 2013. Formulation design, challenges, and development considerations for fixed dose combination (FDC) of oral solid dosage forms. Pharm Dev Technol 18:1265-1276.

12. SHAHI S, SHIVANIKAR S, ZADBUKE N, PADALKAR A 2012. Formulation and evaluation of bilayered tablet of metformin hydrochloride and pioglitazone hydrochloride. International Journal of Pharmacy and Pharmaceutical Sciences 4:380-385.

13. Mandal U, Pal TK 2008. Formulation and in vitro studies of a fixed-dose combination of a bilayer matrix tablet containing metformin HCl as sustained release and glipizide as immediate release. Drug Dev Ind Pharm 34:305-313.

14. Chang S-Y, Li J-x, Sun CC 2017. Tensile and shear methods for measuring strength of bilayer tablets. Int J Pharm 523:121-126.

15. Osei-Yeboah F, Chang S-Y, Sun CC 2016. A critical Examination of the Phenomenon of Bonding Area - Bonding Strength Interplay in Powder Tableting. Pharm Res 33:1126-1132.

16. Food U, Administration D 2014. Code of Federal Regulations Title 21–Food and Drugs (Government Printing Office, Washington, DC) Chapter 1, Part 300, Subpart B, Sec. 300.50. Department of Health and Human Services (Ed) US Food and Drug Administration.

17. P. T 2006. Developing fixed combination drug products– Technical challenges and opportunities. In: The 10th Annual Drug Delivery Partnerships Phoenix, AZ, USA.

18. Lehár J, Krueger AS, Avery W, Heilbut AM, Johansen LM, Price ER, Rickles RJ, Short Iii GF, Staunton JE, Jin X 2009. Synergistic drug combinations tend to improve therapeutically relevant selectivity. Nature biotechnology 27:659.

19. Easton J, Noble S, Perry CM 2003. Amoxicillin/clavulanic acid. Drugs 63:311-340.

20. Coleman JJ, Schuster CR, DuPont RL 2010. Reducing the abuse potential of controlled substances. Pharmaceutical Medicine 24:21-36.

21. Vicknasingam B, Mazlan M, Schottenfeld R, Chawarski M 2010. Injection of buprenorphine and buprenorphine/naloxone tablets in Malaysia. Drug and alcohol dependence 111:44-49.

22. Bangalore S, Kamalakkannan G, Parkar S, Messerli FH 2007. Fixed-dose combinations improve medication compliance: a meta-analysis. Am J Med 120:713-719.

23. Friedland GH, Williams A 1999. Attaining higher goals in HIV treatment: The central importance of adherence. AIDS 13:S61-72.

24. Melikian C, White TJ, Vanderplas A, Dezii CM, Chang E 2002. Adherence to oral antidiabetic therapy in a managed care organization: a comparison of monotherapy, combination therapy, and fixed-dose combination therapy. Clinical therapeutics 24:460-467.

25. Jayaprakash S, Halith SM, Pillai KK, Balasubramaniyam P, Firthouse PM, Boopathi M 2011. Formulation and evaluation of bilayer tablets of amlodipine besilate and metprolol succinate. Pharm Lett 3:143-154.

26. Patra C, Kumar A, Pandit H, Singh S, Devi M 2007. Design and evaluation of sustained release bilayer tablets of propranolol hydrochloride. Acta Pharm 57:479-489.

27. Kulkarni A, Bhatia M 2010. Development and evaluation of regioselective bilayer floating tablets of Atenolol and Lovastatin for biphasic release profile. Iran J Pharm Res 8:15-25.

28. Nirmal J, Saisivam S, Peddanna C, Muralidharan S, Godwinkumar S, Nagarajan M 2008. Bilayer tablets of atorvastatin calcium and nicotinic acid: formulation and evaluation. Chem Pharm Bull 56:1455-1458.

29. Abebe A, Akseli I, Sprockel O, Kottala N, Cuitiño AM 2014. Review of bilayer tablet technology. Int J Pharm 461:549-558.

30. Reddy P, Rao D, Kumar R 2013. Bi-layer technology-an emerging trend, A review. International Journal of Research and Development in Pharmacy and Life Sciences 2:404-411.

31. Kottala N, Abebe A, Sprockel O, Bergum J, Nikfar F, Cuitiño A 2012. Evaluation of ohe performance characteristics of bilayer tablets: Part I. impact of material properties and process parameters on the strength of bilayer tablets. AAPS PharmSciTech 13:1236-1242.

32. Zhang J, Wu C-Y, Storey D, Byrne G 2018. Interfacial strength of bilayer pharmaceutical tablets. Powder Technol 337:36-42.

33. Castrati L, Mazel V, Diarra H, Busignies V, Tchoreloff P 2017. Effect of the curvature of the punches on the shape of the interface and the delamination tendency of bilayer tablets. J Pharm Sci 106:1331-1338.

34. Castrati L, Mazel V, Busignies V, Diarra H, Rossi A, Colombo P, Tchoreloff P 2016. Comparison of breaking tests for the characterization of the interfacial strength of bilayer tablets. Int J Pharm 513:709-716.

35. Papós K, Kása Jr P, Ilič I, Blatnik-Urek S, Regdon Jr G, Srčič S, Pintye-Hódi K, Sovány T 2015. Effect of the surface free energy of materials on the lamination tendency of bilayer tablets. Int J Pharm 496:609-613.

36. Yohannes B, Gonzalez M, Abebe A, Sprockel O, Nikfar F, Kiang S, Cuitiño AM 2017. Discrete particle modeling and micromechanical characterization of bilayer tablet compaction. Int J Pharm 529:597-607.

37. Patel S, Kaushal AM, Bansal AK 2006. Compression physics in the formulation development of tablets. Critical Reviews™ in Therapeutic Drug Carrier Systems 23.

38. Sun CC 2011. Decoding powder tabletability: roles of particle adhesion and plasticity. Journal of Adhesion Science and Technology 25:483-499.

39. Amidon GE, Akseli I, Goldfarb D, He X, Sun CC. Pharmacopeial Forum, 2014.

40. Inman SJ, Briscoe BJ, Pitt KG 2007. Topographic characterization of cellulose bilayered tablets interfaces. Chem Eng Res Des 85:1005-1012.

41. Jivraj M, Martini LG, Thomson CM 2000. An overview of the different excipients useful for the direct compression of tablets. Pharm Sci Technolo Today 3:58-63.

42. Rees JE, Rue PJ 1978. Time-dependent deformation of some direct compression excipients. J Pharm Pharmacol 30:601-607.

43. Duberg M, Nyström C 1981. Studies on direct compression of tablets. Vi. Evaluation of methods for the estimation of particle fragmentation during compaction. Acta Pharm Suec 19:421-436.

44. Patel S, Sun CC 2016. Macroindentation hardness measurement—Modernization and applications. Int J Pharm 506:262-267.

45. Gong X, Sun CC 2015. A new tablet brittleness index. Eur J Pharm Biopharm 93:260-266.

46. Osei-Yeboah F, Sun CC 2015. Validation and applications of an expedited tablet friability method. Int J Pharm 484:146-155.

47. Al-Ibraheemi ZAM, Anuar M, Taip F, Amin M, Tahir S, Mahdi AB 2013. Deformation and mechanical characteristics of compacted binary mixtures of plastic (microcrystalline cellulose), elastic (sodium starch glycolate), and brittle (lactose monohydrate) pharmaceutical excipients. Particulate Science and Technology 31:561-567.

48. Sun W-J, Kothari S, Sun CC 2018. The relationship among tensile strength, Young's modulus, and indentation hardness of pharmaceutical compacts. Powder Technol 331:1-6.

49. Hersey JA, Bayraktar G, Shotton E 1967. The effect of particle size on the strength of sodium chloride tablets. The Journal of pharmacy and pharmacology 19:Suppl: 24S.

50. Shotton E, Ganderton D 1961. The strength of compressed tablets: III. The relation of particle size, bonding and capping in tablets of sodium chloride, aspirin and hexamine. J Pharm Pharmacol 13:144T-152T.

51. McKenna A, McCafferty D 1982. Effect of particle size on the compaction mechanism and tensile strength of tablets. J Pharm Pharmacol 34:347-351.

52. Sun C, Himmelspach MW 2006. Reduced tabletability of roller compacted granules as a result of granule size enlargement. J Pharm Sci 95:200-206.

53. Paul S, Sun CC 2018. Modulating Sticking Propensity of Pharmaceuticals Through Excipient Selection in a Direct Compression Tablet Formulation. Pharm Res 35:113.

54. Almaya A, Aburub A 2008. Effect of particle size on compaction of materials with different deformation mechanisms with and without lubricants. AAPS PharmSciTech 9:414-418.

55. De Boer A, Vromans H, Leur C, Bolhuis G, Kussendrager K, Bosch H 1986. Studies on tableting properties of lactose. Pharmaceutisch weekblad 8:145-150.

56. Eriksson M, Alderborn G 1995. The effect of particle fragmentation and deformation on the interparticulate bond formation process during powder compaction. Pharm Res 12:1031-1039.

57. Chang S-Y, Sun CC 2017. Superior Plasticity and Tabletability of Theophylline Monohydrate. Mol Pharm 14:2047-2055.

58. Stasiak M, Tomas J, Molenda M, Rusinek R, Mueller P 2010. Uniaxial compaction behaviour and elasticity of cohesive powders. Powder Technol 203:482-488.

59. Busignies V, Mazel V, Diarra H, Tchoreloff P 2013. Role of the elasticity of pharmaceutical materials on the interfacial mechanical strength of bilayer tablets. Int J Pharm 457:260-267.

60. Anuar M, Briscoe B 2010. Interfacial elastic relaxation during the ejection of bi-layered tablets. Int J Pharm 387:42-47.

61. Klinzing G, Zavaliangos A 2013. Understanding the effect of environmental history on bilayer tablet interfacial shear strength. Pharm Res 30:1300-1310.

62. Kottala N, Abebe A, Sprockel O, Bergum J, Nikfar F, Cuitiño AM 2012. Evaluation of the performance characteristics of bilayer tablets: part II. Impact of environmental conditions on the strength of bilayer tablets. AAPS PharmSciTech 13:1190-1196.

63. Wang J, Wen H, Desai D 2010. Lubrication in tablet formulations. Eur J Pharm Biopharm 75:1-15.

64. He X, Secreast PJ, Amidon GE 2007. Mechanistic study of the effect of roller compaction and lubricant on tablet mechanical strength. J Pharm Sci 96:1342-1355.

65. NAKABAYASHI K, SHIMAMOTO T, MIMA H 1980. Stability of packaged solid dosage forms. II. Shelf-life prediction for packaged sugar-coated tablets liable to moisture and heat damage. Chemical and pharmaceutical bulletin 28:1099-1106.

66. El Gindy NA, Samaha MW 1982. Tensile strength of some pharmaceutical compacts and their relation to surface free energy. Int J Pharm 13:35-46.

67. Kottala N, Abebe A, Sprockel O, Akseli I, Nikfar F, Cuitiño AM 2013. Characterization of interfacial strength of layered powder-compacted solids. Powder Technol 239:300-307.

68. Franck J, Abebe A, Keluskar R, Martin K, Majumdar A, Kottala N, Stamato H 2015. Axial strength test for round flat faced versus capsule shaped bilayer tablets. Pharmaceutical development and technology 20:139-145.

69. Dietrich P, Bauer-Brandl A, Schubert R 2000. Influence of tableting forces and lubricant concentration on the adhesion strength in complex layer tablets. Drug Dev Ind Pharm 26:745-754.

70. Niwa M, Hiraishi Y, Iwasaki N, Terada K 2013. Quantitative analysis of the layer separation risk in bilayer tablets using terahertz pulsed imaging. Int J Pharm 452:249-256.

71. Podczeck F, Al-Muti E 2010. The tensile strength of bilayered tablets made from different grades of microcrystalline cellulose. Eur J Pharm Sci 41:483-488.

72. Busignies V, Mazel V, Diarra H, Tchoreloff P 2014. Development of a new test for the easy characterization of the adhesion at the interface of bilayer tablets: Proof-of-concept study by experimental design. Int J Pharm 477:476-484.

73. Sun W-J, Aburub A, Sun CC 2018. A mesoporous silica based platform to enable tablet formulations of low dose drugs by direct compression. Int J Pharm 539:184-189.

74. Sun CC, Hou H, Gao P, Ma C, Medina C, Alvarez FJ 2009. Development of a high drug load tablet formulation based on assessment of powder manufacturability: moving towards quality by design. J Pharm Sci 98:239-247.

75. Perumalla SR, Paul S, Sun CC 2016. Enabling the tablet product development of 5-fluorocytosine by conjugate acid base cocrystals. J Pharm Sci 105:1960-1966.

76. Wang C, Perumalla SR, Lu R, Fang J, Sun CC 2016. Sweet berberine. Cryst Growth Des 16:933-939.

77. Shafer E, Wollish E, Engel CE 1956. The „Roche” □ friabilator. Journal of the American Pharmaceutical Association 45:114-116.

78. USP, 2014. USP37/NF32 (Online), General Chapters: Tablet Friability. United States

Pharmacopoeial Convention, Rockville, MD.

79. Podczeck F 2012. Methods for the practical determination of the mechanical strength of tablets—From empiricism to science. Int J Pharm 436:214-232.

80. Joiris E, Di Martino P, Berneron C, Guyot-Hermann A-M, Guyot J-C 1998. Compression behavior of orthorhombic paracetamol. Pharm Res 15:1122-1130.

81. Sun C, Grant DJ 2001. Compaction properties of L-lysine salts. Pharm Res 18:281-286.

82. Wang C, Paul S, Wang K, Hu S, Sun CC 2017. Relationships among crystal structures, mechanical properties, and tableting performance probed using four salts of diphenhydramine. Crystal Growth & Design 17:6030-6040.
83. Sun CC 2009. Materials Science Tetrahedron—A Useful Tool for Pharmaceutical Research and Development. J Pharm Sci 98:1671-1687.
84. Osei-Yeboah F, Sun CC 2015. Tabletability modulation through surface engineering. J Pharm Sci 104:2645-2648.
85. Sun CC, Kleinebudde P 2016. Mini review: Mechanisms to the loss of tabletability by dry granulation. Eur J Pharm Biopharm 106:9-14.

CHAPTER 2.

1. Ruzicka M, Leenen FH 2001. Monotherapy versus combination therapy as first line treatment of uncomplicated arterial hypertension. Drugs 61:943-954.
2. Abdul S, Poddar SS 2004. A flexible technology for modified release of drugs: multi layered tablets. J Control Release 97:393-405.
3. Fassihi RA, Ritschel WA 1993. Multiple-layer, direct-compression, controlled-release system: In vitro and in vivo evaluation. J Pharm Sci 82:750-754.
4. Sun CC, Hou H, Gao P, Ma C, Medina C, Alvarez FJ 2009. Development of a high drug load tablet formulation based on assessment of powder manufacturability: moving towards quality by design. J Pharm Sci 98:239-247.
5. Inman SJ, Briscoe BJ, Pitt KG 2007. Topographic characterization of cellulose bilayered tablets interfaces. Chem Eng Res Des 85:1005-1012.
6. Anuar MS, Briscoe BJ 2010. Interfacial elastic relaxation during the ejection of bi-layered tablets. Int J Pharm 387:42-47.
7. Kottala N, Abebe A, Sprockel O, Bergum J, Nikfar F, Cuitiño A 2012. Evaluation of ohe performance characteristics of bilayer tablets: Part I. impact of material properties and process parameters on the strength of bilayer tablets. AAPS PharmSciTech 13:1236-1242.

8. Kottala N, Abebe A, Sprockel O, Akseli I, Nikfar F, Cuitiño AM 2012. Influence of compaction properties and interfacial topography on the performance of bilayer tablets. Int J Pharm 436:171-178.

9. Akseli I, Abebe A, Sprockel O, Cuitiño AM 2013. Mechanistic characterization of bilayer tablet formulations. Powder Technol 236:30-36.

10. Klinzing G, Zavaliangos A 2013. Understanding the Effect of Environmental History on Bilayer Tablet Interfacial Shear Strength. Pharm Res 30:1300-1310.

11. Wu C-Y, Seville JP 2009. A comparative study of compaction properties of binary and bilayer tablets. Powder Technol 189:285-294.

12. Amin MCIM, Albawani SM, Amjad MW 2012. A comparative study of the compaction properties of binary and bilayer tablets of direct compression excipients. Trop J Pharm Res 11:585-594.

13. Niwa M, Hiraishi Y, Iwasaki N, Terada K 2013. Quantitative analysis of the layer separation risk in bilayer tablets using terahertz pulsed imaging. Int J Pharm 452:249-256.

14. Papós K, Kása Jr P, Ilič I, Blatnik-Urek S, Regdon Jr G, Srčič S, Pintye-Hódi K, Sovány T 2015. Effect of the surface free energy of materials on the lamination tendency of bilayer tablets. Int J Pharm 496:609-613.

15. Podczeck F, Drake KR, Newton JM, Haririan I 2006. The strength of bilayered tablets. Eur J Pharm Sci 29:361-366.

16. Podczeck F, Al-Muti E 2010. The tensile strength of bilayered tablets made from different grades of microcrystalline cellulose. Eur J Pharm Sci 41:483-488.

17. Busignies V, Mazel V, Diarra H, Tchoreloff P 2013. Role of the elasticity of pharmaceutical materials on the interfacial mechanical strength of bilayer tablets. Int J Pharm 457:260-267.

18. Podczeck F 2011. Theoretical And Experimental Investigations Into The Delamination Tendencies Of Bilayer Tablets. Int J Pharm 408:102-112.

19. Busignies V, Mazel V, Diarra H, Tchoreloff P 2014. Development of a new test for the easy characterization of the adhesion at the interface of bilayer tablets: Proof-of-concept study by experimental design. Int J Pharm 477:476-484.

CHAPTER 3.

1. Sabaté E. 2003. Adherence to long-term therapies: evidence for action. ed., WHO.
2. Lee JK, Grace KA, Taylor AJ 2006. Effect of a pharmacy care program on medication adherence and persistence, blood pressure, and low-density lipoprotein cholesterol: a randomized controlled trial. Jama 296:2563-2571.
3. Ho PM, Bryson CL, Rumsfeld JS 2009. Medication adherence: its importance in cardiovascular outcomes. Circulation 119:3028-3035.
4. Delamater AM 2006. Improving patient adherence. Clin Diabetes 24:71-77.
5. Brown MT, Bussell JK 2011. Medication adherence: WHO cares? Mayo Clinic Proc 86:304-314.
6. Desai D, Wang J, Wen H, Li X, Timmins P 2013. Formulation design, challenges, and development considerations for fixed dose combination (FDC) of oral solid dosage forms. Pharm Dev Technol 18:1265-1276.
7. Siew A 2014. Tackling challenges in the development of fixed-dose combinations. Pharm Technol 38:57.
8. Jayaprakash S, Halith SM, Pillai KK, Balasubramaniyam P, Firthouse PM, Boopathi M 2011. Formulation and evaluation of bilayer tablets of amlodipine besilate and metprolol succinate. Pharm Lett 3:143-154.
9. Gupta AK, Arshad S, Poulter NR 2010. Compliance, safety, and effectiveness of fixed-dose combinations of antihypertensive agents: a meta-analysis. Hypertension 55:399-407.
10. Bangalore S, Kamalakkannan G, Parkar S, Messerli FH 2007. Fixed-dose combinations improve medication compliance: a meta-analysis. Am J Med 120:713-719.
11. Patra C, Kumar A, Pandit H, Singh S, Devi M 2007. Design and evaluation of sustained release bilayer tablets of propranolol hydrochloride. Acta Pharm 57:479-489.
12. Kulkarni A, Bhatia M 2010. Development and evaluation of regioselective bilayer floating tablets of Atenolol and Lovastatin for biphasic release profile. Iran J Pharm Res 8:15-25.
13. Nirmal J, Saisivam S, Peddanna C, Muralidharan S, Godwinkumar S, Nagarajan M 2008. Bilayer tablets of atorvastatin calcium and nicotinic acid: formulation and evaluation. Chem Pharm Bull 56:1455-1458.

14. Chang S-Y, Li J-X, Sun CC 2017. Tensile and shear methods for measuring strength of bilayer tablets. Int J Pharm 523:121-126.

15. Kottala N, Abebe A, Sprockel O, Bergum J, Nikfar F, Cuitiño A 2012. Evaluation of ohe performance characteristics of bilayer tablets: Part I. impact of material properties and process parameters on the strength of bilayer tablets. AAPS PharmSciTech 13:1236-1242.

16. Zhang J, Wu C-Y, Storey D, Byrne G 2018. Interfacial strength of bilayer pharmaceutical tablets. Powder Technol 337:36-42.

17. Castrati L, Mazel V, Diarra H, Busignies V, Tchoreloff P 2017. Effect of the curvature of the punches on the shape of the interface and the delamination tendency of bilayer tablets. J Pharm Sci 106:1331-1338.

18. Castrati L, Mazel V, Busignies V, Diarra H, Rossi A, Colombo P, Tchoreloff P 2016. Comparison of breaking tests for the characterization of the interfacial strength of bilayer tablets. Int J Pharm 513:709-716.

19. Papós K, Kása Jr P, Ilič I, Blatnik-Urek S, Regdon Jr G, Srčič S, Pintye-Hódi K, Sovány T 2015. Effect of the surface free energy of materials on the lamination tendency of bilayer tablets. Int J Pharm 496:609-613.

20. Yohannes B, Gonzalez M, Abebe A, Sprockel O, Nikfar F, Kiang S, Cuitiño AM 2017. Discrete particle modeling and micromechanical characterization of bilayer tablet compaction. Int J Pharm 529:597-607.

21. Abebe A, Akseli I, Sprockel O, Kottala N, Cuitiño AM 2014. Review of bilayer tablet technology. Int J Pharm 461:549-558.

22. Osei-Yeboah F, Chang S-Y, Sun CC 2016. A critical Examination of the Phenomenon of Bonding Area - Bonding Strength Interplay in Powder Tableting. Pharm Res 33:1126-1132.

23. Zhou Q, Shi L, Marinaro W, Lu Q, Sun CC 2013. Improving manufacturability of an ibuprofen powder blend by surface coating with silica nanoparticles. Powder Technol 249:290-296.

24. Chang S-Y, Sun CC 2017. Superior Plasticity and Tabletability of Theophylline Monohydrate. Mol Pharm 14:2047-2055.

25. Kottala N, Abebe A, Sprockel O, Akseli I, Nikfar F, Cuitiño AM 2012. Influence of compaction properties and interfacial topography on the performance of bilayer tablets. Int J Pharm 436:171-178.

26. Amidon GE, Akseli I, Goldfarb D, He X, Sun CC. Pharmacopeial Forum, 2014.

27. Sun W-J, Kothari S, Sun CC 2018. The relationship among tensile strength, Young's modulus, and indentation hardness of pharmaceutical compacts. Powder Technol 331:1-6.

28. Podczeck F, Drake KR, Newton JM, Haririan I 2006. The strength of bilayered tablets. Eur J Pharm Sci 29:361-366.

29. Inman SJ, Briscoe BJ, Pitt KG 2007. Topographic characterization of cellulose bilayered tablets interfaces. Chem Eng Res Des 85:1005-1012.

30. Podczeck F, Al-Muti E 2010. The tensile strength of bilayered tablets made from different grades of microcrystalline cellulose. Eur J Pharm Sci 41:483-488.

31. Busignies V, Mazel V, Diarra H, Tchoreloff P 2013. Role of the elasticity of pharmaceutical materials on the interfacial mechanical strength of bilayer tablets. Int J Pharm 457:260-267.

32. Ryshkewitch E 1953. Compression strength of porous sintered alumina and zirconia. J Am Ceram Soc 36:65-68.

33. Rees JE, Rue PJ 1978. Time-dependent deformation of some direct compression excipients. J Pharm Pharmacol 30:601-607.

34. Duberg M, Nyström C 1981. Studies on direct compression of tablets. Vi. Evaluation of methods for the estimation of particle fragmentation during compaction. Acta Pharm Suec 19:421-436.

35. Patel S, Sun CC 2016. Macroindentation hardness measurement—Modernization and applications. Int J Pharm 506:262-267.

36. Gong X, Sun CC 2015. A new tablet brittleness index. Eur J Pharm Biopharm 93:260-266.

37. Osei-Yeboah F, Sun CC 2015. Validation and applications of an expedited tablet friability method. Int J Pharm 484:146-155.

38. Paul S, Chang S-Y, Sun CC 2017. The phenomenon of tablet flashing—its impact on tableting data analysis and a method to eliminate it. Powder Technol 305:117-124.

39. Sun CC 2006. A material-sparing method for simultaneous determination of true density and powder compaction properties—Aspartame as an example. Int J Pharm 326:94-99.
40. Fell J, Newton J 1970. Determination of tablet strength by the diametral-compression test. J Pharm Sci 59:688-691.
41. Paul S, Sun CC 2017. The suitability of common compressibility equations for characterizing plasticity of diverse powders. Int J Pharm 532:124-130.
42. Train D 1956. An Investigation Into The Compaction Of Powders. J Pharm Pharmacol 8:745-761.

CHAPTER 4.

1. Desai D, Wang J, Wen H, Li X, Timmins P 2013. Formulation design, challenges, and development considerations for fixed dose combination (FDC) of oral solid dosage forms. Pharm Dev Technol 18:1265-1276.
2. Siew A 2014. Tackling challenges in the development of fixed-dose combinations. Pharm Technol 38:57.
3. Bangalore S, Kamalakkannan G, Parkar S, Messerli FH 2007. Fixed-dose combinations improve medication compliance: a meta-analysis. Am J Med 120:713-719.
4. Gupta AK, Arshad S, Poulter NR 2010. Compliance, safety, and effectiveness of fixed-dose combinations of antihypertensive agents: a meta-analysis. Hypertension 55:399-407.
5. Friedland GH, Williams A 1999. Attaining higher goals in HIV treatment: The central importance of adherence. AIDS 13:S61-72.
6. Patra C, Kumar A, Pandit H, Singh S, Devi M 2007. Design and evaluation of sustained release bilayer tablets of propranolol hydrochloride. Acta Pharm 57:479-489.
7. Nirmal J, Saisivam S, Peddanna C, Muralidharan S, Godwinkumar S, Nagarajan M 2008. Bilayer tablets of atorvastatin calcium and nicotinic acid: formulation and evaluation. Chem Pharm Bull 56:1455-1458.

8. Kulkarni A, Bhatia M 2010. Development and evaluation of regioselective bilayer floating tablets of Atenolol and Lovastatin for biphasic release profile. Iran J Pharm Res 8:15-25.

9. Shiyani B, Gattani S, Surana S 2008. Formulation and evaluation of bi-layer tablet of metoclopramide hydrochloride and ibuprofen. AAPS PharmSciTech 9:818-827.

10. Mandal U, Pal TK 2008. Formulation and in vitro studies of a fixed-dose combination of a bilayer matrix tablet containing metformin HCl as sustained release and glipizide as immediate release. Drug Dev Ind Pharm 34:305-313.

11. Department of Justice. October 26 2010. GlaxoSmithKline to Plead Guilty & Pay $750 Million to Resolve Criminal and Civil Liability Regarding Manufacturing Deficiencies at Puerto Rico Plant.

12. Kottala N, Abebe A, Sprockel O, Bergum J, Nikfar F, Cuitiño A 2012. Evaluation of ohe performance characteristics of bilayer tablets: Part I. impact of material properties and process parameters on the strength of bilayer tablets. AAPS PharmSciTech 13:1236-1242.

13. PharmTech. Mar 10 2005. US Marshals Seize Supplies of GSK Paxil CR, Avandamet. ed.

14. Osei-Yeboah F, Chang S-Y, Sun CC 2016. A critical Examination of the Phenomenon of Bonding Area - Bonding Strength Interplay in Powder Tableting. Pharm Res 33:1126-1132.

15. Sun CC, Kleinebudde P 2016. Mini review: Mechanisms to the loss of tabletability by dry granulation. Eur J Pharm Biopharm 106:9-14.

16. Osei-Yeboah F, Sun CC 2015. Tabletability modulation through surface engineering. J Pharm Sci 104:2645-2648.

17. Duncan-Hewitt WC 1996. Modeling the compression behavior of particle assemblies from the mechanical properties of individual particles. Drug Pharm Sci 71:375-418.

18. Ryshkewitch E 1953. Compression strength of porous sintered alumina and zirconia. J Am Ceram Soc 36:65-68.

19. Chang S-Y, Sun CC 2019. Insights into the effect of compaction pressure and material properties on interfacial bonding strength of bilayer tablets. Powder Technol 354:867-876.

20. Chang S-Y, Sun CC 2017. Superior Plasticity and Tabletability of Theophylline Monohydrate. Mol Pharm 14:2047-2055.

21. Sun C, Grant DJ 2001. Influence of crystal structure on the tableting properties of sulfamerazine polymorphs. Pharm Res 18:274-280.

22. Dey S, Chattopadhyay S, Mazumder B 2014. Formulation and evaluation of fixed-dose combination of bilayer gastroretentive matrix tablet containing atorvastatin as fast-release and atenolol as sustained-release. Biomed Res Int 2014.

23. Luo D, Kim JH, Park C, Oh E, Park J-B, Cui J-H, Cao Q-R, Lee B-J 2017. Design of fixed dose combination and physicochemical characterization of enteric-coated bilayer tablet with circadian rhythmic variations containing telmisartan and pravastatin sodium. Int J Pharm 523:343-356.

24. Yohannes B, Gonzalez M, Abebe A, Sprockel O, Nikfar F, Kiang S, Cuitiño A 2017. Discrete particle modeling and micromechanical characterization of bilayer tablet compaction. Int J Pharm 529:597-607.

25. Busignies V, Mazel V, Diarra H, Tchoreloff P 2014. Development of a new test for the easy characterization of the adhesion at the interface of bilayer tablets: Proof-of-concept study by experimental design. Int J Pharm 477:476-484.

26. Chang S-Y, Li J-X, Sun CC 2017. Tensile and shear methods for measuring strength of bilayer tablets. Int J Pharm 523:121-126.

27. Zhang J, Wu C-Y, Storey D, Byrne G 2017. Interfacial strength of bilayer pharmaceutical tablets. Powder Technol 337:36-42.

28. Rees JE, Rue PJ 1978. Time-dependent deformation of some direct compression excipients. J Pharm Pharmacol 30:601-607.

29. Duberg M, Nyström C 1981. Studies on direct compression of tablets. Vi. Evaluation of methods for the estimation of particle fragmentation during compaction. Acta Pharm Suec 19:421-436.

30. Patel S, Sun CC 2016. Macroindentation hardness measurement—Modernization and applications. Int J Pharm 506:262-267.

31. Gong X, Sun CC 2015. A new tablet brittleness index. Eur J Pharm Biopharm 93:260-266.
32. Osei-Yeboah F, Sun CC 2015. Validation and applications of an expedited tablet friability method. Int J Pharm 484:146-155.
33. Paul S, Chang S-Y, Sun CC 2017. The phenomenon of tablet flashing—its impact on tableting data analysis and a method to eliminate it. Powder Technol 305:117-124.
34. Sun CC 2006. A material-sparing method for simultaneous determination of true density and powder compaction properties—Aspartame as an example. Int J Pharm 326:94-99.
35. Fell J, Newton J 1970. Determination of tablet strength by the diametral-compression test. J Pharm Sci 59:688-691.
36. Al-Ibraheemi ZAM, Anuar M, Taip F, Amin M, Tahir S, Mahdi AB 2013. Deformation and mechanical characteristics of compacted binary mixtures of plastic (microcrystalline cellulose), elastic (sodium starch glycolate), and brittle (lactose monohydrate) pharmaceutical excipients. Part Sci Technol 31:561-567.
37. Dun J, Osei-Yeboah F, Boulas P, Lin Y, Sun CC 2018. A systematic evaluation of dual functionality of sodium lauryl sulfate as a tablet lubricant and wetting enhancer. Int J Pharm 552:139-147.
38. Kottala N, Abebe A, Sprockel O, Akseli I, Nikfar F, Cuitiño AM 2012. Influence of compaction properties and interfacial topography on the performance of bilayer tablets. Int J Pharm 436:171-178.
39. Hogan J 1989. Hydroxypropylmethylcellulose sustained release technology. Drug Dev Ind Pharm 15:975-999.

CHAPTER 5.

1. Shotton E, Ganderton D 1961. The strength of compressed tablets: III. The relation of particle size, bonding and capping in tablets of sodium chloride, aspirin and hexamine. J Pharm Pharmacol 13:144T-152T.
2. Sun C, Grant DJ 2001. Effects of initial particle size on the tableting properties of L-lysine monohydrochloride dihydrate powder. Int J Pharm 215:221-228.

3. McKenna A, McCafferty D 1982. Effect of particle size on the compaction mechanism and tensile strength of tablets. J Pharm Pharmacol 34:347-351.

4. Herting MG, Kleinebudde P 2007. Roll compaction/dry granulation: Effect of raw material particle size on granule and tablet properties. Int J Pharm 338:110-118.

5. Nyström C, Mazur J, Sjögren J 1982. Studies on direct compression of tablets II. The influence of the particle size of a dry binder on the mechanical strength of tablets. Int J Pharm 10:209-218.

6. Sebhatu T, Alderborn G 1999. Relationships between the effective interparticulate contact area and the tensile strength of tablets of amorphous and crystalline lactose of varying particle size. Eur J Pharm Sci 8:235-242.

7. Almaya A, Aburub A 2008. Effect of particle size on compaction of materials with different deformation mechanisms with and without lubricants. AAPS PharmSciTech 9:414-418.

8. Sun C, Himmelspach MW 2006. Reduced tabletability of roller compacted granules as a result of granule size enlargement. J Pharm Sci 95:200-206.

9. De Boer A, Vromans H, Leur C, Bolhuis G, Kussendrager K, Bosch H 1986. Studies on tableting properties of lactose. Pharmaceutisch weekblad 8:145-150.

10. Eriksson M, Alderborn G 1995. The effect of particle fragmentation and deformation on the interparticulate bond formation process during powder compaction. Pharm Res 12:1031-1039.

11. Desai D, Wang J, Wen H, Li X, Timmins P 2013. Formulation design, challenges, and development considerations for fixed dose combination (FDC) of oral solid dosage forms. Pharmaceutical development and technology 18:1265-1276.

12. Kulkarni A, Bhatia M 2010. Development and evaluation of regioselective bilayer floating tablets of Atenolol and Lovastatin for biphasic release profile. Iran J Pharm Res 8:15-25.

13. Nirmal J, Saisivam S, Peddanna C, Muralidharan S, Godwinkumar S, Nagarajan M 2008. Bilayer tablets of atorvastatin calcium and nicotinic acid: formulation and evaluation. Chem Pharm Bull 56:1455-1458.

14. Sun C, Grant DJ 2001. Influence of crystal structure on the tableting properties of sulfamerazine polymorphs. Pharm Res 18:274-280.

15. Osei-Yeboah F, Chang S-Y, Sun CC 2016. A critical Examination of the Phenomenon of Bonding Area - Bonding Strength Interplay in Powder Tableting. Pharm Res 33:1126-1132.

16. Joiris E, Di Martino P, Berneron C, Guyot-Hermann A-M, Guyot J-C 1998. Compression behavior of orthorhombic paracetamol. Pharm Res 15:1122-1130.

17. Chang S-Y, Sun CC 2019. Insights into the effect of compaction pressure and material properties on interfacial bonding strength of bilayer tablets. Powder Technol 354:867-876.

18. Chang S-Y, Sun CC Manuscript under review. Understanding the interfacial bonding mechanism of formulated bilayer tablets. Eur J Pharm Biopharm:Unpublished work.

19. Inman S, Briscoe B, Pitt K 2007. Topographic characterization of cellulose bilayered tablets interfaces. Chem Eng Res Des 85:1005-1012.

20. Abebe A, Akseli I, Sprockel O, Kottala N, Cuitiño AM 2014. Review of bilayer tablet technology. Int J Pharm 461:549-558.

21. Yohannes B, Gonzalez M, Abebe A, Sprockel O, Nikfar F, Kiang S, Cuitiño AM 2017. Discrete particle modeling and micromechanical characterization of bilayer tablet compaction. Int J Pharm 529:597-607.

22. Department of Justice. October 26 2010. GlaxoSmithKline to Plead Guilty & Pay $750 Million to Resolve Criminal and Civil Liability Regarding Manufacturing Deficiencies at Puerto Rico Plant.

23. Kottala N, Abebe A, Sprockel O, Bergum J, Nikfar F, Cuitiño A 2012. Evaluation of ohe performance characteristics of bilayer tablets: Part I. impact of material properties and process parameters on the strength of bilayer tablets. AAPS PharmSciTech 13:1236-1242.

24. Zhang J, Wu C-Y, Storey D, Byrne G 2017. Interfacial strength of bilayer pharmaceutical tablets. Powder Technol 337:36-42.

25. Chang S-Y, Li J-X, Sun CC 2017. Tensile and shear methods for measuring strength of bilayer tablets. Int J Pharm 523:121-126.

26. Paul S, Chang S-Y, Sun CC 2017. The phenomenon of tablet flashing—its impact on tableting data analysis and a method to eliminate it. Powder Technol 305:117-124.

27. Sun CC 2006. A material-sparing method for simultaneous determination of true density and powder compaction properties—Aspartame as an example. Int J Pharm 326:94-99.
28. Fell J, Newton J 1970. Determination of tablet strength by the diametral-compression test. J Pharm Sci 59:688-691.
29. Ryshkewitch E 1953. Compression strength of porous sintered alumina and zirconia. J Am Ceram Soc 36:65-68.
30. Sun CC, Kleinebudde P 2016. Mini review: Mechanisms to the loss of tabletability by dry granulation. Eur J Pharm Biopharm 106:9-14.
31. Sun CC 2008. Mechanism of moisture induced variations in true density and compaction properties of microcrystalline cellulose. Int J Pharm 346:93-101.
32. Duberg M, Nyström C 1981. Studies on direct compression of tablets. Vi. Evaluation of methods for the estimation of particle fragmentation during compaction. Acta Pharm Suec 19:421-436.
33. Patel S, Sun CC 2016. Macroindentation hardness measurement—Modernization and applications. Int J Pharm 506:262-267.
34. Gong X, Sun CC 2015. A new tablet brittleness index. Eur J Pharm Biopharm 93:260-266.
35. Osei-Yeboah F, Sun CC 2015. Validation and applications of an expedited tablet friability method. Int J Pharm 484:146-155.

CHAPTER 6.

1. Jayaprakash S, Halith SM, Pillai KK, Balasubramaniyam P, Firthouse PM, Boopathi M 2011. Formulation and evaluation of bilayer tablets of amlodipine besilate and metprolol succinate. Pharm Lett 3:143-154.
2. Mandal U, Pal TK 2008. Formulation and in vitro studies of a fixed-dose combination of a bilayer matrix tablet containing metformin HCl as sustained release and glipizide as immediate release. Drug Dev Ind Pharm 34:305-313.
3. Shiyani B, Gattani S, Surana S 2008. Formulation and evaluation of bi-layer tablet of metoclopramide hydrochloride and ibuprofen. AAPS PharmSciTech 9:818-827.

4. PharmTech. Mar 10 2005. US Marshals Seize Supplies of GSK Paxil CR, Avandamet. ed.

5. Department of Justice. October 26 2010. GlaxoSmithKline to Plead Guilty & Pay $750 Million to Resolve Criminal and Civil Liability Regarding Manufacturing Deficiencies at Puerto Rico Plant.

6. Kottala N, Abebe A, Sprockel O, Bergum J, Nikfar F, Cuitiño A 2012. Evaluation of ohe performance characteristics of bilayer tablets: Part I. impact of material properties and process parameters on the strength of bilayer tablets. AAPS PharmSciTech 13:1236-1242.

7. Zhang J, Wu C-Y, Storey D, Byrne G 2017. Interfacial strength of bilayer pharmaceutical tablets. Powder Technol 337:36-42.

8. Castrati L, Mazel V, Diarra H, Busignies V, Tchoreloff P 2017. Effect of the curvature of the punches on the shape of the interface and the delamination tendency of bilayer tablets. J Pharm Sci 106:1331-1338.

9. Zhang J, Wu C-Y, Storey D, Byrne G 2018. Interfacial strength of bilayer pharmaceutical tablets. Powder Technol 337:36-42.

10. Akseli I, Abebe A, Sprockel O, Cuitiño AM 2013. Mechanistic characterization of bilayer tablet formulations. Powder Technol 236:30-36.

11. Anuar MS, Briscoe BJ 2010. Interfacial elastic relaxation during the ejection of bi-layered tablets. Int J Pharm 387:42-47.

12. Inman SJ, Briscoe BJ, Pitt KG 2007. Topographic characterization of cellulose bilayered tablets interfaces. Chem Eng Res Des 85:1005-1012.

13. Kottala N, Abebe A, Sprockel O, Bergum J, Nikfar F, Cuitiño A 2012. Evaluation of the Performance Characteristics of Bilayer Tablets: Part II. Impact of Environmental Conditions on the Strength of Bilayer Tablets. AAPS PharmSciTech 13:1190-1196.

14. Klinzing G, Zavaliangos A 2013. Understanding the Effect of Environmental History on Bilayer Tablet Interfacial Shear Strength. Pharm Res 30:1300-1310.

15. Wu C-Y, Seville JP 2009. A comparative study of compaction properties of binary and bilayer tablets. Powder Technol 189:285-294.

16. Amin MCIM, Albawani SM, Amjad MW 2012. A comparative study of the compaction properties of binary and bilayer tablets of direct compression excipients. Trop J Pharm Res 11:585-594.

17. Niwa M, Hiraishi Y, Iwasaki N, Terada K 2013. Quantitative analysis of the layer separation risk in bilayer tablets using terahertz pulsed imaging. Int J Pharm 452:249-256.

18. Papós K, Kása Jr P, Ilič I, Blatnik-Urek S, Regdon Jr G, Srčič S, Pintye-Hódi K, Sovány T 2015. Effect of the surface free energy of materials on the lamination tendency of bilayer tablets. Int J Pharm 496:609-613.

19. Podczeck F, Drake KR, Newton JM, Haririan I 2006. The strength of bilayered tablets. Eur J Pharm Sci 29:361-366.

20. Podczeck F, Al-Muti E 2010. The tensile strength of bilayered tablets made from different grades of microcrystalline cellulose. Eur J Pharm Sci 41:483-488.

21. Busignies V, Mazel V, Diarra H, Tchoreloff P 2013. Role of the elasticity of pharmaceutical materials on the interfacial mechanical strength of bilayer tablets. Int J Pharm 457:260-267.

22. Podczeck F 2011. Theoretical And Experimental Investigations Into The Delamination Tendencies Of Bilayer Tablets. Int J Pharm 408:102-112.

23. Busignies V, Mazel V, Diarra H, Tchoreloff P 2014. Development of a new test for the easy characterization of the adhesion at the interface of bilayer tablets: Proof-of-concept study by experimental design. Int J Pharm 477:476-484.

24. Castrati L, Mazel V, Busignies V, Diarra H, Rossi A, Colombo P, Tchoreloff P 2016. Comparison of breaking tests for the characterization of the interfacial strength of bilayer tablets. Int J Pharm 513:709-716.

25. Chang S-Y, Li J-X, Sun CC 2017. Tensile and shear methods for measuring strength of bilayer tablets. Int J Pharm 523:121-126.

26. Sun CC, Hou H, Gao P, Ma C, Medina C, Alvarez FJ 2009. Development of a high drug load tablet formulation based on assessment of powder manufacturability: moving towards quality by design. J Pharm Sci 98:239-247.

27. USP, 2014. USP37/NF32 (Online), General Chapters: Tablet Friability. United States

Pharmacopoeial Convention, Rockville, MD.

28. Perumalla SR, Paul S, Sun CC 2016. Enabling the tablet product development of 5-fluorocytosine by conjugate acid base cocrystals. J Pharm Sci 105:1960-1966.

29. Wang C, Perumalla SR, Lu R, Fang J, Sun CC 2016. Sweet berberine. Cryst Growth Des 16:933-939.

30. Osei-Yeboah F, Sun CC 2015. Validation and applications of an expedited tablet friability method. Int J Pharm 484:146-155.

31. Rees JE, Rue PJ 1978. Time-dependent deformation of some direct compression excipients. J Pharm Pharmacol 30:601-607.

32. Duberg M, Nyström C 1981. Studies on direct compression of tablets. Vi. Evaluation of methods for the estimation of particle fragmentation during compaction. Acta Pharm Suec 19:421-436.

33. Patel S, Sun CC 2016. Macroindentation hardness measurement—Modernization and applications. Int J Pharm 506:262-267.

34. Gong X, Sun CC 2015. A new tablet brittleness index. Eur J Pharm Biopharm 93:260-266.

35. Rehula M, Adamek R, Spacek V 2012. Stress relaxation study of fillers for directly compressed tablets. Powder Technol 217:510-515.

36. Chang S-Y, Sun CC 2019. Insights into the effect of compaction pressure and material properties on interfacial bonding strength of bilayer tablets. Powder Technol 354:867-876.

37. Griffith AA 1921. VI. The phenomena of rupture and flow in solids. Philosophical transactions of the royal society of london Series A, containing papers of a mathematical or physical character 221:163-198.

Appendix I. Relationship between hydrate stability and accuracy of true density measured by helium pycnometry

Synopsis

Mechanical properties of a material, such as hardness and elastic modulus, depend on porosity exponentially. Thus, accurate characterization of material mechanical properties requires correct porosity, which depends on the accuracy of measured true density. Helium pycnometry is the most common technique for determining true density of a powder material but it is not suitable for materials containing volatile components. For unstable hydrates, dehydration during measurement releases water and invalidates the ideal gas law used for calculating sample volume. Consequently, measured true density is over-estimated, which causes gross errors in mechanical properties extrapolated to zero porosity. This work shows that physical stability and the dehydration kinetics, determined by both types of water-bonding structures and bonding energy, directly affect the magnitude of error in measured true density.

Introduction

The true density of a substance may be defined as "the average mass per unit volume, exclusive of all voids that are not a fundamental part of the molecular packing arrangement. [1 1 1 1 1 1 1 1 1] In the context of solid mechanics, true density is a critical material property because it is required to calculate porosity of tablets, granules, and other solid specimens. Porosity is vital in controlling several important material properties and functions of solids, including mechanical strength, [2] drug dissolution, [3] gas adsorption capacity, [4] effectiveness of catalysts.[5] As a useful parameter to describe tablet structure,[6] important pharmaceutical properties of tablet, such as tablet tensile strength, [2] Young's modulus, [7] indentation hardness, [8,9] brittleness, [10,11] friability, [12] and disintegration time, [8,13] depend on tablet porosity. Extrapolation of the property – tablet porosity relationship to zero porosity provides insight into intrinsic properties of the material. However, results from such extrapolation are very sensitive to errors in true density (Figure A.1). [14] For example, a 5% error in true density can lead to a 60% error in the property extrapolated to zero porosity. [14] Fitting porosity-compaction pressure by an appropriate model, e.g., the Heckel equation [15-17] or Kuentz-Leuenberger equation,[18,19] can yield parameters that correlate with material plasticity, which plays a central role in powder compaction. A more plastic material undergoes more permanent plastic deformation during compaction, which facilitates the development of tablet mechanical strength by effectively reducing tablet porosity and forming larger bonding area between neighboring particles. [20] The tabletability (tensile strength vs. compaction pressure) of viscoelastic powders depends on compaction speeds, which is usually faster during scale up and commercial manufacturing. However, the much less dependence on compaction

speed makes powder compactibility (tensile strength vs. tablet porosity) useful to guide the scale up of a tableting process.[8,21] Clearly, accurate porosity is important in all above mentioned applications. As a result, the role of porosity on powder compaction is of particular relevance to pharmaceutical tablet formulation and manufacturing.

To calculate tablet porosity (ε), tablet density (ρ_{tablet}) and true density of the powder (ρ_{true}) are required (Eqn. 1). The ρ_{tablet} can be calculated from tablet weight and volume. For tablets with a simple geometry, e.g., rectangular, square, or cylindrical tablets, dimensions can be conveniently and accurately measured using a caliper to calculate volume, provided tablet flashing is properly removed. [22] For a tablet with a complex geometry, tablet volume can be measured using an appropriate envelop density analyzer. [23]

$$\varepsilon = 1 - \frac{\rho_{tablet}}{\rho_{true}} \qquad (1)$$

For highly plastic powders, tablet density after the compression - decompression cycle generally approaches true density, i.e., ε approaches zero, with increasing compaction pressure, as long as any phase transformation and macro defects are absent. However, for less compressible powders that do not reach zero porosity even under relatively high pressures, helium pycnometry is the most commonly used instrument to measure powder true density because it is straightforward to perform, applicable to powder mixtures, and the measurement is conducted at the ambient temperature. Helium pycnometry measures sample volume by monitoring pressure change when helium gas expands to a chamber of known volume (Figure A.2), based on the ideal gas law with the assumption of constant total number of gas molecules in a closed system. The true density of the material can

then be calculated from the sample weight and measured volume. Helium pycnometry can yield adequately accurate true density of materials if no sealed pores are present in the sample because helium is small enough to enter pores or crevices larger than 0.2 nm in size. [24-26] However, significant errors can be introduced if a sample releases volatile components into the helium atmosphere, such as dehydration of water-containing materials, during the course of measurement. [24] Such an effect by surface water can be eliminated by purging the sample in situ to eliminate a small amount (usually < 0.5%) of surface water before starting the measurement. However, helium purging or rigorous drying before helium pycnometry is unfit for samples containing significant amount of water. For example, a hydrate can transform to a lower degree hydrate or an anhydrate with a different true density than the original hydrate. [27] In addition, the density of a hygroscopic polymer depends on water content.[28,29] Thus, a completely dried sample possesses true density different from that of the sample in its natural state before drying. However, despite the inherent problem with water-containing materials, helium pycnometry has been routinely used to measure true density of hydrates in the literature. [30-34]

It is conceivable that the impact of dehydration of sample during helium pycnometric measurement depends on the dehydration kinetics. Faster water removal during measurement is expected to result in larger errors. The stability of a hydrate depends on its crystal structure and strength of interactions between water and host molecules. Different types of hydrates, such as isolated hydrates, channel hydrate, and ion assisted hydrates, likely exhibit different stability. For stable hydrates, it is still possible to obtain accurate true density using helium pycnometry. However, the relationship between

dehydration kinetics and accuracy of measured true density by helium pycnometry has not been systematically explored. The goals of the present work were to 1) quantify the impact of the dehydration kinetics of hydrates on accuracy of true density measurement by helium pycnometry and 2) explain diverse dehydration kinetics of crystalline hydrates by considering their crystal structures and interaction energies.

Materials and Methods

Materials

Sodium chloride (NaCl, EMD, lot VL13L, Darmstadt, Germany), theophylline anhydrous (THa, BASF, Lot 045701AX10, Ludwigshafen, Germany), p-hydroxybenzoic acid anhydrous (HBAa, Aldrich, Batch 11718LA, St. Louis, MO), lactose monohydrate (LM, Sigma, lot 85H0770, St. Louis, MO) were used in this work. NaCl and LM were used as received. THa and HBAa, were dried at 40 ˚C in a container with Drierite until a constant weight was attained. Theophylline monohydrate (THm) was prepared by cooling a 70 ˚C saturated aqueous solution of theophylline to room temperature. The needle-shaped THm crystals were gently ground to reduce particle size and stored at 57% RH prior to further analysis to avoid unintended dehydration of THm. [35] HBA monohydrate (HBAm) was obtained using vapor mediated conversion by equilibrating 10 g of as-received HBAa in a 93% RH chamber with intermittent stirring using a spatula until a constant weight was attained after one week. [36]

Methods

True Density Measurement by Helium Pycnometry

A helium pycnometer (Ultrapyc 1200e) was used to measures true density. System performance was verified using a standard stainless ball with known volume before testing each new material to ensure accuracy. An accurately weighed sample was placed in the sample cell and the lid was closed. Approximately 75% of the sample cell volume was filled by the sample, as instructed in the instrument manual. [37] Helium was purged through the chambers for 10 min to remove air and moisture in the chambers. After the valve between the sample and expansion chambers was closed. Helium was introduced into the sample chamber until the preset pressure (~17 Pa) was reached. The system was given 300s to stabilize before the chamber pressure, P_1, was recorded. The valve was then opened to allow pressurized helium in the sample chamber flow into the expansion chamber and establish a new pressure, P_2, in 300 s. The volume of the sample was calculated using Eqn. (2).

$$V_{Sample} = V_{Cell} + \frac{V_{Exp}}{\frac{P_1 - Pa}{P_2 - Pa} - 1} \qquad (2)$$

Where V_{Sample}, V_{Cell} , V_{Exp} are sample volume, sample cell volume, and expansion cell volume, respectively. P_a is the ambient pressure. Each run of the above-mentioned procedure generates a sample volume value. When the volume standard deviation (VSD) of last five runs was smaller than 0.005 %, the average of the last five values was taken as sample volume. The measurement cycle was terminated after 100 runs if VSD did not reach within 0.005 %. Finally, true density was calculated after each run from the sample

weight and the measured volume. Within each measurement cycle, measured density from individual runs usually rose to a plateau. In this work, only values from the last five runs in a cycle are shown for visual clarity.

Powder X-ray Diffraction (PXRD)

X-ray powder diffraction pattern was obtained on a wide-angle diffractometer (Bruker-AXS D5005, Siemens) using a 2.2 kW sealed Cu Kα source run at 45 kV voltage and 40 mA amperage. Each sample was scanned with a step size of 0.02° in the two theta range of 5−35° and a dwell time of 0.5 s. Powders were gently pressed by a glass slide to ensure the surfaces of powder and the holder were coplanar.

Dynamic Vapor Sorption (DVS)

Dehydration kinetics of the materials was studied using an automated moisture balance (DVS 1000, Surface Measurement Systems Ltd., Alperton, Middlesex, UK) at 25 °C. The nitrogen flow rate was 50 mL/min. Before being exposed to 0% RH to record the weight loss, the sample was equilibrated for at least 12 hours at 95% RH. Weight vs. time data was plotted to assess dehydration kinetics.

Crystal Energy Framework

Crystallographic information files (cif) of THm (Refcode: THEOPH01), HBAm (Refcode: PHBZAC01), and LM (Refcode: LACTOS10) were retrieved from the Cambridge Structural Database. Crystal structure visualization was performed using Mercury (v3.7, Cambridge Crystallographic Data Centre, Cambridge, UK). The pairwise intermolecular interaction energy was estimated with B3LYP-D2/6-31G(d,p) molecular wavefunctions using the experimental crystal geometry (CrystalExplorer V.17 and Gaussian09).[38,39] Before each calculation, hydrogen atoms were automatically placed at bond lengths corresponding to standard neutron diffraction values. The intermolecular interaction energy was the sum of electrostatic, polarization, dispersion and exchange-repulsion terms. Each term was properly scaled based on values from a large training set.[40,41] The total interaction energies of water with all molecules having any atom within 3.8 Å were calculated and summed to obtain the total energy. The water – host molecule interaction energies were represented by cylinders, where cylinder thickness was proportional to the total intermolecular interaction energy. The interaction energies below 5 kJ/mol were omitted from the graph for clarity.

RESULTS

System calibration and performance verification

Using the stainless steel sphere with a volume of 7.0699 cm^3, calibration of helium pycnometry was carried out by following the procedure prescribed in the instrument user manual. After the calibration, the accuracy and stability of helium pycnometer was verified by measuring the true density of the same standard stainless ball with sample weight of 7.0699 g entered. As expected for accurate volume measurement, the reported

density was unity (1.0009 g/cm^3 ± 0.0009, n = 30) (Figure A.S1), with a relative standard deviation < 0.1%.

Crystalline anhydrates

NaCl, THa, and HBAa powders were used as control samples to check any unexpected measurement errors for measuring real powder samples that do not release volatile medium during the measurement (Figure A.3). The measured true density of NaCl, 2.156 ± 0.001 g/cm^3, was 0.4% lower than the true density value calculated from a room temperature crystal structure (2.166 g/cm^3). [42] The measured true density of THa, 1.493 ± 0.001 g/cm^3 , was identical to the density (1.493 g/cm^3) calculated from its single crystal structure determined at room temperature. [43] The measured true density of HBAa, 1.468 ± 0.0005 g/cm^3, was 1.9% lower than the calculated density (1.497 g/cm^3) based on crystal structure determined at room temperature. [44]

All three anhydrous materials showed negligible change in weight (< 0.02%) after the first few cycles (Figure A.3). The consistent small weight gain of THa after true density measurement is attributed to a smaller error in initial weight of the sample. Thereafter, the density measurement was continuously performed without taking out the samples for weighing to avoid any possible water adsorption during sample handling. At the end of the whole experiment, sample weight was again measured. No weight change was observed for all samples. Thus, the measured sample true densities were considered accurate within the system accuracy, since no volatiles were released by the samples.

Crystalline hydrates

The PXRD pattern of ground THm matches that calculated from the single crystal structure determined at 173 K, where the small peak shifts to higher two-theta angles in the simulated XRD pattern were attributed to the phenomenon of crystal lattice contraction upon cooling (Figure A.S2). [45] The PXRD pattern of HBAm matched excellently with that of calculated PXRD (Figure A.S3), confirming phase purity.

Both THm and HBAm powders dehydrated during pycnometric measurement, shown as the progressive decrease in sample weight after each cycle of measurement until the weight corresponding to pure anhydrous powder was reached (Figure A.4a & Figure A.4b). In both cases, the measured true density values were higher than those calculated from the single crystal structures of THm (173 K) and HBAm (room temperature). [46,47] Thus, dehydration caused over-estimation of measured true density of these two hydrates. Considering the calculated true density of THm from the sub-ambient temperature crystal structure is higher than that at room temperature because of the thermal expansion effect, [48] the helium pycnometry overestimated true density value even more. It is interesting to point out that the positive deviation from the expected true density of both hydrates increased with repeated cycles and reached the maximum, corresponding to the near completion of the dehydration reaction. With additional measurement cycles, the measured true density quickly dropped to the value of the corresponding anhydrates.

In contrast to THm and HBAm, LM does not undergo detectable weight loss during pycnometric measurement. Correspondingly, the measured density (1.547 ± 0.005 g/cm^3) was comparable to the calculated density from a single crystal structure solved at room temperature, 1.543 g/cm^3 (Figure A.4c). [49]

Discussion

Anhydrous materials

The results from the standard stainless sphere suggested that the instrument is capable of better than 0.1% accuracy and precision (Figure A.S1). Thus, the accuracy of measured true density of a sample is at best ~0.1%. Because of the volumetric nature of the pycnometric measurements, relative accuracy of the measured density results depends on total volume of the measured sample. Therefore, if the same sample weight is used, the error in the measured true density is proportional to the actual true density. Although anhydrous materials do not contain water in the lattice, surface adsorbed moisture is still expected, the amount of which depends on the environment. Such surface moisture can generally be eliminated by the helium purge (10 min in this work) at the beginning of each cycle and prior to each true density measurement.

NaCl is an inorganic material with high purity and degree of crystallinity. The measured true density (2.156 g/cm^3) is 0.4% lower than the true density value calculated from its room temperature crystal structure (Figure A.3a). Since the pycnometer gives a 0.09% deviation from the ideal value for the standard sphere, the measured true density of NaCl is significantly lower than that of a perfect NaCl crystal. Because the measured values are repeatable (Figure A.3), this discrepancy is not due to random events during measurement. We have attributed it to the presence of imperfections in NaCl crystals, which reduces packing efficiency and density, instead of measurement errors. This view is supported by the observation that the true density value of THa measured by the

helium pycnometry (1.493 ± 0.001 g/cm^3) is identical to that calculated from the single crystal structure (1.493 g/cm^3) in Figure A.3b. The true density values of THa suggests that, within the error of the experiment, the crystallinity of the THa sample was 100%. This high degree crystallinity of THa is consistent with its fast crystallizing tendency. [50] The assertion of accuracy in the measured density is important for interpreting measured true density of HBAa (1.468 ± 0.0005 g/cm^3), which is 1.9% lower than the calculated density (1.497 g/cm^3) in Figure A.3c. This data strongly suggests that the crystals in the HBAa commercial sample are considerably disordered. This is supported by the observation that the measured density of HBAa dehydrated from HBAm by exposing to helium during density measurement, 1.478 g/cm^3, is closer to the calculated density of a perfect HBAa crystal (1.2% lower). Thus, the commercial manufacturing process of HBAa likely involved more stressful conditions than drying by helium and generated more defects. The relative standard deviations of measured density from the last cycle for the three anhydrates ranged 0.02% - 0.07%, indicating high precision of the helium pycnometric measurement for physically stable materials. Overall, the helium pycnometry generated accurate and precise true density values for these crystalline anhydrates.

Although the true density of a crystalline solid may be approximated by calculation from the corresponding single crystal structures (cell volume and molecular content in the unit cell), not every material has solved crystal structure. Also, sub-ambient temperatures are routinely used to improve quality of the solved crystal structure. This usually leads to higher calculated density because of the contraction of unit cell volume at lower temperatures.[48,51,52] Even for crystal structures solved at ambient temperature, the

calculated true density is for a perfect crystal, which is higher than real crystals that often contain defects, such as in the cases of HBAa and NaCl.

Unstable hydrates

The measured density of THm and HBAm (Figure A.4a & Figure A.4b) is always higher than that calculated from its single crystal structure. In the case of THm, the calculated true density (1.476 g/cm^3) from the single crystal structure of THm solved at ~173 K is expected to be higher than that at room temperature. Yet, the measured density values are still significantly higher. This means that the error in measured density introduced by dehydration of THm is even more significant.

When dehydration occurs, the released water molecules enter the gas phase and increase the total number of gas molecules in the system. This introduces a positive error into the measured pressure of P_2, which leads to a smaller estimated volume of the sample according to Eqn. (2). Consequently, the measured density is larger than that without dehydration. The faster water releasing into the gas phase, the larger positive deviation is expected.

With repeated number of run, both THm and HBAm underwent weight loss nearly linearly (Figure A.4a & Figure A.4b). This was accompanied by the gradual increase in the deviation of measured density from their actual true density until the complete dehydration was nearly completed. This trend in measured true density can be explained by the constant dehydration kinetics and the gradual conversion of hydrates to corresponding higher true density anhydrates with time. The constant dehydration rate

means the same amount of water was released during every run, which would have introduced the same amount of error to the volume measurement. At the same time, the denser anhydrous crystal occupies smaller volume. Consequently, measured true density by helium pycnometry increased as the dehydration proceeded because of the presence of a higher fraction of anhydrate. Near the end of dehydration of THm, the rate of dehydration was noticeably slower (Figure A.4a). This corresponded to the gradual decrease of the measured true density to eventually reach the value of THa when the conversion from THm to THa completed (Figure A.4a). For HBAm, dehydration rate maintained constant until completion, which is accompanied by the immediate drop in measured true density to that of the HBAa (Figure A.4b). In both cases, accurate true density of the unstable hydrate could not be obtained by helium pycnometry.

These two hydrates showed distinct dehydration kinetics, which resulted in different extents of elevation in true density measurement. HBAm lose 0.2567 g of water over 1425 runs (0.18 mg/run) while THm lose 0.3628 g of water over 3447 runs (0.105 mg/run) (Figure A.4a & Figure A.4b). Thus, the dehydration rate of HBAm is approximately 80% faster than that of THm. When assessed under continuous flow of dry nitrogen in DVS, the dehydration kinetics of THm (0.04 mg/min) was again slower than HBAm (0.1 mg/min) in the linear range of the plot (Figure A.5e & Figure A.5f). The nearly first order dehydration kinetics of THm and the zero order dehydration kinetics of HBAm may be related to the channeled and isolated hydrate structures, respectively. The maximum deviation from the accurate density of HBAm (15% or 0.15 g/mL) is about 3 times that of THm (5% or 0.05 g/mL). This correlation between faster dehydration and

larger error in measured true density confirms the expected role of released water on the accuracy of measured true density.

However, the rate of dehydration is affected by not only the inherent stability of a hydrate but also the surface area. Therefore, we also examined stability of hydrates using energy framework to more firmly link true density measurement errors with kinetic stability of hydrates. THm shows a typical structure of a channel hydrate, in which each water molecule is connected to two other water molecules on either sides along the water chain via a O-H···O hydrogen bond (2.726 and 2.744 Å) (Figure A.5a). Each water molecule also interacts with a nearby theophylline dimer through a O-H···N hydrogen bond (2.900 Å). The energy framework suggests removing water from the THm crystal requires overcoming the energy barrier of -76.3 kJ/mol (Figure A.5c). In HBAm, water molecules are isolated from each other (Figure A.5b). Each water molecule connects to three surrounding HBA molecules through three O-H···O hydrogen bonds (2.603, 2.811, and 2.827 Å) for a total of -83.4 kJ/mol interaction energy (Figure A.5d). HBAm possessed higher energy barrier (-83.4 kJ/mol) than THm (-76.3 kJ/mol) for water removal. This suggests that isolated hydrates are not necessarily always more stable than channel hydrates. Despite the higher energy barrier for dehydration, HBAm still exhibited faster dehydration rate than THm. This is explained by the larger particle size of THm than HBAm, which reduced the dehydration rate THm. Although a complete separation of the effects by surface area and inherent stability is beyond the scope of this work, it is useful to mention that the prediction of hydrate stability based on packing features alone may be erroneous without considering particle size, environment humidity, and water – host interaction energy.

Stable hydrates

As shown earlier, the release of water from a crystalline hydrate affects the accuracy of measured true density when dehydration occurs during pycnometric measurement. However, when a hydrate does not undergo dehydration when exposed to dry helium, no error due to water release on measured true density is expected. LM is an example of such stable hydrate, which did not loss lattice water after true density measurement using helium pycnometry (Figure A.4c) or during continuous dry nitrogen purge (Figure A.6c). The initial slight weight loss (~0.5%) when RH was changed from 95% to 0% corresponds to surface adsorbed water. The weight essentially did not change during an 18 hr period after surface moisture was removed by dry nitrogen. Correspondingly, true density of LM measured by helium pycnometry matched well with calculated density. Therefore, accurate true density of hydrates can be acquired as long as no water is released during pycnometric measurement. The excellent stability of LM implies strong interactions between water and lactose molecules. LM is also an isolated hydrate, where each water molecule forms an O-H···O hydrogen bond (2.736, 2.762, 2.775, and 2.949Å) with one of four surrounding lactose molecules (Figure A.6a) for a total interaction energy of -114.5 kJ/mol (Figure A.6b). Thus, removing water from LM requires overcoming a significantly higher energy barrier than HBAm and THm. Therefore, in the case of predicting stability of hydrates, the quantitative energy framework approach is more reliable than the qualitative crystal structure visualization. However, accurate assessment of hydrate stability should be performed experimentally instead of solely

relying on crystal structure analysis before the relationship between interaction energy and stability is established.

Conclusions

Despite its convenience and wide acceptance in measuring true density, helium pycnometry must be applied with caution. Accurate true density cannot be obtained for unstable hydrates that release lattice water when exposed to dry helium during measurement. The accuracy of measured density value of a hydrate strongly correlate with its solid-state stability. Sample dehydration causes positive deviation in measured true density and the effect is greater for less stable hydrates. A hydrate is more stable when the strength of interactions between water and host molecules is stronger. Therefore, solid-state stability must be confirmed before helium pycnometry is applied to measure true density of a hydrate. Conversely, the magnitude of relative error in measured true density may be used to assess stability of crystalline hydrates.

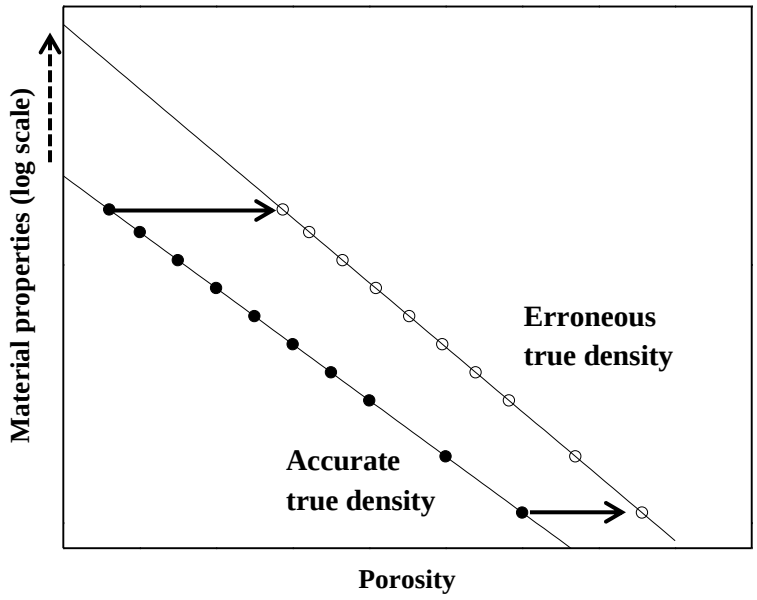

Figure A.1 The effect of overestimated true density on extrapolated material properties (hardness, elastic moduli, tensile strength, and brittleness) to zero porosity. The horizontal shift of porosity for each measured values of material property leads to significant shift in the extrapolated properties at zero porosity.

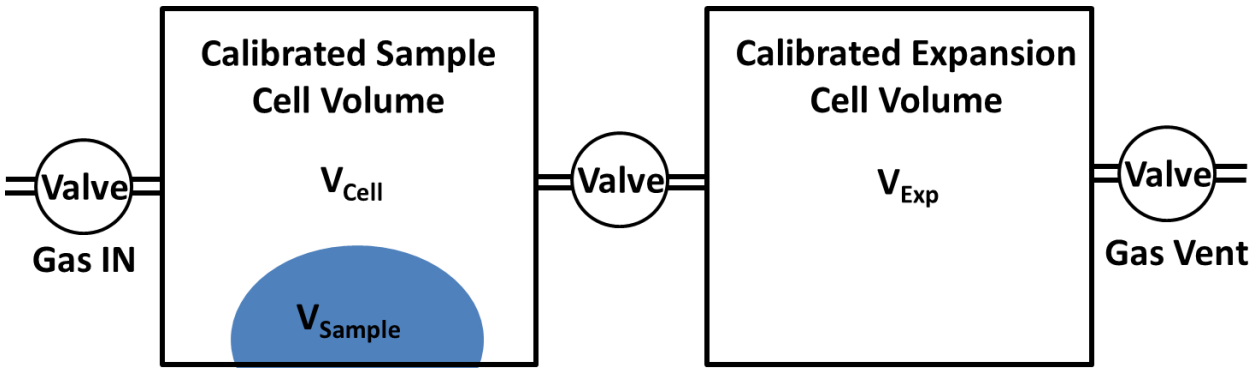

Figure A.2 Schematic illustration of the key components in a helium pycnometer.

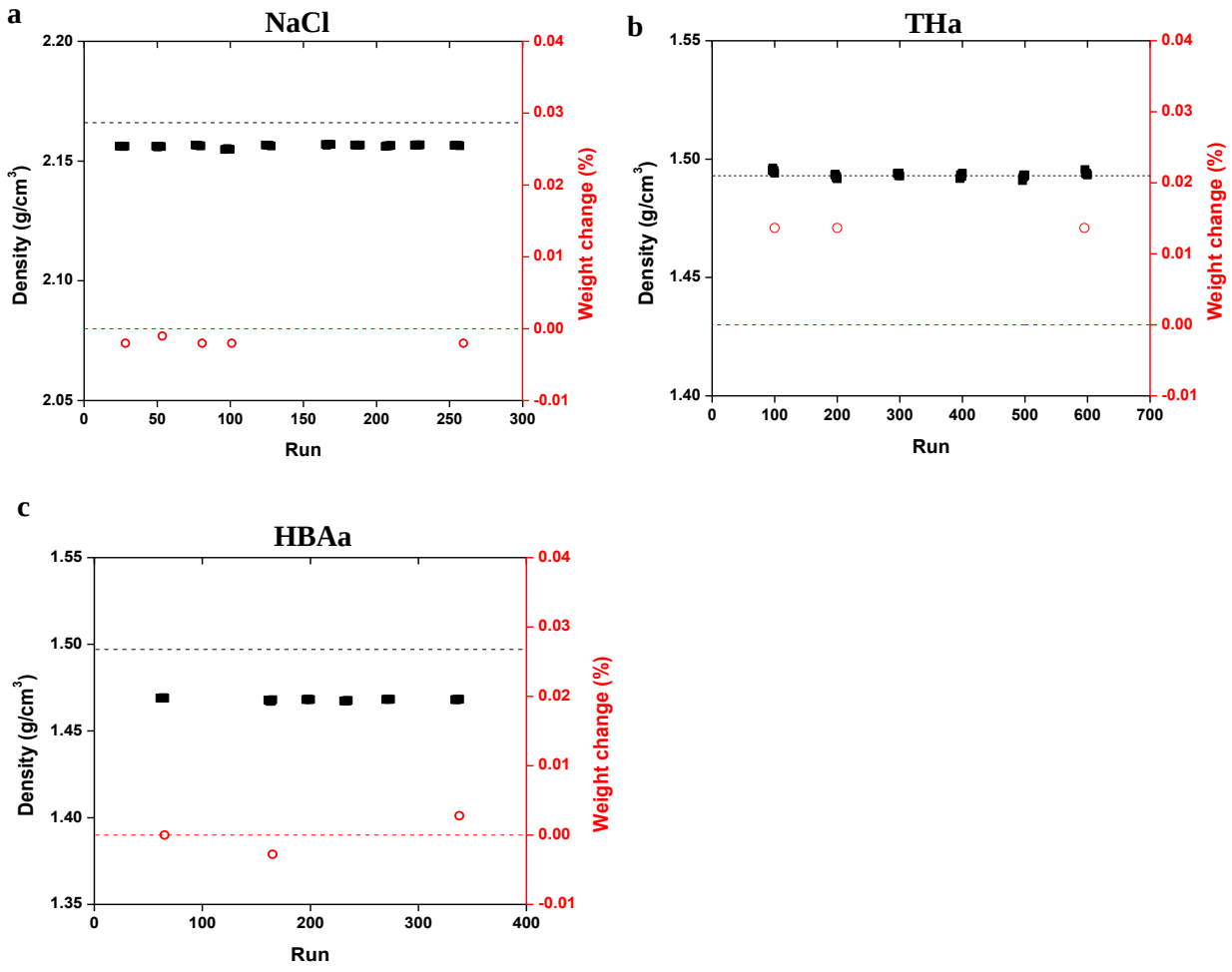

Figure A.3 Measured true density (solid squares) and sample weight (open circles) as a function of number of runs for a) NaCl, b) THa, and c) HBAa. Upper dashed line in each graph is the calculated density from each corresponding single crystal structure and lower dashed line is initial sample weight.

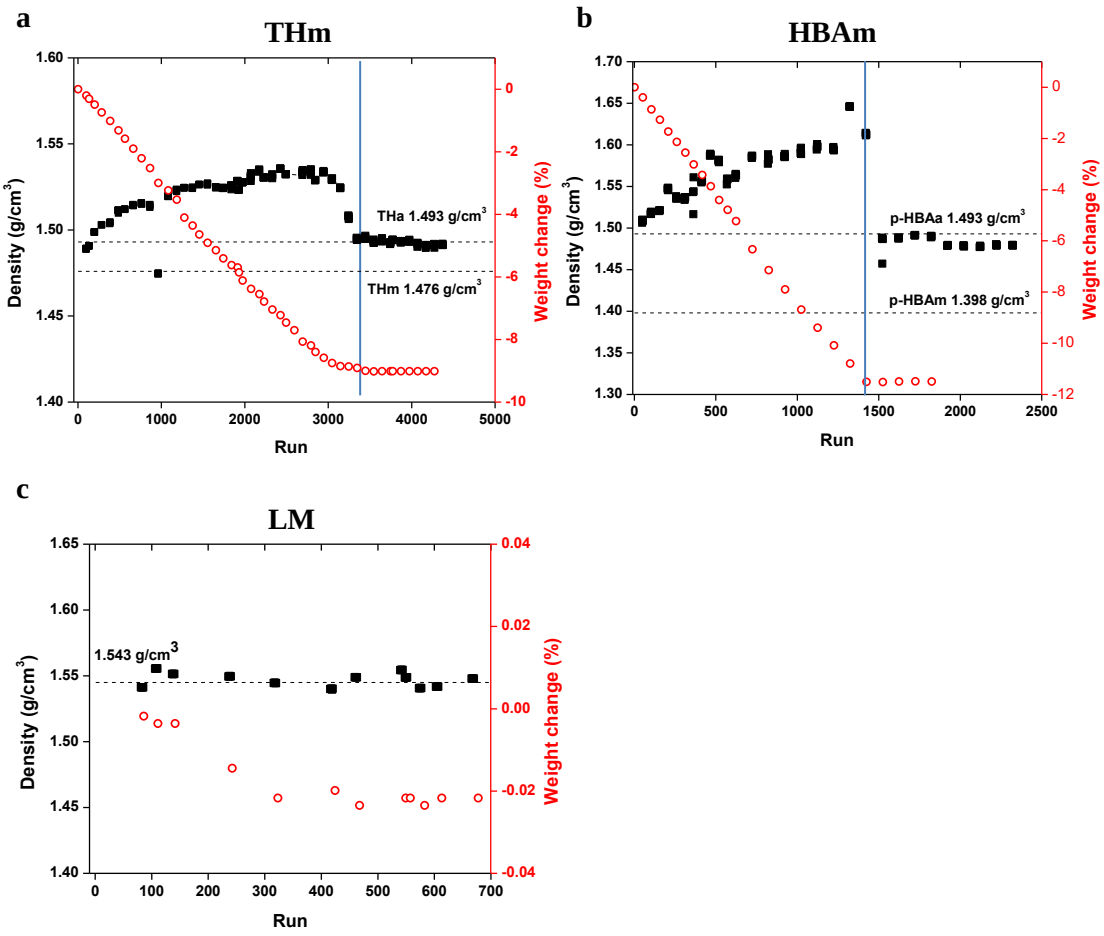

Figure A.4 Measured true density (solid squares) and weight change (open circles) as a function of run for a) THm, b) HBAm and c) LM. Dashed lines indicate density values calculated from corresponding single crystal structures with values shown.

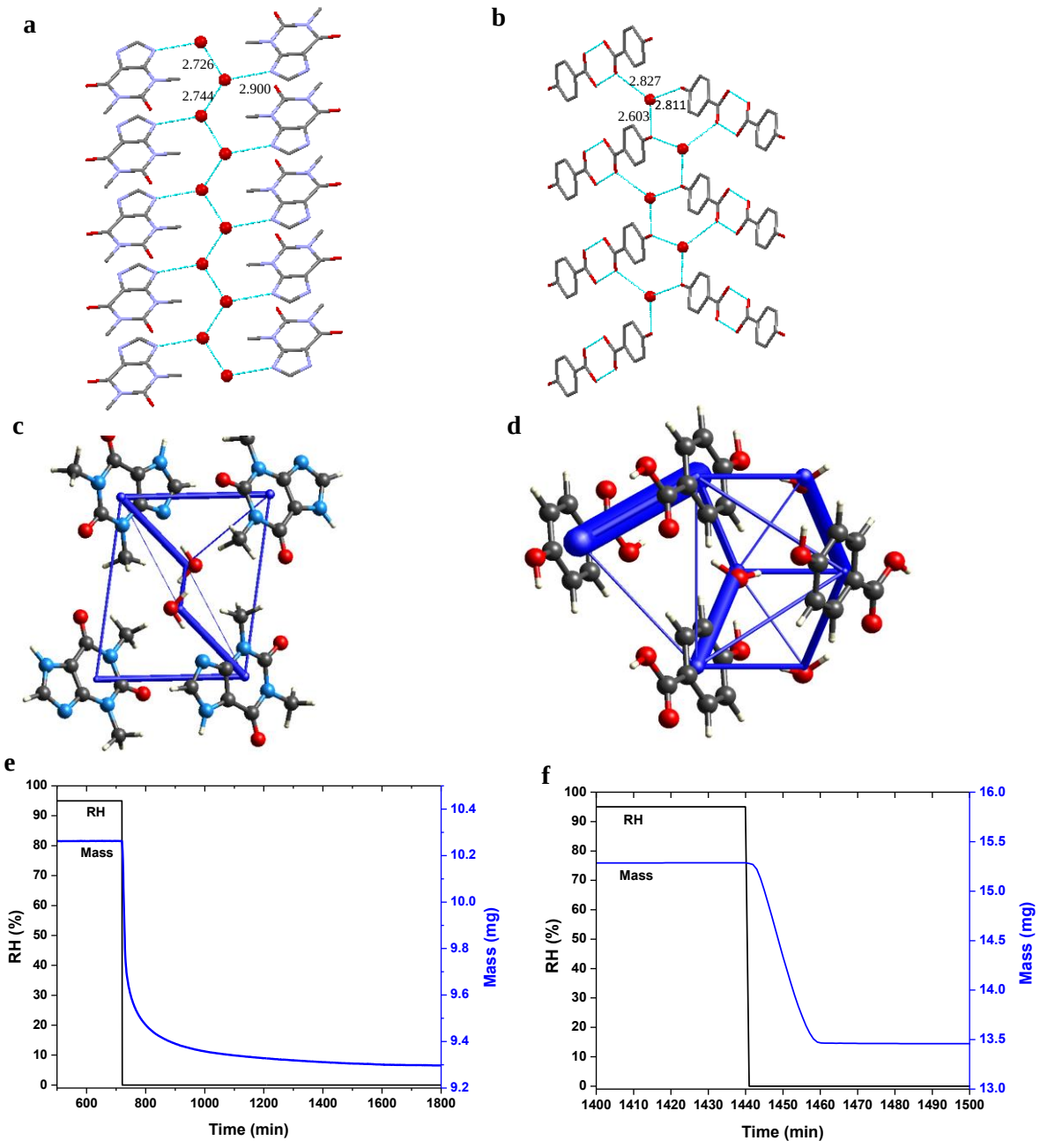

Figure A.5 Crystal structures of a) THm and b) p-HBAm. Energy framework of c) THm and d) HBAm. Drying curves in DVS of e) THm and f) HBAm. Samples were equilibrated in 95% RH for 12 hours for THm and 24 hours for HBAm before drying at 0% RH.

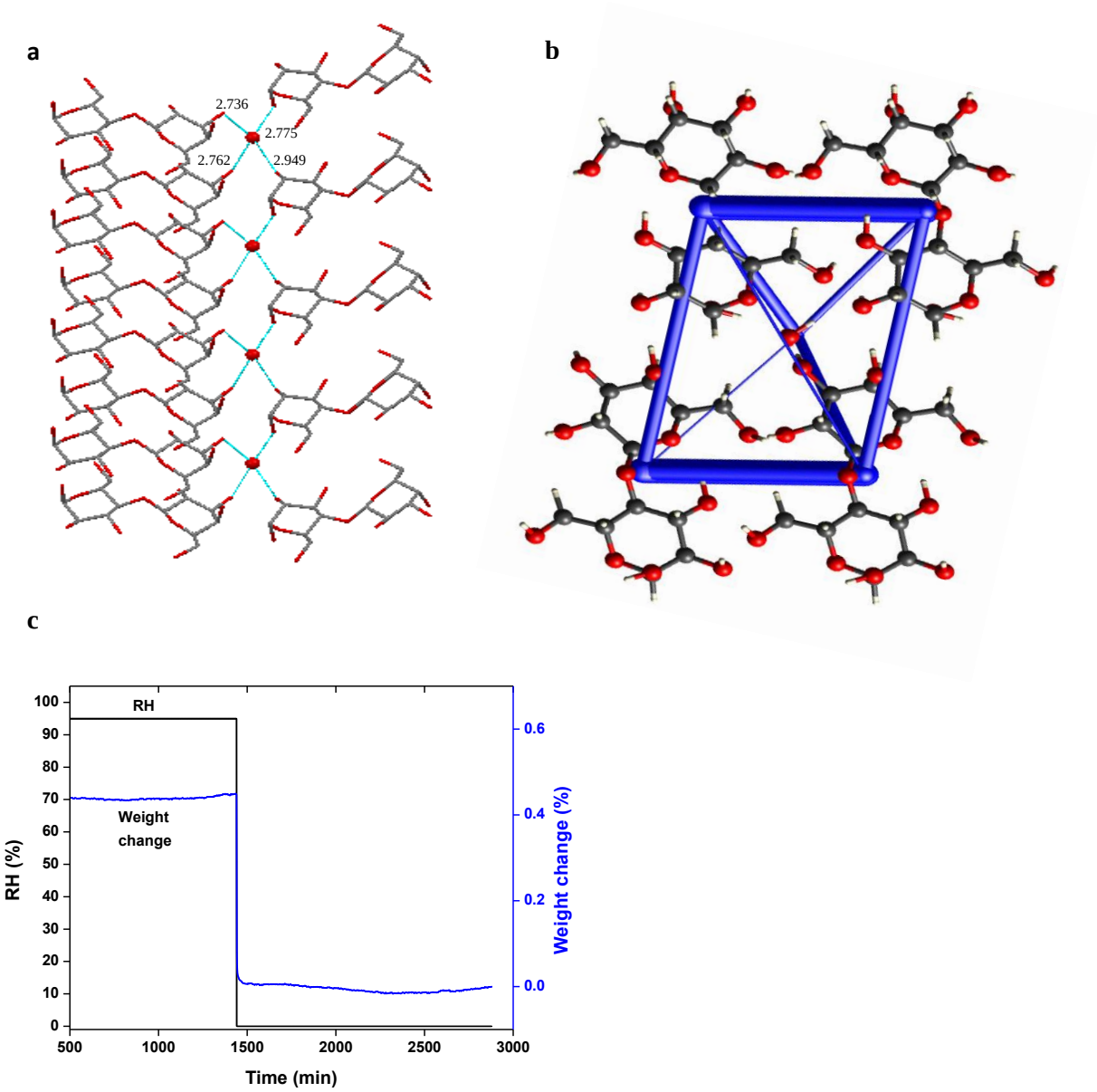

Figure A.6. a) LM crystal structure (hydrogen bond lengths are indicated). b) Energy framework of LM. c) Drying curves of LM in DVS under nitrogen purge. Samples were equilibrated in 95% RH for 24 hours before drying at 0% RH.

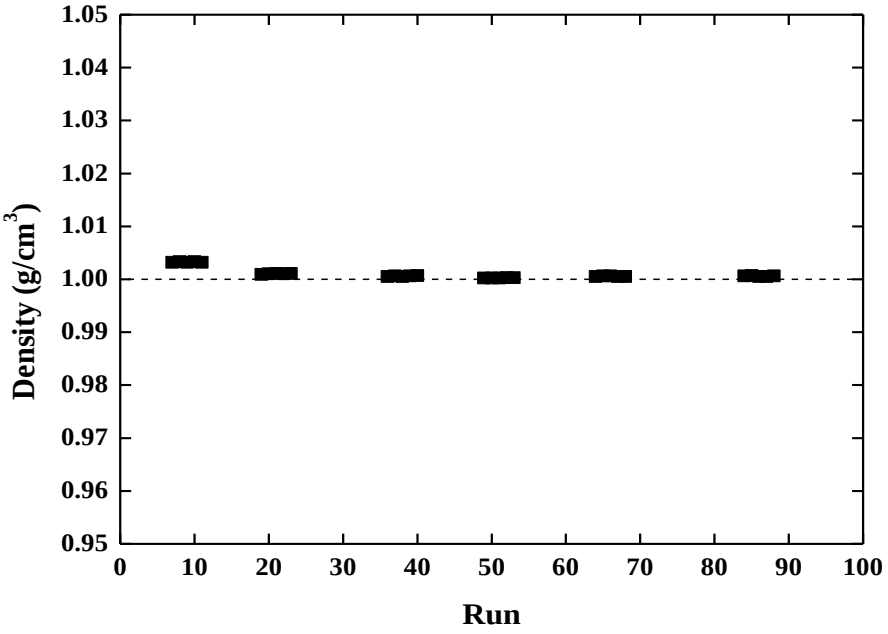

Figure A.S1 Measured true density of a standard stainless ball as a function of number of runs. The dashed line is at 1.00 g/cm^3.

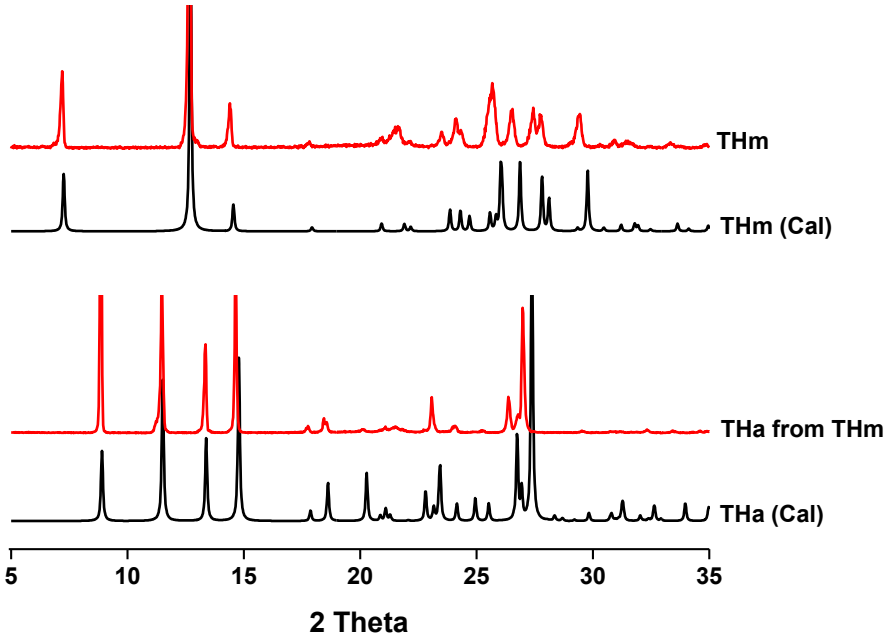

Figure A.S2 X-ray diffraction profiles for starting THm and THa dehydrated from THm. Both are compared with corresponding theoretical XRD patterns calculated from single crystal structures.

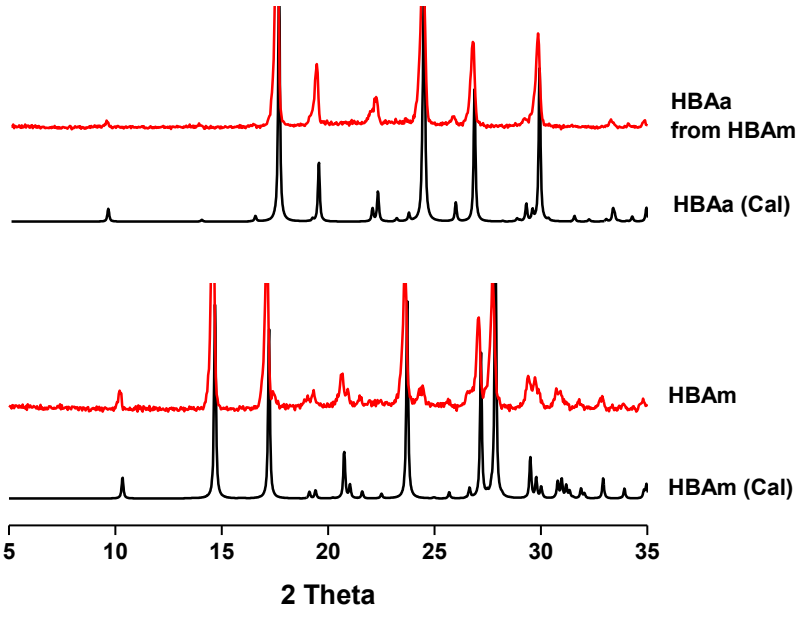

Figure A.S3 X-ray diffraction patterns of HBAa from dehydration of HBAm and starting HBAm. Patterns calculated from corresponding single crystal structures are shown for comparison.

References

1. Pharmacopeia US. 2006, pp 2669.
2. Ryshkewitch E 1953. Compression strength of porous sintered alumina and zirconia. J Am Ceram Soc 36:65-68.
3. Colombo P, Bettini R, Massimo G, Catellani PL, Santi P, Peppas NA 1995. Drug diffusion front movement is important in drug release control from swellable matrix tablets. J Pharm Sci 84:991-997.
4. Li J-R, Kuppler RJ, Zhou H-C 2009. Selective gas adsorption and separation in metal–organic frameworks. Chemical Society Reviews 38:1477-1504.
5. Pérez-Ramírez J, Christensen CH, Egeblad K, Christensen CH, Groen JC 2008. Hierarchical zeolites: enhanced utilisation of microporous crystals in catalysis by advances in materials design. Chemical Society Reviews 37:2530-2542.
6. Sun CC 2017. Microstructure of tablet—pharmaceutical significance, assessment, and engineering. Pharm Res 34:918-928.
7. Sun W-J, Kothari S, Sun CC 2018. The relationship among tensile strength, Young's modulus, and indentation hardness of pharmaceutical compacts. Powder Technol 331:1-6.
8. Sun C 2005. Critical roles of porosity in tableting properties characterization and solids formulation development. Am Pharmaceut Rev 8:102.
9. Patel S, Sun CC 2016. Macroindentation hardness measurement—Modernization and applications. Int J Pharm 506:262-267.
10. Gong X, Chang S-Y, Osei-Yeboah F, Paul S, Perumalla SR, Shi L, Sun W-J, Zhou Q, Sun CC 2015. Dependence of tablet brittleness on tensile strength and porosity. Int J Pharm 493:208-213.
11. Gong X, Sun CC 2015. A new tablet brittleness index. Eur J Pharm Biopharm 93:260-266.
12. Paul S, Sun CC 2017. Dependence of friability on tablet mechanical properties and a predictive approach for binary mixtures. Pharm Res 34:2901-2909.
13. Sunada H, Bi Y 2002. Preparation, evaluation and optimization of rapidly disintegrating tablets. Powder Technol 122:188-198.

14. Sun CC 2005. Quantifying errors in tableting data analysis using the Ryshkewitch equation due to inaccurate true density. J Pharm Sci 94:2061-2068.

15. Heckel R 1961. Density-pressure relationships in powder compaction. Trans Metall Soc AIME 221:671-675.

16. Heckel W 1961. An analysis of powder compaction phenomena. Trans Metall Soc AIME 221:671-675.

17. Sonnergaard J 1999. A critical evaluation of the Heckel equation. Int J Pharm 193:63-71.

18. Kuentz M, Leuenberger H 1999. Pressure susceptibility of polymer tablets as a critical property: A modified heckel equation. J Pharm Sci 88:174-179.

19. Paul S, Sun CC 2017. The suitability of common compressibility equations for characterizing plasticity of diverse powders. Int J Pharm 532:124-130.

20. Osei-Yeboah F, Chang S-Y, Sun CC 2016. A critical Examination of the Phenomenon of Bonding Area - Bonding Strength Interplay in Powder Tableting. Pharm Res 33:1126-1132.

21. Tye CK, Sun CC, Amidon GE 2005. Evaluation of the effects of tableting speed on the relationships between compaction pressure, tablet tensile strength, and tablet solid fraction. J Pharm Sci 94:465-472.

22. Paul S, Chang S-Y, Sun CC 2017. The phenomenon of tablet flashing—its impact on tableting data analysis and a method to eliminate it. Powder Technol 305:117-124.

23. Iyer RM, Hegde S, Singhal D, Malick W 2014. A novel approach to determine solid fraction using a laser-based direct volume measurement device. Pharm Dev Technol 19:577-582.

24. Sun CC 2004. A novel method for deriving true density of pharmaceutical solids including hydrates and water-containing powders. J Pharm Sci 93:646-653.

25. Higuchi T, Rao AN, Busse J, Swintosky J 1953. The physics of tablet compression. II. The influence of degree of compression on properties of table. J Am Pharm Assoc 42:194-200.

26. Higuchi T, Elowe L, Busse L 1954. The physics of tablet compression. V. Studies on aspirin, lactose, lactose-aspirin, and sulfadiazine tablets. J Am Pharm Assoc 43:685-689.

27. Raijada D, Bond AD, Larsen FH, Cornett C, Qu H, Rantanen J 2013. Exploring the solid-form landscape of pharmaceutical hydrates: transformation pathways of the sodium naproxen anhydrate-hydrate system. Pharm Res 30:280-289.

28. Sun CC 2005. True density of microcrystalline cellulose. J Pharm Sci 94:2132-2134.

29. Sun CC 2008. Mechanism of moisture induced variations in true density and compaction properties of microcrystalline cellulose. Int J Pharm 346:93-101.

30. Lee H-J, Kang J-H, Lee H-G, Kim D-W, Rhee Y-S, Kim J-Y, Park E-S, Park C-W 2016. Preparation and physicochemical characterization of spray-dried and jet-milled microparticles containing bosentan hydrate for dry powder inhalation aerosols. Drug Des Devel Ther 10:4017.

31. Maggi L, Conte U, Bettinetti G 1998. Technological properties of crystalline and amorphous α-cyclodextrin hydrates. Int J Pharm 172:211-217.

32. Flicker F, Eberle VA, Betz G 2011. Variability in commercial carbamazepine samples–impact on drug release. Int J Pharm 410:99-106.

33. Leung SS, Padden BE, Munson EJ, Grant DJ 1998. Solid-state characterization of two polymorphs of aspartame hemihydrate. J Pharm Sci 87:501-507.

34. Di Martino P, Malaj L, Censi R, Martelli S 2008. Physico-chemical and technological properties of sodium naproxen granules prepared in a high-shear mixer-granulator. J Pharm Sci 97:5263-5273.

35. Chang S-Y, Sun CC 2017. Superior Plasticity and Tabletability of Theophylline Monohydrate. Mol Pharm 14:2047-2055.

36. Sun CC, Grant DJ 2004. Improved tableting properties of p-hydroxybenzoic acid by water of crystallization: a molecular insight. Pharm Res 21:382-386.

37. Viana M, Jouannin P, Pontier C, Chulia D 2002. About pycnometric density measurements. Talanta 57:583-593.

38. Turner M, McKinnon J, Wolff S, Grimwood D, Spackman P, Jayatilaka D, Spackman M 2017. CrystalExplorer17. University of Western Australia.

39. Gaussian09 RA 2009. 1, MJ Frisch, GW Trucks, HB Schlegel, GE Scuseria, MA Robb, JR Cheeseman, G. Scalmani, V. Barone, B. Mennucci, GA Petersson et al., Gaussian. Inc, Wallingford CT.

40. Turner MJ, Thomas SP, Shi MW, Jayatilaka D, Spackman MA 2015. Energy frameworks: insights into interaction anisotropy and the mechanical properties of molecular crystals. Chem Comm 51:3735-3738.

41. Turner MJ, Grabowsky S, Jayatilaka D, Spackman MA 2014. Accurate and efficient model energies for exploring intermolecular interactions in molecular crystals. J Phys Chem Lett 5:4249-4255.

42. Wang K, Reeber RR 1996. Thermal expansion of alkali halides at high pressure: NaCl as an example. Phys Chem Miner 23:354-360.

43. Ebisuzaki Y, Boyle PD, Smith JA 1997. Methylxanthines. I. Anhydrous theophylline. Acta Crystallogr C 53:777-779.

44. Heath EA, Singh P, Ebisuzaki Y 1992. Structure of p-hydroxybenzoic acid and p-hydroxybenzoic acid-acetone complex (2/1). Acta Crystallogr C 48:1960-1965.

45. Jacobsson TJ, Schwan LJ, Ottosson M, Hagfeldt A, Edvinsson T 2015. Determination of thermal expansion coefficients and locating the temperature-induced phase transition in methylammonium lead perovskites using x-ray diffraction. Inorg Chem 54:10678-10685.

46. Sun C, Zhou D, Grant DJ, Young Jr VG 2002. Theophylline monohydrate. Acta Crystallogr E: Structure Reports Online 58:0368-0370.

47. Colapietro M, Domenicano A, Marciante C 1979. Structural studies of benzene derivatives. VI. Refinement of the crystal structure of p-hydroxybenzoic acid monohydrate. Acta Crystallogr B 35:2177-2180.

48. Sun CC 2007. Thermal expansion of organic crystals and precision of calculated crystal density: a survey of Cambridge crystal database. J Pharm Sci 96:1043-1052.

49. Noordik J, Beurskens PT, Bennema P 1984. Crystal structure, polarity and morphology of 4-0-β-D-galactopyranosyl-α-D-glucopyranose monohydrate (α-lactose monohydrate): a redetermination. Zeitschrift für Kristallographie-Crystalline Materials 168:59-66.

50. Baird JA, Van Eerdenbrugh B, Taylor LS 2010. A classification system to assess the crystallization tendency of organic molecules from undercooled melts. J Pharm Sci 99:3787-3806.

51. Duncan-Hewitt WC, Grant DJ 1986. True density and thermal expansivity of pharmaceutical solids: Comparison of methods and assessment of crystallinity. Int J Pharm 28:75-84.

52. Hancock B, Rowe R 1998. The thermal expansion of pharmaceutical solids. STP Pharma Sci 8:213-220.